UNIVERSITY OF CALGARY

Characterization of the Potassium Channel Isoforms in Mouse Ventricle by Ribonuclease Protection Assay: Developmental Changes and Effect of Thyroid Hormone on mRNA Expression Levels

by

Kathryn Janzen

A THESIS

SUBMITTED TO THE FACULTY OF GRADUATE STUDIES

IN PARTIAL FULFILLMENT OF THE REQUIREMENTS FOR THE

DEGREE OF MASTER OF SCIENCE

DEPARTMENT OF CARDIOVASCULAR/RESPIRATORY SCIENCES

CALGARY, ALBERTA

OCTOBER, 1999

ABSTRACT

Ribonuclease protection assays (RPAs) were used to study the developmental expression pattern of eight K^+ channel α-subunit mRNAs in mouse ventricle. It was determined that Kv1.2, Kv1.5, Kv4.2, Kv4.3 and IRK1 mRNA levels increased during postnatal development and Kv1.4, $KvLQT_1$ and minK mRNA levels decreased. It was hypothesized that the developmental changes in K^+ channel mRNA expression in the mouse ventricle resulted from the developmental increase in thyroid hormone. The effect of thyroid hormone on K^+ channel α-subunit mRNA expression was examined. Ventricular tissues from adult hypothyroid mice had greater Kv1.2, Kv1.4, $KvLQT_1$ and minK mRNA levels than controls; and direct addition of thyroid hormone to neonatal ventricular myocytes in culture caused decreased Kv1.4 and $KvLQT_1$ and increased Kv4.2 mRNA expression after 18-24 hours. Thus, thyroid hormone treatment resulted in changes in mRNA levels for some transcripts, which were somewhat similar to those seen during development.

ACKNOWLEDGMENTS

First, I am very grateful to Dr. Wayne Giles for providing me with the opportunity to work in such a stimulating research environment. My experience at the University of Calgary has been invaluable. As well, I would like to thank him for his enormous amount of support and guidance throughout this project. He has spent a great deal of time teaching me about the fundamentals of cardiac electrophysiology and pharmacology, which have been very enlightening. He has also spent countless time reviewing various drafts of my thesis. His thoughtfulness and support will always be appreciated.

Secondly, I would like to thank Bob Winkfein. He has spent an enormous amount of time and effort in teaching me the fundamentals of molecular biology. His guidance and expertise have definitely aided in the success of this project. I would also like to thank him for his tremendous amount of patience and understanding when dealing with a molecular amateur. Bob has also spent a great amount of time reviewing my thesis and his comments were always very helpful.

I am also indebted to Dr. Robert Clark who was a valuable resource and a great source of encouragement. All of his expert advice was very useful and appreciated. I would like to extend my thanks to Claude Veillette who was very helpful in teaching me the necessary cell culture skills required to successfully complete this project and Marco Perizzolo who was always there when I needed a second set of hands.

TABLE OF CONTENTS

Approval Page ii
Abstract iii
Acknowledgements iv
Table of Contents v
List of Figures vii
List of Abbreviations viii

1. INTRODUCTION 1
1.1. The Cardiac Action Potential 1
1.2. Native K^+ currents in cardiac myocytes 5
1.2.1. The Ca^{2+}-independent transient outward K^+ current (I_{to}) 5
1.2.2. Delayed rectifier K^+ currents (I_{Kr}, I_{Ks}) 6
1.2.3. The rapidly activating slowly inactivating outward K^+ current (I_{sus}) 7
1.2.4. Inward rectifier (I_{K1}) 7
1.3. Potassium Channels 8
1.3.1. Voltage-gated K^+ channels 8
1.3.1.1. Voltage-gated K^+ channel pore-forming subunits 8
1.3.1.2. Accessory (β) subunits of voltage-gated K^+ channels 11
1.3.2. Inward rectifier K^+ channels 12
1.3.3. K^+ channel α-subunit mRNA and protein expression 12
1.4. Relationship Between Cloned K^+ α-Subunits and myocardial K^+ Currents 14
1.4.1. Kv4.2, Kv4.3, and Kv1.4: I_{to} 14
1.4.2. Kv1.5 and Kv1.2: I_{sus} 16
1.4.3. $KvLQT_1$ and minK: I_{Ks} 17
1.5. Regulation of K^+ Channel Expression in the Heart: Thyroid Hormone 18
1.6. RNase Protection Assay 19
1.7. Project Objectives 20

2. METHODS 21
2.1. Mouse Ventricular Total RNA Samples 21
2.1.1. Whole ventricular muscle 21
2.1.2. Neonatal ventricular muscle 22
2.1.2.1. Cell isolation and digestion solutions 22
2.1.2.2. Myocyte and fibroblast isolation and culture 22
2.1.3. Total RNA isolation 23
2.2. Preparation of Template DNA for Riboprobe Synthesis 25
2.2.1. K^+ channel isoform-specific DNA fragments 25
2.2.1.1. Template cDNA 26
2.2.1.2. Oligonucleotide PCR Primers 26
2.2.1.3. PCR amplification 30
2.2.2. Subcloning cDNA fragments into a plasmid vector 30

2.3. Synthesis of Riboprobes 33
2.4. RNase Protection Assays 35
2.5. Data Analysis 36
2.6. Statistics 37
2.7. Materials 38

3. RESULTS 39
3.1. Riboprobes 39
3.2. Mouse Ventricular RNA Samples 44
3.3. Internal Controls 49
3.4. RNase Protection Assay: Methodological Findings 49
3.5. Mouse Ventricular K^+ Channel mRNA Levels 55
3.5.1. mRNA expression during development 55
3.5.2. mRNA expression in adult hypothyroid diet mice 66
3.5.3. mRNA expression in myocytes and fibroblasts 75
3.5.4. mRNA expression in high-density myocyte cultures 84

4. DISCUSSION 103
4.1. Method Evaluation: The RNase Protection Assay 103
4.2. Neonatal Ventricular Myocyte Cell Culture 104
4.2.1. mRNA levels in ventricular myocytes and fibroblasts 105
4.3. K^+ Channels in the Developing Mouse Heart 108
4.3.1. mRNA expression during development 108
4.3.2. Relationship between mRNA levels and electrophysiology 109
4.3.2.1. Kv4.2, Kv4.3 and Kv1.4: I_{to} 109
4.3.2.2. Kv 1.5 and Kv1.2: I_{sus} 111
4.3.2.3. $KvLQT_1$ and minK: I_{Ks} 113
4.3.2.4. IRK1 (Kir2.1): I_{K1} 114
4.4. Thyroid Hormone and Postnatal Development of the Mouse Heart 115
4.4.1. Effect of thyroid hormones on K^+ currents 116
4.4.2. Effect of thyroid hormones on mRNA expression 117
4.4.2.1. mRNA expression in hypothyroid ventricles 118
4.4.2.2. Effect of T_3 on myocyte mRNA expression 119
4.5. Correlation of mRNA Levels: Development and Thyroid Hormone 120
4.6. Limitation of Study and Future Directions 122
4.7. Overall Relevance 124

5. REFERENCES 125

APPENDIX I : pBluescript® II SK- Phagemid and DNA Ladder 141

APPENDIX II : Detailed RPA Protocols 143

APPENDIX III : RPA Gel Phosphorimaging Data 145

LIST OF FIGURES

Figure 1.1: Schematic diagram of the cardiac action potential 3
Figure 1.2: Postulated one-dimensional membrane-spanning arrangements 9

Figure 2.1: Synthetic oligonucleotide primers: K^+ channels 28
Figure 2.2: Synthetic oligonucleotide primers: Internal controls 31

Figure 3.1: Mouse ventricle total RNA and primary strand cDNA 40
Figure 3.2: Cloned K^+ channel cDNA fragments 42
Figure 3.3: Nucleotide sequence of the antisense RPA fragments 45
Figure 3.4: Mouse ventricle total RNA samples 47
Figure 3.5: RPA gel autoradiograms - Internal controls 50
Figure 3.6: Hybspeed™ RPA versus RPA III™ kits (Ambion) 53
Figure 3.7: RPA gel autoradiogram - seeDNA™ 56
Figure 3.8: Developmental expression of Kv1.5 and IRK1 mRNA 58
Figure 3.9: Developmental expression of Kv4.2 and Kv4.3 mRNA 60
Figure 3.10: Developmental expression of $KvLQT_1$ and minK 62
Figure 3.11: Developmental expression of Kv1.4 and Kv1.2 64
Figure 3.12: Kv1.5 and IRK1 mRNA expression in hypothyroid mice 67
Figure 3.13: Kv4.2 and Kv4.3 mRNA expression in hypothyroid mice 69
Figure 3.14: $KvLQT_1$ and minK mRNA expression in hypothyroid mice 71
Figure 3.15: Kv1.4 and Kv1.2 mRNA expression in hypothyroid mice 73
Figure 3.16: Kv1.5 and IRK1 mRNA expression in isolated ventricular cells 76
Figure 3.17: Kv4.2 and Kv4.3 mRNA expression in isolated ventricular cells 78
Figure 3.18: KvLQT1 and minK mRNA expression in isolated ventricular cells 80
Figure 3.19: Kv1.4 and Kv1.2 mRNA expression in isolated ventricular cells 82
Figure 3.20: Kv1.5 and IRK1 mRNA expression in myocytes (pellet culture) 85
Figure 3.21: Kv1.5 and IRK1 mRNA expression in T_3-treated myocytes 87
Figure 3.22: Kv4.2 and Kv4.3 mRNA expression in myocytes (pellet culture) 89
Figure 3.23: Kv4.2 and Kv4.3 mRNA expression in T_3-treated myocytes 91
Figure 3.24: $KvLQT_1$ and minK mRNA expression in myocytes (pellet culture) 93
Figure 3.25: $KvLQT_1$ and minK mRNA expression in T_3-treated myocytes 95
Figure 3.26: Kv1.4 and Kv1.2 mRNA expression in myocytes (pellet culture) 97
Figure 3.27: Kv1.4 and Kv1.2 mRNA expression in T_3-treated myocytes 99

LIST OF ABBREVIATIONS

4-AP - 4-aminopyridine

α-DTX - α-dendrotoxin

BLAST - Basic Local Alignment Search Tool

cDNA - complementary DNA

GAPDH - glyceraldehyde-3-phosphate dehydrogenase

MMI - methimazole

mRNA - messenger RNA

PCR - polymerase chain reaction

PTU- propylthyouracil

RNase - Ribonuclease

RPA - Ribonuclease Protection Assay

T_3 - 3,3'5-triiodo-L-thyronine

T_4 - thyroxine

1. INTRODUCTION

Transgenic mouse models allow researchers to study complex biological systems *in vivo*, using animals that have been specifically engineered to express a given phenotype. For example, these models have become powerful tools for the investigation of the cellular and molecular physiology of the heart (Milano *et al.*, 1994; Chien, 1995; Becker *et al.*, 1996; Ben-Yehuda & Rockman, 1996; Christensen *et al.*, 1997), and cardiovascular abnormalities including hypertension, hypertrophy, and some cardiomyopathies (Boyden & Jeck, 1995; Kubalak *et al.*, 1996; Ackerman & Clapham, 1997). Despite the potential importance of this approach, relatively little is known regarding the ionic basis of the cardiac action potential or the exact molecular identity of the ionic currents responsible for the different phases of the action potential in the mouse heart throughout normal cardiac development.

Myocardial K^+ currents function to control resting membrane potential, the height and duration of action potentials, and refractoriness and automaticity of the mammalian heart (Campbell *et al.*, 1995; Barry & Nerbonne, 1996; Deal *et al.*, 1996; Giles *et al.*, 1996). Numerous K^+ channel genes have been identified by molecular cloning (Chandy & Gutman, 1993) and individual myocardial cells express multiple types of K^+ channels (Barry & Nerbonne, 1996). Identification of the K^+ channel α-subunits which are expressed in mouse ventricular myocytes throughout development, and defining the relationship between these K^+ channel α-subunits and the functional K^+ currents identified in these cells, is an important step in the overall understanding of the murine cardiac action potential.

1.1. The Cardiac Action Potential

The size and shape of the cardiac action potential is determined by the net current resulting from the movement of Na^+, Ca^{2+}, K^+, and Cl^- (in some species) ions across the sarcolemmal membrane (Deal *et al.*, 1996; Lindblad *et al.*, 1996). The cardiac action potential waveform can be considered to consist of five phases: Phase 0, the upstroke, or

rapid depolarization; Phase 1, early rapid (incomplete) repolarization; Phase 2, the plateau; Phase 3, final repolarization; and Phase 4, the resting membrane potential (Figure1.1).

The depolarization phase (Phase 0) of the cardiac action potential is mediated by a rapid inward movement of Na^+ through voltage-gated Na^+ channels (Fozzard, 1994). Phase 1 is mediated by the efflux of K^+ through transiently activated K^+ channels (both Ca^{2+}-independent and dependent). These channels determine the initial plateau potential and, therefore, regulate the behaviour of other voltage-dependent channels and the overall duration of the action potential (Carmeliet, 1993; Deal *et al.*, 1996). The ionic currents that underlie the plateau phase of the cardiac action potential are not fully understood. However, it is known that the action potential duration is governed by a balance of the inward Ca^{2+} current and one or two outward K^+ currents; and repolarization occurs as the Ca^{2+} channels inactivate and as delayed rectifier K^+ channels open (Weidmann, 1956; Hoffman & Cranfield, 1960). This simplified model needs to be adapted to take account of the expression of two distinct types of Ca^{2+} channels (e.g. L-type and T-type) and a variety of K^+ channels and Cl^- channels in particular cardiac tissues or cell types. Moreover, the important role of current generated by both Na^+-Ca^{2+} exchange and the Na^+-K^+ pump in repolarization needs to be accounted for (Noble, 1984; Hume & Uehara, 1985; Schouten & ter Keurs, 1985; Carmeliet, 1993; Katz, 1993).

The final repolarization phase of the action potential is controlled by the time-dependent increase in K^+ permeability through delayed rectifier K^+ channels, and the activation of inwardly rectifying K^+ channels at more negative potentials. The resting membrane potential is maintained primarily by the inwardly rectifying K^+ channels as well as by currents generated by the Na^+/K^+ pump and the Na^+/Ca^{2+} exchanger proteins (Giles, 1989; Janvier & Boyette, 1996).

Figure 1.1: Schematic diagram of the mammalian cardiac action potential waveform. Phase 0, the upstroke, or rapid depolarization; Phase 1, early rapid (incomplete) repolarization; Phase 2, the plateau; Phase 3, final repolarization; and Phase 4, the resting membrane potential. The main ionic currents involved in each phase of the action potential are listed. Those shown in bold-face type are mose relevant to this project.

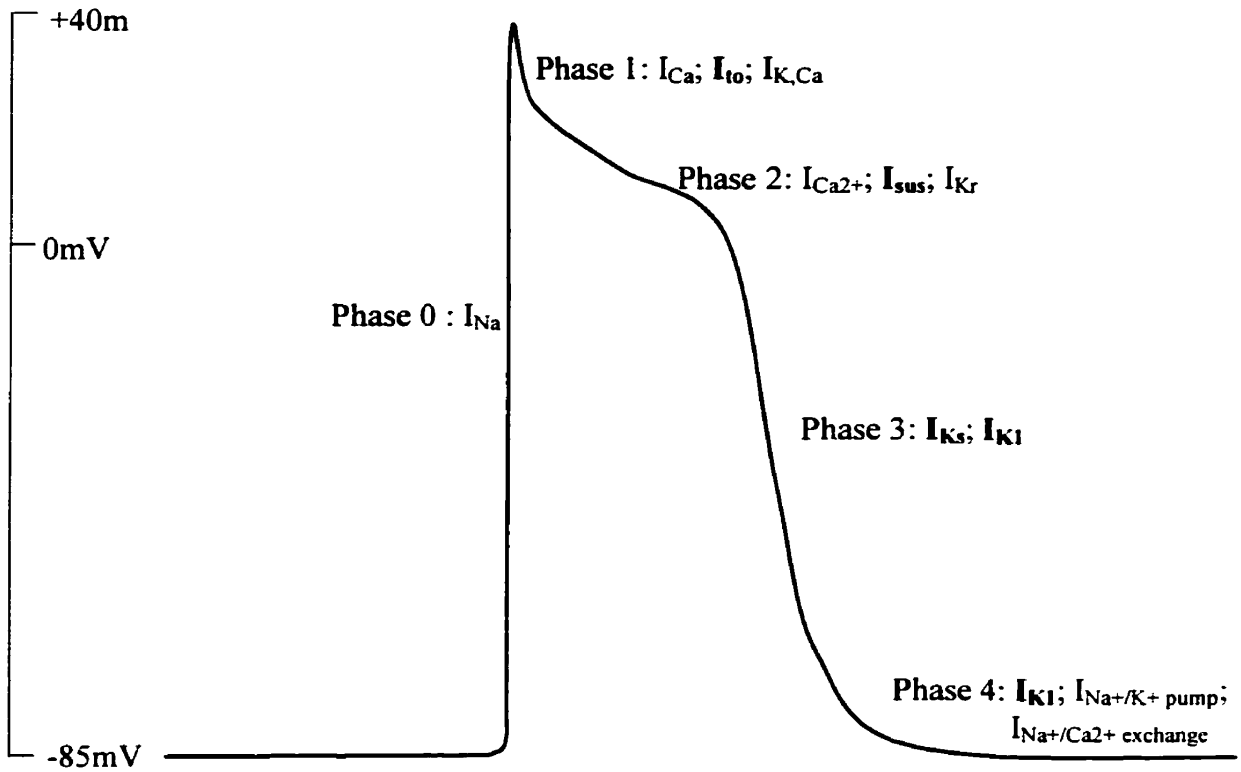
+40m
0mV
-85mV
Phase 0 : I_{Na}
Phase 1: I_{Ca}; $\mathbf{I_{to}}$; $I_{K,Ca}$
Phase 2: I_{Ca2+}; $\mathbf{I_{sus}}$; I_{Kr}
Phase 3: $\mathbf{I_{Ks}}$; $\mathbf{I_{K1}}$
Phase 4: $\mathbf{I_{K1}}$; $I_{Na+/K+\ pump}$; $I_{Na+/Ca2+\ exchange}$

It is important to note that the action potential waveform is not uniform when various regions of the same heart are compared (Lindbald *et al.*, 1996) and that there are also important species-dependent differences (Giles, 1989; Shibata *et al.*, 1989). This suggests that the ionic basis of the action potential is also tissue- and species-specific. Furthermore, age-dependent differences in cardiac electrophysiology are apparent since the action potential waveform changes during development (Jeck & Boyden, 1992; Adolph, 1996; Wang *et al.*, 1996; Wetzel & Klitzner, 1996; Wang & Duff, 1997; Nerbonne, 1998). Pathophysiological states, such as congestive heart failure, also give rise to changes in the cardiac action potential waveform, as a result of altered expression of specific ion channels in the heart (Kaab *et al.*, 1998).

1.2. Native K^+ Currents in Cardiac Myocytes

It is evident that numerous, distinct K^+ currents are involved in shaping the cardiac action potential as well as maintaining the resting conductance in cardiac myocytes (Benndorf *et al.*, 1987; Tseng & Hoffman, 1989; Apkon & Nerbonne, 1991; Wang *et al.*, 1993; Wang *et al.*, 1994). The properties of the K^+ currents that are most relevant to this study are outlined in the following sections (indicated in boldface type on Figure 1.1).

1.2.1. The Ca^{2+}-independent transient outward K^+ current (I_{to})

A transient outward K^+ current (I_{to}) plays an essential role in the early repolarization of the cardiac action potential in a variety of species (Campbell *et al.*, 1995; Giles *et al.*, 1996; Nerbonne *et al.*, 1998). It is characterized by its rapid activation and inactivation kinetics and sensitivity to 4-aminopyridine (4-AP) in the millimolar concentration range. Rat, mouse, rabbit, canine, and human cardiomyocytes exhibit this type of transient outward K^+ current (Escande *et al.*, 1985; Benndorf *et al.*, 1987; Giles & Imaizumi, 1988; Shibata *et al.*, 1989; Tseng & Hoffman, 1989; Apkon & Nerbonne, 1991). I_{to} currents may be generated by more than one channel subtype, since differing inactivation kinetics have been observed in some tissues and species (Nerbonne, 1998). For example, in rabbit atrial and ventricular myocytes (Giles & Imaizumi, 1988) and rat atrial myocytes (Boyle

& Nerbonne, 1992) I_{to} inactivates more slowly than in mouse and rat ventricular cells (Benndorf & Nilius, 1988; Apkon & Nerbonne, 1991). As well, rates of inactivation and recovery are significantly faster in epicardial than in endocardial cells isolated from ferret left ventricle (Brahmajothi *et al.*, 1999).

In mouse, I_{to} is an important repolarizing K^+ current in adult ventricular myocytes (Benndorf *et al.*, 1987; Benndorf & Nilius, 1988; Fiset *et al.*, 1997a; Xu *et al.*, 1999). Developmental increases in I_{to} density have been reported (Nuss & Marban, 1994; Wang & Duff, 1997). Recently, a detailed analysis of the depolarization-activated K^+ currents in adult mouse ventricular myocytes indicated that there are two distinct I_{to} currents, $I_{to,fast}$ ($I_{to,f}$, I_{to} previously identified in mouse cardiomyocytes) and $I_{to,slow}$ ($I_{to,s}$) that have differing inactivation kinetics (fast and slow), sensitivities to *Heteropoda* toxin-3 ($I_{to,f}$ is selectively blocked by nanomolar concentrations of *Heteropoda* toxin-3 and $I_{to,s}$ is unaffected) and distribution patterns (Xu *et al.*, 1999).

1.2.2. Delayed rectifier K^+ currents (I_{Kr}, I_{Ks})

A time- and voltage-dependent delayed rectifier K^+ current (I_K) is important in the regulation of the action potential duration in most mammalian hearts (Tseng & Hoffman, 1989; Sanguinetti & Jurkiewicz, 1991). It consists of at least two components: a rapidly activating current, I_{Kr} and a slowly activating current I_{Ks} (Sanguinetti & Jurkiewicz, 1991). Together, I_{Kr} and I_{Ks} produce a small net outward current that increases with time (Attali, 1996). In mouse ventricle, both I_{Kr} and I_{Ks} change significantly during development (Nuss & Marban, 1994; Davies *et al.*, 1996; Wang & Duff, 1996; Wang *et al.*, 1996). I_{Kr} is the dominant repolarizing K^+ current in fetal mouse ventricular myocytes but is not present in adult ventricular myocytes (Wang & Duff, 1996; Wang *et al.*, 1996). I_{Ks} density increases in the late embryonic heart, becoming consistently detectable just before birth (Davies *et al.*, 1996): it subsequently decreases during postnatal development (Nuss & Marban, 1994; Davies *et al.*, 1996; Wang *et al.*, 1996) and is not prominent in the adult mouse ventricle (Wang *et al.*, 1996; Xu *et al.*, 1999).

1.2.3. The rapidly activating slowly inactivating outward K^+ current (I_{sus})

A rapidly activating, slowly inactivating outward K^+ current, I_{sus} (also referred to as $I_{K,slow}$ and I_{Kur}) has been identified in human atrium (Wang *et al.*, 1993), canine atrium (Yue *et al.*, 1996), neonatal rat ventricle (Guo *et al.*, 1997a), and mouse ventricle (Fiset *et al.*, 1997b; London *et al.*, 1998; Zhou *et al.*, 1998; Xu *et al.*, 1999). I_{sus} activates during the earliest stages of repolarization and plays an important role in shaping the action potential, distinct from the other classic delayed rectifiers (I_{Kr} and I_{Ks}) (Backx & Marban, 1993). I_{sus} can be blocked selectively by micromolar (3-50 μM) concentrations of 4-AP.

In adult mouse ventricle, I_{sus} plays important roles in regulating action potential duration and phasic contraction of the mouse heart (Fiset *et al.*, 1997b; London *et al.*, 1998b; Zhou *et al.*, 1998; Xu *et al.*, 1999). It is a major repolarizing current that significantly contributes to the early and middle repolarization process (Zhou *et al.*, 1998). I_{sus} current density has been found to increase during postnatal development in mouse ventricular myocytes (C. Fiset and R. Clark, unpublished observations).

1.2.4. Inward rectifier (I_{K1})

The inward rectifier current (I_{K1}) is present in cardiac myocytes of most species, including mouse ventricular myocytes, and has been reported to increase during postnatal development (Wahler, 1992; Masuda & Sperelakis, 1993; Sanchez-Chapula *et al.*, 1994; Nakamura *et al.*, 1999). I_{K1} currents, which flow through IRK1 channels, are relatively large at negative potentials, but generate only very small outward currents at more positive membrane potentials (Nichols *et al.*, 1996). I_{K1} contributes little to the early phases of repolarization, since virtually no outward current is present at potentials positive to -40mV (Vandenberg, 1995; Shimoni *et al.*, 1997); however, it does contribute to the terminal phase of repolarization (-60 to -85 mV), and is the dominant K^+ conductance maintaining the negative resting membrane potential (Heidbuchel *et al.*, 1990; Vandenberg, 1995).

1.3. Potassium Channels

Over the last decade a large number of K^+ channel genes have been identified in both vertebrates and invertebrates, including genes for voltage-dependent transient and delayed-rectifier channels, for inwardly rectifying channels, calcium-dependent K^+ channels, and ATP-sensitive channels (Gintant *et al.*, 1992; Barry & Nerbonne, 1996).

1.3.1. Voltage-gated K^+ channels

1.3.1.1. Voltage-gated K^+ channel pore-forming subunits

The first voltage-gated K^+ channel (Kv) pore-forming (α) subunit clone was obtained using *Drosphila* genetics (Papizan *et al.*, 1987). It was discovered that the *Shaker* phenotype (i.e. abnormal leg shaking in response to ether) was caused by a defect in a K^+ channel gene (Chandy & Gutman, 1993). Subsequently, the isolation of this gene led to the cloning of the first voltage-gated K^+ channel (Pongs *et al.*, 1988; Tempel *et al.*, 1988).

Sequence analysis of *Shaker* combined with hydropathy analysis suggested the protein had six transmembrane domains (S1-S6) with both the N- and C-termini located intracellularly (Figure 1.2A; Tempel *et al.*, 1987). The fourth transmembrane domain (S4) is homologous to the corresponding region in voltage-gated Na^+ and Ca^{2+} channels placing *Shaker* in the S4 superfamily of voltage-gated channels (Jan & Jan, 1992). The S4 segment consists of a number of positively charged amino acid resides and is thought to act as a voltage sensor (Mathur *et al.*, 1997). The H5-loop between S5 and S6 contributes to forming the K^+-selective pore (Jan & Jan, 1992; Pongs *et al.*, 1988). Domains that control inactivation have been characterized within the N-terminus, the pore and S6 (Wei *et al.*, 1990; Rudy *et al.*, 1991; Pongs, 1993).

Figure 1.2: Postulated one-dimensional membrane-spanning arrangements of A. *Shaker*-like K^+ channels; B. minK-type K^+ channel accessory subunit; and C. Inward rectifier-type K^+ channels in mammalian heart (adapted from Deal *et al.* 1996).

A. Shaker-type K^+ Channel

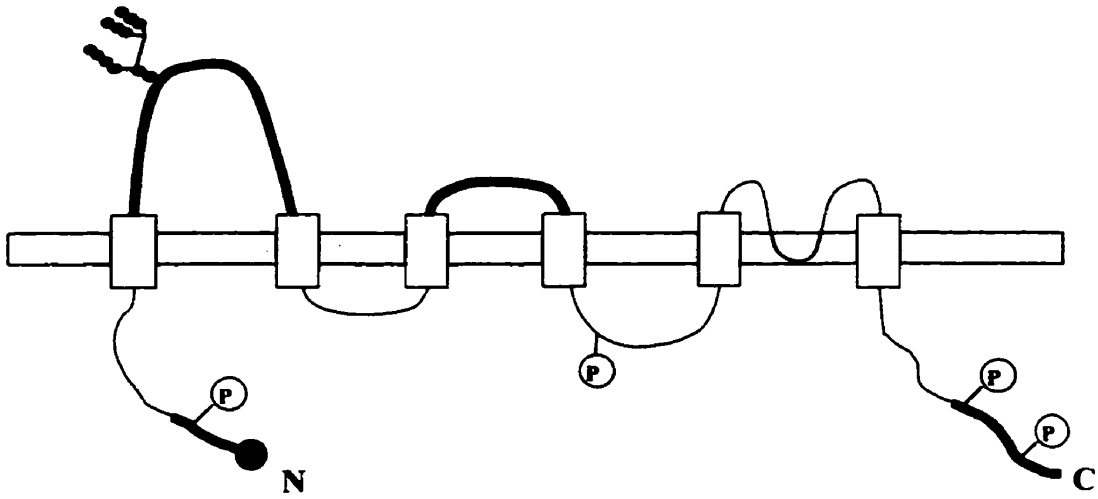

B. MinK: K^+ Channel Regulator

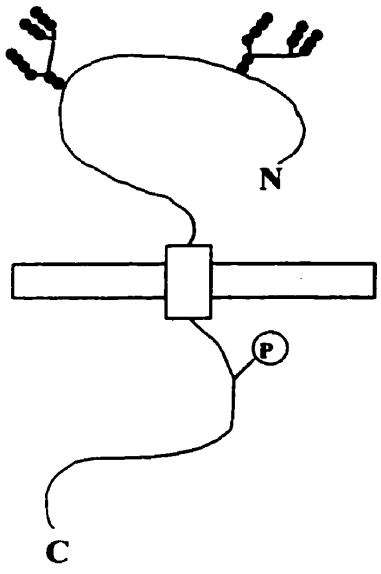

C. Inward Rectifier-type K^+ Channel

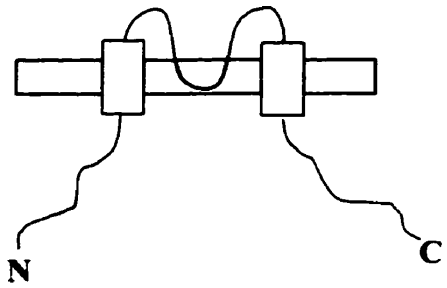

Three highly homologous subfamilies of Kv α-subunits, *Shab*, *Shaw*, and *Shal*, have subsequently been cloned from *Drosophila* (Wei *et al.*, 1990). All four *Drosophila* K^+ channel α-subunit genes have been found to have vertebrate homologues named the Kv1 (Shaker), Kv2 (Shab), Kv3 (Shaw), and Kv4 (Shal) subfamilies (Chandy, 1991; Chandy & Gutman, 1993). Further homology screening has led to the identification of multiple members of each Kv subfamily (Roberds *et al.*, 1993; Barry & Nerbonne, 1996). Furthermore, genes encoding additional subfamilies of voltage-gated K^+ channel α-subunits, such as $KvLQT_1$ (a gene responsible for some forms of long QT and Jervell and Lange-Nielsen syndromes; Wang *et al.*, 1998) and Kv5 through Kv9 (Salinas *et al.*, 1997), have also been identified in mammals using various homology and positional cloning strategies.

Heterologous expression of each of the Shaker-type genes in Xenopus oocytes produced functional voltage-gated K^+ channels that consist of a tetramer of α-subunits (Timpe *et al.*, 1988; Wei *et al.*, 1990; Pak *et al.*, 1991; MacKinnon, 1991). Both homomultimeric and heteromultimeric channel proteins may form *in vivo* since cells express multiple Kv α-subunit genes (Covarrubias *et al.*, 1991). Co-injection experiments have revealed that heteromultimeric Kv channels form in oocytes following injection of two different cRNAs belonging to the same subfamily but do not form if the cRNAs are from two different subfamilies (Christie *et al.*, 1990; Isacoff *et al.*, 1990; Ruppersberg *et al.*, 1990; Covarrubias *et al.*, 1991; Po *et al.*, 1993).

1.3.1.2. Accessory (β) subunits of voltage-gated K^+ channels

In addition to genes that encode pore-forming K^+ channel α-subunits, genes that encode additional proteins that regulate the function and/or the assembly and trafficking of K^+ channel α-subunits have also been identified (Papazian, 1999). For example, a family of cytoplamsic β-subunits have been described. These proteins can combine with voltage-gated K^+ channel α-subunits with a proposed stoichiometry of α4β4 (Isom *et al.*, 1994;

Rettig *et al.*, 1994; Shi *et al.*, 1996). Coexpression of α- and β-subunits results in significant alterations in channel gating kinetics which suggests that K^+ channels may be differentially regulated by association with variable β-subunits (Breitwieser, 1996).

The single-spanning transmembrane protein, minK (Figure 1.2B), is also considered a regulatory K^+ channel subunit (Attali *et al.*, 1993; Freeman & Kass, 1993; Barhanin *et al.*, 1997; Romey *et al.*, 1997; Sanguinetti *et al.*, 1997). The minK protein coassembles with $KvLQT_1$ and ERG channels altering both the gating and permeation properties of these channels (Barhanin *et al.*, 1996; Romey *et al.*, 1997; Sanguinetti *et al.*, 1997).

1.3.2. Inward rectifier-type K^+ channels

The first inwardly rectifying K^+ channel α-subunits (ROMK1 and IRK1) were cloned from rat kidney and a mouse macrophage cell line, respectively (Kubo *et al.*, 1993; Ho *et al.*, 1993). The cDNAs encoding inwardly rectifying K^+ channels are much smaller than the *Shaker* channels (Kubo *et al.*, 1993; Iizuka *et al.*, 1995). Sequence analysis and hydropathy analysis indicated that these inward rectifier channels only have two hydrophobic segments (M1 and M2) and a linker region (H5), homologous to the S5, S6 and H5 segments of voltage-gated K^+ channels (Figure 1.2C; Doupnik *et al.*, 1995). Subsequently, homology screening of cDNA libraries combined with heterologous expression has revealed numerous members of the inwardly rectifying superfamily, including ROMK (Kir1.x), IRK (Kir2.x), and GIRK (Kir3.x) (Barry & Nerbonne, 1996).

1.3.3. K^+ channel α-subunit mRNA and protein expression in the heart

Successful cloning of numerous voltage-gated K^+ channel α-subunit genes from cardiac cDNA libraries and the expression of these Kv subunits in the mammalian heart have been reported (Roberds *et al.*, 1993; Barry & Nerbonne, 1996). Six different K^+ channel α-subunits have been detected by Northern blot analysis in rat heart Kv1.1, Kv1.2, Kv1.4, Kv1.5, Kv2.1, and Kv4.2 (Roberds & Tamkun, 1991). Using quantitative ribonuclease

(RNase) protection assays (RPAs), Dixon & McKinnon (1993) and Dixon *et al.* (1996) have examined the abundance of 15 different voltage-activated K^+ channel α-subunits in adult rat and canine hearts. Kv1.2, Kv1.4, Kv1.5, Kv2.1, Kv4.2, and Kv4.3 α-subunit mRNAs were significantly expressed in rat atria and ventricles, while in canine left ventricle Kv1.1, Kv1.3, Kv1.4, Kv1.5, Kv1.6, Kv2.1, Kv3.4, and Kv4.3 α-subunit mRNAs were abundant (Dixon & McKinnon, 1993; Dixon *et al.*, 1996). Interestingly, the expression levels of several of the mRNA transcripts are significantly different when rat and canine ventricles were compared, which suggests that there is species-specific regulation of K^+ channel α-subunit expression (Dixon & McKinnon, 1993; Dixon *et al.*, 1996).

Using Kv α-subunit-specific antibodies against Kv1.2, Kv1.4, Kv1.5, Kv2.1, and Kv4.2 channel proteins, Barry *et al.* (1995) found detectable levels of Kv1.2, Kv1.5, Kv2.1 and Kv4.2 proteins in adult rat heart by Western blot analysis. Since the anti-Kv4.2 antibody used recognizes a sequence that is highly homologous between Kv4.2 and Kv4.3, it is likely that both proteins were detected by this assay (anti-Kv4.2/4.3; Nerbonne, 1998).

The developmental expression of Kv α-subunit mRNAs and proteins has also been examined in the rat heart (Xu *et al.*, 1996; Wickenden *et al.*, 1997). It was found that Kv1.2, Kv1.5, Kv2.1 Kv4.2 and Kv4.3 mRNA levels increase significantly during postnatal development and that Kv1.4 mRNA levels decrease (Xu *et al.*, 1996; Wickenden *et al.*, 1997). Western analysis revealed that Kv1.2 and Kv4.2/4.3 protein expression increases and Kv1.4 and Kv2.1 protein expression decreases during postnatal developmental, while no change in Kv1.5 protein expression was detected (Xu *et al.*, 1996). Mismatches in the Kv α-subunit mRNA and protein expression patterns during development are therefore evident (Xu *et al.*, 1996).

$KvLQT_1$, minK, and IRK1 K^+ channel subunits have been cloned from or shown to be expressed in mammalian hearts (Honore *et al.*, 1991; Felipe *et al.*, 1994; Ishii *et al.*, 1994; Wible *et al.*, 1995; Wood *et al.*, 1995; Barhanin *et al.*, 1996; Sanguinetti *et al.*, 1996). $KvLQT_1$ mRNA expression has been identified in the adult rat heart (Takimoto *et al.*, 1997), while minK mRNA expression has been reported in the neonatal rat heart (Folander *et al.*, 1990) but is not detectable in the adult rat atria and ventricles (Dixon & McKinnon, 1994). In contrast, minK mRNA has been detected in adult mouse and human heart (Swanson *et al.*, 1991; Lesage *et al.*, 1992), and an appreciable developmental decrease in the mouse has been reported (Felipe *et al.*, 1994).

1.4. Relationship Between Cloned K^+ α-Subunits and Myocardial K^+ Currents

1.4.1. Kv4.2, Kv4.3, and Kv1.4: I_{to}

Three of the voltage-gated K^+ channels α-subunits cloned from the heart produce Ca^{2+}-independent 4-AP-sensitive, rapidly activating and inactivating voltage-gated currents that resemble the I_{to} currents expressed in native cardiac cells. The candidate K^+ channel α-subunits include Kv1.4 (Tseng-Crank *et al.*, 1990; Roberds & Tamkun, 1991; Tamkun *et al.*, 1991; Po *et al.*, 1992), Kv4.2 (Blair *et al.*, 1991; Roberds & Tamkun, 1991), and Kv4.3 (Dixon *et al.*, 1996).

Kv1.4 was the first K^+ channel cloned that generated K^+ currents that resemble cardiac I_{to}, however, these channels display very slow recovery from inactivation when compared to native channels (Tseng-Crank *et al.*, 1990, Po *et al.*, 1992; Peterson & Nerbonne, 1999). Subsequently, K^+ channel α-subunits of Kv4 subfamily have become the more likely candidates generating the predominant cardiac I_{to}. Kv4.2 recovers from inactivation much faster than Kv1.4 (Yeola & Synders, 1997), and the mRNA and protein levels of Kv4.2 in rat heart are much more abundant than Kv1.4 (Dixon & McKinnon, 1994; Barry *et al.*, 1995; Xu *et al.*, 1996). Furthermore, a gradient of Kv4.2 mRNA expression exists across the ventricular wall that resembles the pattern of I_{to} current expression from endocardium

to epicardium (Fedida & Giles, 1991; Roberds & Tamkun, 1991; Clark *et al.*, 1993; Dixon & McKinnon, 1994). Kv4.3 has also been found to have biophysical and pharmacological properties that are similar to the native I_{to}, suggesting that it to underlies a fraction of the I_{to} current in some species (Dixon *et al.*, 1996; Fiset *et al.*, 1997a; Shimoni *et al.*, 1997; Kaab *et al.*, 1999). As well, using antisense oligonucleotides Fiset *et al.* (1997a) have clearly shown that Kv4.2 and Kv4.3 are essential components of I_{to} in rat ventricular myocytes.

The roles of Kv4 and Kv1.4 channels in generating I_{to} in the heart have also been investigated using transgenic mice. Barry *et al.* (1998) generated a pore mutant of Kv4.2 (Kv4.2W362F) that also functions as a dominant negative construct. Expression of Kv4.2W362F in transgenic mice results in the functional knockout of I_{to} (Barry *et al.*, 1998). London *et al.* (1998a) engineered mice lacking a functional copy of the Kv1.4 gene. These Kv1.4$^{-/-}$ transgenic mice were found to have normal cardiac action potentials with no significant change in I_{to} recorded from adult ventricular myocytes (London *et al.* 1998a). Overall, the evidence suggests that members of the Kv4 subfamily underlie I_{to} in rat and mouse heart.

More slowly inactivating I_{to} currents have recently been identified in cardiac myocytes from several species (Brahmajothi *et al.*, 1999; Wickenden *et al.*, 1999; Xu *et al.*, 1999). Slow I_{to} currents have been recorded from endocardial myocytes of the ferret left ventricle (Brahmajothi *et al.*, 1999) and the septum and right free wall of the rat ventricle (Wickenden *et al.*, 1999). In the adult mouse heart, a distinct distribution pattern of fast and slow I_{to} currents ($I_{to,f}$ and $I_{to,s}$) has also been reported (Xu *et al.*, 1999). 80% of septum myocytes express both $I_{to,f}$ and $I_{to,s}$ and the remaining 20% of septum myocytes only express $I_{to,s}$ (Xu *et al.*, 1999). The proposed molecular correlate for the slowly inactivating I_{to} currents is Kv1.4 and not Kv4 α-subunits. Firstly, Kv1.4 channels are known to generate more slowly decaying transient K^+ currents (Tseng-Crank *et al.*, 1990; Peterson & Nerbonne, 1999). Secondly, regional differences in the expression of

Kv4.2/4.3 and Kv1.4 transcripts have been reported. For example, in the ferret left ventricle Kv1.4 transcripts are prominent in the endocardium, which supports Kv1.4 in underlying the slow I_{to} recorded in these cells (Brahmajothi *et al.*, 1998). Furthermore, in rat ventricle Kv1.4 mRNA and protein expression has been found to correlate well with the expression pattern of the slowly recovering I_{to} (Wickenden *et al.*, 1999). Lastly, Barry *et al.* (1998) have reported the upregulation of a more slowly inactivating I_{to} current in the ventricular myocytes of Kv4.2W362F transgenic mice in which the Kv4 α-subunits have been selectively eliminated by genetic knock-out. From the above, it seems likely that Kv1.4 and not Kv4 α-subunits underlie the slow I_{to} currents however, additional experiments are still required to further support this hypothesis.

1.4.2. Kv1.5 and Kv1.2: I_{sus}

Of the cloned channels, the isoforms which are candidates for the K^+ current classified as the rapidly activating slowly inactivating outward K^+ current, I_{sus}, include Kv1.2 and Kv1.5 (Paulmichl *et al.*, 1991; Roberds & Tamkun, 1991; Fiset *et al.*, 1997b). The kinetics of these two channels have been found to be nearly indistinguishable, however, there is a major pharmacological difference between Kv1.2 and Kv1.5 in their sensitivity to α-dendrotoxin (α-DTX). Kv1.5 is relatively insensitive to α-DTX (>1μM), while Kv1.2 is highly sensitive (0.4nM) (Snyders *et al.*, 1993; Wang *et al.*, 1993; Grissmer *et al.*, 1994). The native I_{sus} currents seen in human atria and mouse ventricle are not sensitive to DTX, which favours Kv1.5 as the corresponding K^+ channel isoform (Wang *et al.*, 1993; Xu *et al.*, 1999). As well, Kv1.5 is highly sensitive to 4-AP (165-270μM), like the native currents, while Kv1.2 is less sensitive (590μM) (Grissmer *et al.*, 1994).

The use of molecular biology techniques has provided further evidence that Kv1.5 channels underlie I_{sus} currents in the heart. Using antisense oligodeoxynucleotides directed against Kv1.5 mRNA, Feng *et al* (1997) found that the I_{sus}-like current in adult human atrial myocytes was specifically inhibited. Furthermore, London *et al.* (1998b)

have recently characterized transgenic mice expressing a truncated Kv1.1 α-subunit that co-assembles with Kv1.5 α-subunits, such that no Kv1.5 channel proteins are expressed at the cell surface. The functional consequence of blocked Kv1.5 channel expression resulted in inhibition of an I_{sus}-type current in the ventricular myocytes of these mice (London *et al.*, 1998b).

1.4.3. $KvLQT_1$ and minK: I_{Ks}

Heterologous expression of $KvLQT_1$ in Xenopus oocytes reveals voltage-gated K^+-selective currents that are small, activate rapidly and display little or no inactivation (Barhanin *et al.*, 1996; Sanguinetti *et al.*, 1997). However, coexpression of $KvLQT_1$ with minK produces a very slowly activating K^+ current very similar to I_{Ks} (Barhanin *et al.*, 1996; Sanguinetti *et al.*, 1997). Direct biochemical evidence for coassembly of $KvLQT_1$ and minK in the mammalian heart, has not been provided to date (Nerbonne, 1998), however, in the inner ear it has been shown that the cytoplasmic end of minK interacts directly with the pore region of $KvLQT_1$ creating a very slowly activating K^+ current (Romey *et al.*, 1997).

Genetic studies have shown that mutations in either the $KvLQT_1$ (Wang *et al.*, 1998) or the minK (Splaski *et al.*, 1997) genes are implicated in the Jervelle and Lange-Nielsen syndrome (JLN, a congenital long QT syndrome). I_{Ks} is strongly downregulated or abolished in the ventricular myocytes of patients with JLN, which supports the hypothesis that $KvLQT_1$ and minK are both required to form the functional I_{Ks} current (Drici *et al.*, 1998). The importance of minK in generating I_{Ks} has been further supported by the generation of minK null mutant mice with a targeted disruption of the minK gene (Drici *et al.*, 1998; Kupershmidt *et al.*, 1999). The heart cells from these animals have no detectable I_{Ks}, which further supports the role for minK in modulating this current (Drici *et al.*, 1998; Kupershmidt *et al.*, 1999).

1.5. Regulation of K^+ Channel Expression in the Heart : Thyroid Hormone

It has been demonstrated that the cardiac action potential shortens during postnatal development (Wetzel & Klitzner, 1996) and it has been postulated that an increase in the density of the repolarizing K^+ currents is partly responsible for this phenomena (Xu *et al.*, 1996; Shimoni *et al.*, 1997; Wickenden *et al.*, 1997; Nerbonne, 1998). Subsequently, increased expression of several K^+ channel α-subunits (mRNA and protein) has been described (Xu *et al.*, 1996; Wickenden *et al.*, 1997). However, the molecular mechanisms mediating changes in the functional expression of K^+ channel α-subunits during cardiac development are not fully understood (Nerbonne, 1998). Understanding the molecular basis of the cardiac action potential during development and identifying the factors that can regulate these events is of interest since re-expression of a neonatal genetic programme is a common feature of cardiac hypertrophy and failure (Lompre *et al.*, 1979; Schwartz *et al.*, 1986).

It has been hypothesized that thyroid hormone may be one of the factors controlling the changes in K^+ channel α-subunit expression during normal cardiac development (Shimoni *et al.*, 1997; Wickenden *et al.*, 1997). K^+ channel genes are known to be under dynamic control by a variety of physiological and pathological stimuli (Levitan & Takimoto, 1998). For example, glucocorticoids have been shown to induce Kv1.5 gene transcription thereby increasing mRNA levels in a variety of tissues (Takimoto & Levitan, 1994; Levitan *et al.*, 1996).

The serum levels of the thyroid hormone(s) (T_3, 3,3'5-triiodo-L-thyoinine and T_4, thyroxine) increase postnatally, with early neonates being strongly hypothyroid due to a poorly developed hypothalamic pituitary-thyroid axis (Vigouroux, 1976; Dubois & Dussault, 1977). This thyroid hormone surge is believed to play a role in several important developmental events in the heart such as, the postnatal isoform switching of the myosin heavy chain genes (Gustafson *et al.*, 1987), the Na^+,K^+-ATPase genes (Kamitani *et al.*, 1992), and the protein kinase C genes (Rybin & Steinberg, 1996).

Thyroid hormone has been shown to exert effects on cardiac K^+ channel/current expression (Shimoni *et al.*, 1992; 1995; 1997; Wickenden *et al.*, 1997). For example T_3 was found to upregulate Kv4.2 and Kv4.3 mRNAs in the rat ventricle which corresponds to the increases in I_{to} current density also reported (Levitan & Takimolo, 1998; Shimoni *et al.*, 1997). Abe *et al.* (1998) also reported that Kv1.2 mRNA levels were suppressed in rats made hyperthyroid by hormone injection and enhanced in rats made hypothyroid by propylthyouracil (PTU, a thyroid hormone synthesis inhibitor) treatment. As well, Kv1.5 mRNA expression was downregulated, while Kv1.4 mRNA expression was upregulated in hypothyroid animals (Abe *et al.*, 1998).

1.6. RNase Protection Assay

Dixon & McKinnon (1993), Dixon *et al.* (1996) Shimoni *et al.* (1997) and Wickenden *et al.* (1997) have studied K^+ channel α-subunit mRNA levels in rat and canine heart using the RNase protection assay. Identification of RNA levels with RNase is extremely sensitive, approximately 20-fold greater than is attainable with double-stranded DNA probes or end-labelled single-stranded DNA probes (Krieg & Melton, 1987). As well, the digestion of RNA:RNA hybrids with RNase creates fewer artifacts than digestion of RNA:DNA hybrids with nuclease S1 (Krieg & Melton, 1987). The RPA technique has therefore become the standard method to quantitate mRNA molecules due to its simplicity, flexibility, and superior sensitivity (Krieg & Melton, 1987).

It must be remembered, however, that the presence of mRNA does not guarantee the presence of the encoded protein. mRNA mapping only provides information on the cell specificity of K^+ channel gene expression (Deal *et al.*, 1996). Other techniques that employ isoform-specific antibodies and transgenic knock-out strategies should also be used to complement the preliminary information gained at the mRNA level. In combination these techniques can be used to demonstrate direct sarcolemma/cellular

expression of the gene products, which is required to more confidently define the functional roles of genes.

1.7. Project Objectives

The primary goal of this project is to identify and quantify K^+ channel α-subunit mRNAs present in mouse ventricular tissue throughout development by means of the RPA. The K^+ channels selected for study include: Kv1.5, which is thought to be responsible for I_{sus}; Kv1.2, another less likely candidate for I_{sus} in the mouse ventricle; Kv1.4, Kv4.2, and Kv4.3, which are candidates for I_{to} in mouse heart; $KvLQT_1$ and minK, which are thought to underlie I_{Ks}; and IRK1, which generates the cardiac inward rectifier (I_{K1}). The information obtained in these molecular studies complement detailed electrophysiological work being performed in parallel in mouse ventricular myocytes in our laboratory.

Specifically, the message level (mRNA level) of the eight K^+ channels mentioned above were investigated in 0-1 day, 10 day, 21 day, and adult (>6 weeks) mouse ventricle total RNA samples. As well, the effect of thyroid hormone levels on the K^+ channel mRNA expression were studied, using ventricles from mice raised on a hypothyroid diet, and by culturing isolated myocytes in the presence of thyroid hormone. Causal relationships between the changes seen during development and with hypo- and hyperthyroid treatments were then examined.

2. METHODS

The mRNA expression levels of Kv1.2, Kv1.4, Kv1.5, Kv4.2, Kv4.3, $KvLQT_1$, minK and IRK1 K^+ channel α-subunits in mouse ventricular tissues and cells were determined using the RNase protection assay technique. RPAs were designed such that two K^+ channel isoforms could be quantified simultaneously in a single total RNA sample. An internal control probe was also included in RPA reactions to confirm that samples were not lost or degraded and to standardize sample loading. Methods required to set-up and run the multiple target RPA experiments, include: isolation of total RNA samples from ventricular tissues and cells, synthesis of channel-specific cDNA fragments, and generation of radioactive RNA probes (riboprobes).

2.1. Mouse Ventricular Total RNA Samples

2.1.1. Whole ventricular muscle

Whole ventricular muscle samples were isolated from 0-1 day, 10 day, 21 day, and young adult (approximately 6-9 weeks) CD-1 mice (Charles River) as well as adult control and hypothyroid C57b6 mice (the hypothyroid mice were a generous gift from Dr. W. Dillmann, San Diego, CA). The mice were made hypothyroid (T_3, levels below 20 ng/dl and T_4, levels below 0.5 μg/dl) by maintaining them on an iodine deficient rodent chow (Harlan Teklad) supplemented with 0.15% PTU for 4 weeks.

All 21 day and adult animals were anaesthetized by inhalation of methoxyflurane. After cervical dislocation, the hearts were excised and washed in Tyrode solution (10 mM HEPES, pH 7.4; 130 mM NaCl; 5.4 mM KCl; 1 mM $CaCl_2$; 1 mM $MgCl_2$; 5 mM glucose). Hearts were removed from the 0-1 day and 10 day pups immediately after decapitation. Only the lower ¾ of the ventricles were used to ensure no atrial or aortic tissue was present. Excised segments of ventricle were blotted on gauze to remove excess liquid and then immediately frozen in 50 ml Falcon tubes on dry ice.

2.1.2. Neonatal mouse ventricular cells

2.1.2.1. Cell isolation and digestion solutions

Solution A (isolation solution): Minimal essential medium (S-MEM) supplemented with 24 mM $NaHCO_3$, 1 mM DL-carnitine, 0.6 mM $MgSO_4 \cdot 7H_2O$; pH 7.4

Solution B (enzyme digestion solution): Solution A with 1% bovine serum albumin, 20 mM taurine, and 0.23 mg/ml collagenase (Yakult).

Solution C (plain media): DMEM-HAM F12 (1:1) with 26 mM $NaCO_3$; pH 7.4

Solution D (complete media): Solution C supplemented with 5% fetal bovine serum (Hyclone), 1 μg/ml bovine insulin, 1% PEN/STREP (Penicillin G: 10000 units/ml and Streptomycin: 10 mg/mL).

Solution E (neutralization solution): Solution D with added fetal bovine serum to 10%.

Solution F (serum-free media): Solution C supplemented with 1 nM LiCl, 25 μg/ml ascorbic acid, 5 μg/ml bovine apotransferrin, 1 μg/ml bovine insulin, 1 nM Na_2SeO_4 and 1% PEN/STREP.

2.1.2.2. Myocyte and fibroblast isolation and short-term culture

Two litters of 0-1 day-old CD-1 mouse pups (between 16-30 pups; Charles River) were pooled for preparation of each batch of ventricular myocytes. Pups were killed by decapitation and the hearts were quickly removed aseptically, and placed into a petri dish containing Solution A (all solutions were filter sterilized prior to use with Whatman disk filters or Nalgene bottle filters). Using aseptic technique, the atria and major blood vessels were removed and the ventricles were placed into a new petri dish containing fresh Solution A. Once all of the ventricles had been collected, they were rinsed again to remove residual blood, and then transferred to a petri dish containing 2 ml of Solution B. The ventricles were then minced using scissors, and transferred to a small sterile beaker (10 ml). The first aliquot of Solution B was subsequently discarded and replaced. The minced heart tissue was stirred with a small stir bar in a dry 37°C block heater (Fisher Scientific) to disperse cells. The supernatant fractions, containing the cells, were collected every 5 minutes. The presence of isolated myocytes (small rounded cells) was

checked visually with an inverted microscope and the first 2-3 collections were discarded, as they contained mostly red blood cells and debris (damaged myocytes). Thereafter, all of the other freed-cell fractions (approximately 10-12 collections) were collected and placed in solution E to neutralize the collagenase.

When the cell dissociation was complete, the cell suspension was filtered through a 150 μm mesh filter and then centrifuged for 5 minutes at 600 x *g*. The pelleted cells were re-suspended with 10 ml of Solution C and plated on a 100 mm plastic petri dish and incubated at 37°C in a 95% O_2-5% CO_2 humidified atmosphere for 20 minutes. This step was used to selectively remove non-myocytes (primarily fibroblasts) based on differential adhesive strength. Fibroblasts stick to the plastic plate and myocytes remain unattached in suspension (Hyde *et al.*, 1969). The myocyte-rich supernatant was transferred to a 50 ml tube and the volume was increased to 30 ml with Solution F. Several of the plastic petri dishes, with attached fibroblasts, were re-fed with Solution F and returned to the incubator.

The myocyte-rich fraction was centrifuged for 5 minutes at 600 x *g* and subsequently re-suspended in 12 ml of Solution F with or without 100 nM T_3 added to it, and either plated on 100 mm glass petri dishes or transferred to 15 ml conical culture tubes. The samples were returned to the 37°C incubator for 18-24 hours. The myocytes plated on the 100 mm glass dishes were referred to as low-density, plate cultures. The myocytes cultured in suspension in 15 ml conical tubes settled by gravity forming pellet and were thus referred to as high-density or pellet cultured myocytes (Hershman & Levitan, 1998). The fibroblast plates were grown for 3 days, washed with serum-free media to remove loosely attached cells, and then incubated for an additional day.

2.1.3. Total RNA isolation

TRIzol® Reagent (GibcoBRL) was used to isolate total RNA from all ventricular samples according to the manufacturers' protocol. Whole ventricle total RNA samples were

produced from pooled ventricles from the hearts of 4-20 animals, depending on age. 1 ml of TRIzol® Reagent, per 50-100 mg of tissue, was added directly to the 50 ml Falcon tubes in which the pooled ventricular samples had been frozen. To obtain total RNA from the isolated ventricular cells (myocytes and fibroblasts), 4 ml of TRIzol® Reagent was added directly to their 100 mm petri dishes after the culture media had been carefully discarded. A rubber policeman was used to aid in the thorough lysing and collection of these cells. The solution was then transferred to a 15 ml conical tube. The myocytes cultured directly in 15 ml conical tubes were briefly centrifuged (600 x *g*) to collect the cells and then the media was discarded and replaced with 4 ml of TRIzol® Reagent.

Immediately after TRIzol® Reagent addition (and transfer to a conical tube if required) samples were homogenized with a Tekmar TISSUMIZER® for approximately 30 to 60 seconds to thoroughly lyse the cells and shear the DNA. 0.2 ml of 100% chloroform per 1 ml of TRIzol® Reagent was then added and the samples were centrifuged at 12,000 x *g* for 15 minutes to promote phase separation. The aqueous phase, which contains the extracted RNA, was then collected. The RNA was subsequently precipitated overnight with an equal volume of isopropanol at -20°C. To pellet the precipitated RNA, the samples were centrifuged at 10,000 x *g* for 20 minutes at 4°C. The RNA pellet was then re-dissolved in 50 to 200 µl of diethylpyrocarbonate (DEPC) treated water (Research Genetics). To ensure the samples were free of DNA contamination 1-4 units of RNase-free RQ1 DNase (1 U/µl Promega) and the appropriate amount of buffer (NEB 3 restriction buffer: 50 mM Tris-HCl, pH 7.9; 10 mM $MgCl_2$; 100 mM NaCl; 1 mM dithiothreitol, DTT, New England Biolabs) were added. The reaction was then incubated at 37°C for 30 minutes. The DNased total RNA samples were subsequently purified using RNeasy® spin columns (Qiagen®) following the manufacturer's protocol.

The purity and concentration of the total RNA samples were determined by spectophotometric analysis using a Beckman DU® 640 spectrophotometer. Total RNA samples were said to be pure and thus relatively free of protein contamination if the

absorbance, $A_{260/280}$, ratios were greater than 1.8 (DU® 600 series instruction manual, Beckman). The integrity and concentration of the total RNA were then confirmed by agarose gel electrophoresis. Briefly, 1 μg of total RNA was run on a 1% agarose gel in TAE buffer (100 mM Tris acetate (pH 8.0), 1 mM EDTA with 0.5 μg/ml ethidium bromide) at 250 V for approximately 30 minutes. When irradiated with an ultraviolet light source the ethidium bromide bound to the nucleotides emits fluorescence that can be visualized (Maniatis *et al.*, 1982). Photographs of gels were made using transmitted UV light and a Polariod DS-34 Camera with Type 667 high-speed film (ISO 3000).

2.2. Preparation of Template DNA for Riboprobe Synthesis

Riboprobes used in RPAs are routinely produced by *in vitro* transcription using plasmid DNA templates. The riboprobes are synthesized with an RNA polymerase by run-off transcription, thus the plasmid DNA must be linearized with a restriction enzyme downstream of the insert to be transcribed. Riboprobes must be synthesized in the antisense orientation in order to detect mRNA from a total RNA sample. The total size of the riboprobes equals the vector sequence between the RNA polymerase promoter and the beginning of the insert, plus the length of the insert itself, plus the vector sequence between the end of the insert and the linearization site.

In this project, we used the pBluescript® II SK- phagmid (Stratagene, see Appendix I for sequence and restriction map) as a plasmid vector with the T7 RNA polymerase. Isoform-specific K^+ channel cDNA fragments that contained restriction sites on their 5' and 3' ends were synthesized and then inserted in the polylinker of pBluescript® II in the antisense orientation downstream of the T7 RNA polymerase promoter. The methods used to construct the DNA templates used are outlined in the following subsections.

2.2.1. K^+ channel isoform-specific DNA fragments

cDNA fragments, specific to the eight K^+ channel α-subunits studied, were synthesized by reverse transcription followed by PCR (polymerase chain reaction) amplification,

using mouse ventricle cDNA as template. The materials necessary to synthesize cDNA fragments via PCR include: 1) template cDNA; 2) specific primers flanking the fragment; 3) the PCR reagents (GibcoBRL); and 4) a GeneAmp PCR System (2400/9700, Perkin Elmer) or equivalent (Maniatis *et al.*, 1982).

2.2.1.1. Template cDNA

Template mouse ventricle DNA, in the form of primary strand (or first-strand) cDNA, was obtained from poly(A)$^+$ RNA. Poly(A)$^+$ RNA was purified from stock samples of mouse ventricular total RNA (isolated using TRIzol® Reagent, as previously described) by affinity chromatography using oligo(dT)-cellulose spin columns (polyA Spin™ mRNA Isolation Kit, New England Biolabs). First-strand cDNA was subsequently synthesized from the poly(A$^+$) RNA using Superscript™ II Reverse Transcriptase according to the manufacturers' protocol (GibcoBRL). Briefly, oligo $(dT)_{12-18}$ primers (500 μg/ml, Pharmacia Biotech) or random hexanucleotide primers (50-250 ng, University of Calgary DNA synthesis laboratory) were added to 1-5 μg of poly(A$^+$) RNA. The reaction was heated for 10 minutes at 70°C and quickly chilled on ice to allow the primers to anneal to the RNA. 5X First Strand Buffer (GibcoBRL), 0.1 M DTT (GibcoBRL), 0.5 mM dNTP mix (Pharmacia Biotech), 3.77 units of RNAGuard® RNase inhibitor (Pharmacia Biotech) and 80 units of Superscript™ II Reverse Transcriptase (GibcoBRL) were added to the primer annealed RNA. The reaction was incubated at 42°C for 1 hour, inactivated by heating at 70°C for 15 minutes and the resulting first-strand cDNA was analyzed by agarose gel electrophoresis. The cDNA was purified using QIAquick™ spin columns (Qiagen®) following the manufacturer's protocol.

2.2.1.2. Oligonucleotide PCR primers

In designing the oligonucleotide primers required to amplify the eight K^+ channel cDNA fragments, several important aspects were considered. 1) The sequence flanked by the primers needed to be isoform-specific and not have long uninterrupted regions complementary to any transcripts other than the one being tested. 2) The size of the

amplified cDNA fragment must be carefully determined since they define the size of the protected fragments in the multi-probe RPAs. 3) Restriction sites must be added to the ends of the primers to allow ligation of the fragments with pBluescript® II SK- (Stratagene) in the correct antisense orientation.

Complete mouse heart cDNA sequences for Kv1.5, IRK1, $KvLQT_1$, minK, Kv1.4 and Kv1.2 and rat heart cDNA sequences for Kv4.2 and Kv4.3 (see Figure 2.1 for GenBank Accession numbers and references) were found in the GenBank database using the Basic Local Alignment Search Tool (BLAST, Altschul *et al.*, 1990) and the WWWEntrez browser on the National Center for Biotechnology Information (NCBI) Internet server (http://www.ncbi.nlm.nih.gov). The nucleotide sequences of each channel were analyzed using GeneRunner© (Version 3.04; Hastings Software Inc.) and the Clustal W1.7 alignment tool (Thompson *et al.*, 1994; http://kiwi.imgen.bcm.tmc.edu:8088/search-launcher) was used to make multiple sequence alignments.

The multiple sequence alignments indicated that the 5' and 3' ends of the K^+ channel cDNAs have the lowest amount of homology between channels. Thus nucleotide sequences (100 to 200 nucleotides in length) from these regions were considered for making the riboprobes. Each potential sequence was entered into the BLAST search engine to ensure that the target fragments were not complementary to any unexpected sequences found in GenBank.

Once a sequence was confirmed to be unique, forward and reverse oligonucleotide primers were constructed containing approximately 16 to 20 nucleotides of each end of the target sequence (Figure 2.1 shows the forward and reverse primer sequences). Additional restriction sites were added to the 5' ends (shown in lower case in Figure 2.1) of the primers, such that the cDNA fragments created contained convenient restriction sites on both ends (either BamH I/Kpn I or BamH I/EcoR I). The primers were produced using a Beckman Oligo1000® DNA Synthesizer and accompanying reagents.

Figure 2.1. Synthetic oligonucleotide primers used to amplify cDNA fragments by PCR for synthesis of K^+ channel α-subunit riboprobes for RPAs. Oligonucleotide primers were synthesized using a Beckman Oligo1000® DNA Synthesizer and accompanying reagents. For each template, the forward and reverse primers that were synthesized are shown. The reference nucleotide sequence is given in brackets corresponding to the GenBank sequences. (Primer sequence given in lowercase represents the added restriction site plus additional bases 5' to the cut-site required by the restriction enzymes to properly recognize and cut the fragments close to the end of the molecules.)

Synthetic Oligonucleotide Primers: K^+ Channels

IRK_1- sequence: 106bp (nucleotides 1 to 106, GenBank Acs.#AF021136; Rae & Shepard, 1997)

primers: forward- 5' gcgggatccATGGGCAGTGTGAGAA
reverse- 5' cgcggtaccTACTCTTGCCATTCCC

Kv1.5- sequence: 181bp (nucleotides 298 to 478, GenBank Acs.#L22218; Attali *et al.*, 1993)

primers: forward- 5' gcgggatccATGGAGATCTCCCTGG
reverse- 5' gcggaattcCCGCATCCTCGTGTGT

Kv4.2- sequence: 181bp (nucleotides 233-413, GenBank Acs.#M59980; Roberds & Tamkun, 1991)

primers: forward- 5' gcgggatccATGGCAGCCGGTGTTG
reverse- 5' gcggaattcGTTCCAGGGTGTCTTG

Kv4.3- sequence: 111bp (nucleotides 21-131, GenBank Acs.#U75448; Dixon *et al.*, 1996)

primers: forward- 5' gcgggatccATGGCGGCAGGAGTTG
reverse- 5' cgcggtaccCCGCTTGTTCTTGTCGG

$KvLQT_1$- sequence: 170bp (nucleotides 991 to 1160, GenBank Acs.#U70068; Barhanin *et al.*, 1996)

primers: forward- 5' gcgggatccGAAGCACTTCAACCGG
reverse- 5' cgcggtaccCCATGACAGACTTTTTAGG

minK- sequence: 106bp (nucleotides 79 to 184, GenBank Acs.#X60457; Honore *et al.*, 1991)

primers: forward- 5' gcgggatccATGAGCCTGCCCAATT
reverse- 5' cgcggtaccGCTGAGACTTACGAGC

Kv1.4- sequence: 178bp (nucleotides 2615 to 2794, GenBank Acs.#U03723; Wymore *et al.*, 1994)

primers: forward- 5' cagggatccTGAAAATGAAGAACAGACC
reverse- 5' cccggtaCCCTGACACTTCTCCTCCT

Kv1.2- sequence: 106bp (nucleotides 2428 to 2540, GenBank Acs.#M30440; Chandy *et al.*, 1990)

primers: forward- 5' cccgGATCCCGTCCTCCCCTGACC
reverse- 5' gggggtaCCTCTCTAAAGTCCTCATTG

Specific primers were also designed for the amplification of mouse β-actin, calsequestrin, glyceraldehyde-3-phosphate dehydrogenase (GAPDH), and ribosomal subunit 18s cDNA fragments (Figure 2.2). These transcripts were used to make internal control riboprobes for the RPAs.

2.2.1.3. PCR amplification

The PCR amplification reactions used to make the K^+ channel cDNA fragments contained 50 ng of template mouse ventricle cDNA, 200 μM of each of the 4 dNTPs (dATP, dCTP, dGTP, dTTP), 2 mM $MgCl_2$, 10X PCR buffer (500 mM KCl and 200 mM Tris-HCL, pH 8.4), 0.5 μM sense and antisense primers and 0.25 units *Taq* DNA polymerase. The standard thermal cycler PCR amplification program began with an initial 5 minute incubation at 94°C to denature template DNA and then included 35 cycles of a 30 second denaturing step at 94°C, a 30 second annealing step at 62°C, and a 45 second primer extension at 72°C. A final 7 minute incubation, at 72 °C, was used to ensure products were full length.

The cDNA fragments generated were visualized by agarose gel electrophoresis, and subsequently isolated as gel slices and purified using the QIAquick™ Gel Extraction Kit (Qiagen®) following the manufacturers' protocol. The PCR-products were then sequenced using the Thermo Sequenase™ Kit (Radiolabeled terminator cycle sequencing kit, Amersham Life Sciences) according to manufacturers' protocols to ensure the cDNA fragment generated corresponded to the expected sequence from which they were based.

2.2.2. Subcloning cDNA fragments into a plasmid vector

In preparation for subcloning the cDNA fragments into pBluescript® II SK- (Stratagene), the fragments were digested for 2 to 4 hours at 37°C with restriction endonucleases that corresponded to the restriction sites on their 5' and 3' ends (either BamH I/Kpn I or BamH I/EcoR I). The digested fragments were then purified using QIAquick™ spin columns (Qiagen®). pBluescript® II SK- vector was also restriction digested with either

Figure 2.2. Synthetic oligonucleotide primers used to amplify cDNA fragments by PCR for synthesis of internal control riboprobes for RPAs. Oligonucleotide primers were synthesized using a Beckman Oligo1000® DNA Synthesizer and accompanying reagents. For each template, the forward and reverse primers that were synthesized are shown. The reference nucleotide sequence is given in brackets corresponding to the GenBank sequences. (Primer sequence given in lowercase represents the added restriction site plus additional bases 5' to the cut-site required by the restriction enzymes to properly recognize and cut the fragments close to the end of the molecules.)

Synthetic Oligonucleotide Primers: Internal Controls

β-**actin**- sequence: 71bp (nucleotides 919 to 989, GenBank Acs.#X03672; Tokunaga *et al.*, 1986)

primers: forward- 5' gcggaattcAGCTCGGTACCACCAGACAGC

reverse- 5' gcgggatccATTCCATCATGAAGTGT

GAPDH - sequence: 69bp (nucleotides 47 to 115; GenBank Acs.#M32599; Sabath *et al.*, 1990)

primers: forward- 5'gcggatccATGGTGAAGGTCGGTGTG

reverse- 5' cgcggtaccACTGCAAATGGCAGCCCTG

Calsequestrin - sequence: 70bp (nucleotides 130 to 200: GenBank Acs.#AF068244; Sato *et al.*, 1998)

primers: forward- 5'gcggaattcATGAAGAGGATTTA

reverse- 5' gcgggatccTCAGCCCCTCTTCT

18s rRNA- sequence: 70bp (nucleotides 601-970: GenBank Acs.#X00686; Raynal *et al.*, 1984)

primers: forward- 5'gcgggaattccGGGCAAGTCTGGTG

reverse- 5' cgcggtaccTTACTGCAGCAAC

BamH I/Kpn I or BamH I/EcoR I, dephosphorylated with calf intestinal alkaline phosphatase (GibcoBRL), and purified using QIAquick™ spin columns (Qiagen®). The Rapid DNA Ligation Kit (Boehringer Mannheim) was then used to ligate the complementary 'sticky ends' of the cDNA fragments and the plasmid vector according to manufacturers' protocols.

Once the ligation reaction was complete the new recombinant plasmids were replicated using a competent bacteria strain. Subcloning Efficiency DH5α™ Competent Cells were used for the transformation reaction according to the manufactures' protocol (GibcoBRL). Aliquots of the transformation reaction were subsequently spread on LB plates containing 100 μg/ml of ampicillin. After an overnight incubation at 37°C, colonies formed and several of these colonies were picked with wooden sticks, spotted on a fresh LB/Amp plate, and then diluted in sterile H_2O (GibcoBRL). These aliquots were heated at 94°C for 20 minutes, and a portion (4 μl) was then used as template in PCR reactions (using T3/T7 primers). 4 μl of the PCR reactions, which would have amplified cDNA fragments inserted into the pBluescript® II SK- polylinker, were then analyzed by agarose gel electrophoresis to determine if an insert of the correct size was present (See Appendix I for DNA ladders used on agarose gels). Positive recombinant clones were grown overnight in 20 to 50 ml of LB and then minipreped using a QIAprep™ Spin Plasmid kit (Qiagen®) to obtain pure plasmid DNA samples that are free of contaminating bacterial proteins and RNA.

2.3. Synthesis of Riboprobes

Plasmid DNA (which contained one of the K^+ channel α-subunit or internal control cDNA fragments) was used as the template to transcribe radioactive antisense RNA probes (riboprobes). Prior to transcription, the plasmids were linearized using a restriction site (XbaI, NotI or BamH I) in the pBluescript® II SK- polylinker that was downstream of the insert. The plasmid restriction digest and subsequent purification were done as before.

The transcription reactions were carried out using the MAXIscript™ In Vitro Transcription Kit (Ambion) according to manufacturers' protocols. Briefly, the plasmid DNA template was incubated for 30 to 60 minutes with unlabelled and labeled dNTPs and 10 units of the T7 RNA Polymerase Ribonuclease inhibitor mix. [α-^{32}P] labeled UTP (400-800 Ci/mmol, 10 mCi/ml; ICN, NCN, or Amersham Life Sciences) was used at a concentration of > 3 μM for synthesizing all of the RNA probes. Unlabelled 'cold' dUTP was only included in the transcription reaction if the transcript being made was highly abundant to decrease the specific activity of the probe (9-20 μM dUTP was added for the synthesis of GAPDH and the other internal controls). After the transcription reaction was complete the DNA template was removed by incubating the samples for 30 minutes at 37°C with 4 units of RNase-free DNase I (Ambion).

The riboprobes were gel isolated prior to use. Briefly, Gel Loading Buffer II (95% formamide/0.025% xylene cyanol/0.025% bromophenol blue /0.5mM EDTA/0.025% SDS) was added directly to the DNased samples. The samples were then electrophoresed on 1.5 mm thick 6% polyacrylamide 8 M urea denaturing gel. Gels were run at 200 volts in Mini-Protean II Electrophoresis Cells (Bio-Rad) filled with TBE buffer (100mM Tris, 20mM boric acid, 1 mM EDTA, pH 8.3) until the bromophenol blue band approached the bottom of the gel (approximately 30 minutes). The gel was carefully exposed to BioMax MS film (Kodak) for approximately 60 seconds to create an autoradiograph that could be aligned with the gel and enable localization of the radioactive transcription product. A gel slice containing the riboprobe was excised and incubated for 4-24 hours in elution buffer (0.5 M ammonium acetate, 1 mM EDTA, 0.1% SDS).

The amount of radiolabel incorporated into the probes was determined by scintillation counting of the eluate. Probes were used at 6 x 10^4 counts·min^{-1}, a concentration that was deemed sufficient by the manufacturer (Ambion) to be in molar excess of abundant messages (e.g. β-actin or GAPDH) in 10 μg total RNA.

2.4. RNase Protection Assays

RPAs were performed using three different RPA kits; Hybspeed™ RPA, RPAII™ or RPAIII™ Kits (Ambion; see Appendix II for explicit details of each protocol). For every RPA reaction 2.5 μg of mouse ventricular total RNA was probed with three antisense riboprobes (6 x 10^4 counts·min^{-1}), two channel riboprobes and one internal control riboprobe. The riboprobe pairs used for all assays were as follows Kv1.5/IRK1; Kv4.2/4Kv4.3; KvLQT1/minK and Kv1.4/Kv1.2.

After the riboprobes were added to tubes containing different sample RNAs, 100 μl of precipitation mix containing 50 μg of yeast tRNA and 0.5 M ammonium acetate was added, followed by the addition of 100% EtOH (2.5 volumes) to precipitate the RNAs. Two control tubes containing the same amount of the labeled probes (but no sample RNA) were also precipitated. The tubes were placed at -20°C for at least 15 minutes prior to pelleting the samples by centrifugation (> 10,000 x *g* for 15 minutes). The pellets were then resuspended in hybridization buffer and incubated under conditions that favor hybridization of complementary transcripts (hybridization times and temperatures varied between Kits, see Appendix II).

All of the tubes containing sample RNA and one of the control tubes were treated with an RNase A/RNase T1 mixture to degrade single-stranded, unhybridized probe. Hybridized probe is protected from ribonuclease digestion and will thus be detected on an RPA gel. No signal should be detected in the digested control tube since no sample RNA was added and thus no homologous sequences should be present. The sizes of the undigested full-length K^+ channel riboprobes and fully protected fragments were as follows (full-length/protected length): Kv1.5, 258/181 nucleotides (nt.); IRK1, 135/106 nt.; Kv4.2, 258/181 nt.; Kv4.3, 139/111 nt.; $KvLQT_1$, 199/170 nt.; minK, 135/106 nt.; Kv1.4, 218/178 nt.; and Kv1.2, 135/106nt. The internal control band sizes were β-actin, 112/71 nt.; GAPDH, 86/69 nt.; calsequestrin 99/70 nt.; and 18s rRNA, 99/70 nt..

RNase digestion was carried out for 30 minutes at 37°C after which the inactivation/ precipitation solution was added and the samples were incubated for 15 minutes at -20°C. The samples were pelleted by centrifugation and resuspended in Gel Loading Buffer II (Ambion). Several 10-well 1-mm thick 8% denaturing polyacrylamide Mini-Protean II gels (Bio-Rad) were prepared in advance depending on the number of sample RNAs. Prior to loading, the samples were incubated 3 minutes at 90-95°C to denature the RNA.

RPA gels were run in Mini-Protean II Electrophoresis Cells (Bio-Rad) at 200 volts in TBE buffer until the xylene cyanol FF marker dye approached the bottom of the gel (approximately 60 minutes). The gels were fixed for 30 minutes with 20% methanol, 5% acetic acid and placed on a piece of Whatman 3MM chromatography paper. The gels were vacuum dried with heating for 1-2 hours on a Slab Dryer (Bio-rad). Dried gels were exposed to BioMax MS film with a Transcreen HE intensifying screen (Kodak) at -70°C for several hours or several days depending on the specific activity of the samples.

2.5. Data Analysis

RPA results were quantified on a Molecular Dynamics Storm™ PhosphorImager™ system using ImageQuant® software (Molecular Dynamics). Briefly, RPA gels were exposed to storage phosphor screens for 3 days. The storage phosphor screen captures the image produced by β- and γ-emissions from the radioactive samples (Molecular Dynamics instruction manual). The PhosphorImager™ count values (arbitrary units of measure that describe the intensity of the photon emissions released from the screen during scanning) reported in ImageQuant® were used to quantify the RPA bands (Molecular Dynamics). All data analysis was done using Microsoft® Excel 97. The individual count values for channel riboprobes were normalized to the value of the internal control (expressed as % internal control), since there was a significant amount of variability between samples resulting from gel loading.

GAPDH was chosen as the internal control for all of the studies performed. However, the level of GAPDH mRNA was found to vary between experimental groups (e.g. hypothyroid diet samples had approximately 1.5 fold higher GAPDH mRNA than control). This affected the data significantly when expressed as % GAPDH since the group with the lower GAPDH levels would have artificially high values. Thus, a correction factor was required to compensate for these differences. By dividing the average GAPDH counts between groups, a correction factor was obtained. This correction factor was then used as a multiplier to normalize the discrepancies in GAPDH band densities between the study groups. The corrected GAPDH counts were then used to yield the % internal control values for the channels.

Corrections for differences in specific activity of the probes due to different numbers of UTP residues were also made, based on the assumption that the specific activity was directly proportional to the number of UTP residues in each sequence. The Kv 4.2 probe was arbitrarily chosen as the probe to which all others were normalized. The channel multipliers (# UTP Kv4.2 / # UTP channel) were as follows: Kv4.2 (1), Kv1.5 (0.87), Kv4.3 (2.05), Kv1.4 (0.67), Kv1.2 (1.05), IRK_1 (1.39), $KvLQT_1$ (0.95), and minK (2.05).

Two of the K^+ channel probes, IRK_1 and $KvLQT_1$, produced unexpected bands (doublets) in the RPAs. The more intense band was used for data analysis purposes in both cases.

2.6. Statistics

All data are expressed as mean±sem (n=3). One-way ANOVA with Tukey's post test was performed using GraphPad InStat version 3.01 for Windows 95 (GraphPad Software) to evaluate the means of the K^+ channel development data set (4 age groups). Unpaired t-tests (assuming equal variance) were used to determine the statistical significance of the variance between means for all other "two-group" comparisons (Microsoft® Excel 97). $P<0.05$ was considered statistically significant.

2.7. Materials

All standard chemicals and biochemicals were obtained from either VWR Canlab or Sigma Chemical Company. Restriction endonucleases were obtained from and used in buffers recommended by either New England BioLabs or GibcoBRL. Standard cell culture media (DMEM-HAMF12, S-MEM) and supplements were from either GibcoBRL or Sigma Chemical Company. All glassware used with RNA samples was treated with RNase Away™ (GibcoBRL), which removes RNase and DNA contamination. Glassware and instruments used for cell culture were sterilized by autoclaving. All plasticware (microfuge tubes, disposable pipette tips) was either pre-sterilized (by the manufacturer) or was sterilized by autoclaving. For work with RNA, the plasticware was pre-sterilized, siliconized and guaranteed to be free of RNase and DNase contamination by the manufacturer (DiaMed Lab Supplies Inc. or VWR Canlab).

3. RESULTS

The levels of selected K^+ channel α-subunit gene expression in mouse ventricle were measured using RNase protection assays. Measurements were made from ventricles of mice at various ages and defined hormone status (0-1 day, 10 day, 21 day and 4-6 weeks (adult) CD-1 mice and hypothyroid diet C57b6 mice), as well as isolated ventricular myocytes and fibroblasts. The K^+ channels of interest in this study included Kv1.2, Kv1.4, Kv1.5, Kv4.2, Kv4.3, IRK1, $KvLQT_1$, and minK.

3.1. Riboprobes

The riboprobes (RNA probes) required for the RPA experiments were transcribed from cloned cDNA fragments generated by PCR amplification. For the PCR reactions, the mouse DNA template was obtained by extracting total RNA from mouse ventricular muscle (Figure3.1A). The ratio of 28:18s ribosomal RNA was approximately 2:1, indicating little degradation of the RNA. This total mouse ventricular RNA was then used to isolate poly(A)$^+$ RNA, which was subsequently used to prepare the first-strand complementary DNA (cDNA). Figure 3.1B is a picture of an agarose gel of first-strand cDNA synthesized by both random and oligo(dT) primed reverse transcription. Note the broad smear of material generated (from 200 bp to greater than the highest band of the marker ~13,000 bp) indicating successful reverse transcription of the various mRNA species present in the poly(A)$^+$ RNA.

Synthetic primers were designed, using published mouse and rat sequences, to amplify specific regions of each K^+ channel α-subunit mRNA in the PCR reaction. The resulting cDNA fragments were cloned into pBluescript® II SK- (Stratagene) and then linearized downstream of the insert with XbaI, BamHI or NotI (Figure 3.2A). Figure 3.2B shows the nucleotide sequences of the eight K^+ channel fragments chosen for use as probes. These regions were determined to be unique using multiple sequence alignments and BLAST searches (Altschul *et al.*, 1990) of the GenBank database (data not shown).

Figure 3.1: A. Agarose gel electrophoresis of 3 µl of mouse ventricle total RNA made from pooled ventricles of four adult male CD-1 mice. Total RNA was isolated using TRIzol® Reagent (GibcoBRL). The 28s, 18s and 5s bands represent ribosomal RNA subunits, the 4s banding results from tRNA, and the background smear is the various sized mRNAs. B. Agarose gel electrophoresis of 3 µl of primary strand cDNA made from random-primed (RP) and oligo(dT)-primed (dT) reverse transcription of poly(A)$^+$ RNA. Refer to Appendix I for information regarding the DNA markers (M) used.

A. **Mouse Ventricle Total RNA**

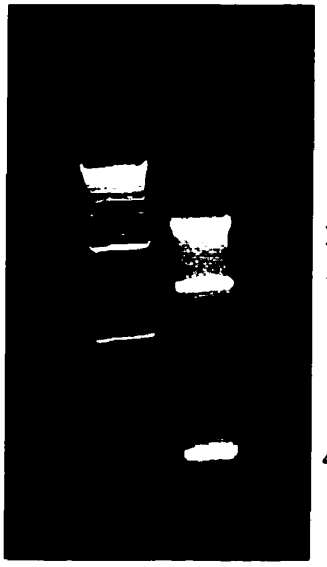

B. **Mouse Ventricle Primary Strand cDNA**

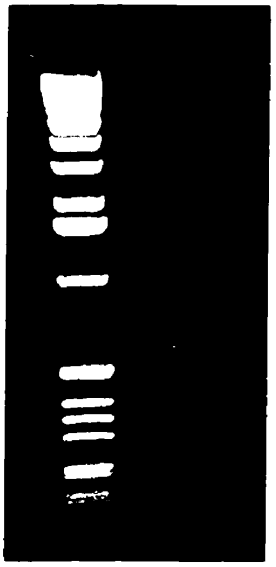

Figure 3.2: A. Agarose gel electrophoresis of the PCR derived cDNA fragments cloned into pBluescript® II SK- (Stratagene). Each lane contains 4 µl (amount used in the synthesis reaction to make the [α-^{32}P] UTP labelled riboprobes, MAXIscript™ protocol, Ambion) of the linearized plasmid containing the respective insert. Refer to Appendix I for information regarding the DNA marker (M) used on the gel. B. Nucleotide sequence of the eight K^+ channel fragments created (nucleotide sequence length excludes the restriction sites incorporated in the primers, approx. 12 bp).

A.

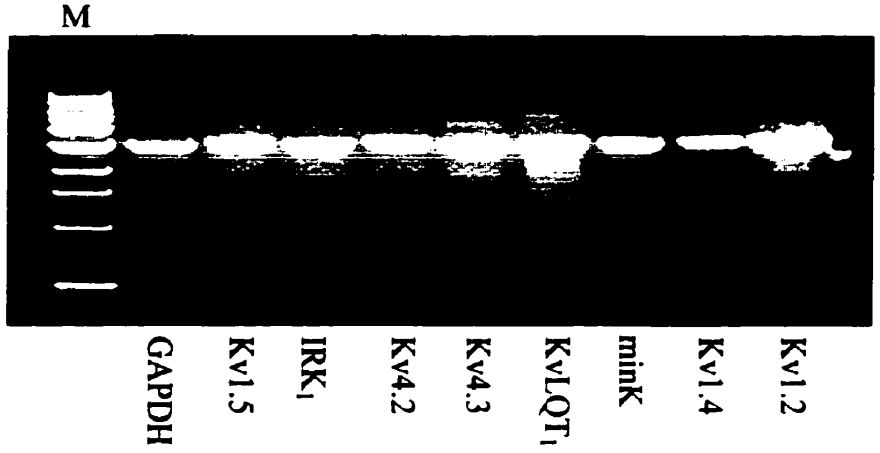

B.

```
Kv1.5   ATGGAGATCTCCCTGGTGCCCATGGAGAACGGCAGTGCCATGACCCTCAGAGGAGGAGGGGAGGCAGGGGCAA
IRK1    ATGGGCAGTGTGAGAACCAACCGCTACAGCATCGTCTCTTCGGAGGAAGATGGCATGAAGCTGGCCACTATGG
Kv4.2   ATGGCAGCCGGTGTTGCAGCATGGCTGCCCTTTGCCAGGGCAGCCGCCATTGGGTGGATGCCTGTTGCTTCGG
Kv4.3   ATGGCGGCAGGAGTTGCAGCCTGGCTGCCTTTTGCCCGGGCTGCGGCCATTGGATGGATGCCAGTGGCCAACT
KvLQT1  GAAGCACTTCAACCGGCAGATCCCAGCTGCAGCCTCACTCATCCAGACTGCATGGAGGTGCTATGCCGCTGAG
minK    ATGAGCCTGCCCAATTCCACGACTGTTCTGCCCTTTCTGGCCAGGCTGTGGCAGGAGACAGCTGAACAGGGCG
Kv1.4   TGAAAATGAAGAACAGACCCAGCTGACACAAAACGCAGTCAGTTGTCCATACCTACCTTCTAATTTGCTCAAG
Kv1.2   GATCCCGTCCTCCCCTGACCTAAAGAAAAGTAGAAGTGCCTCTACCATAAGTAAGTCTGATTACATGGAGATA

Kv1.5   GCTGTGTGCAGAGCCCCAGGGGAGAGTGTGGGTGCCCTCCGACGGCTGGACTCAATAATCAGTCCAAAGAAAC
IRK1    CAGTTGCCAATGGCTTTGGGAATGGCAAGAGTA (106bp)
Kv4.2   GGCCTATGCCTGCGCCCCCAAGACAGGAGAGAAAAAGGACTCAGGACGCTCTGATAGTGCTGAACGTGAGTGG
Kv4.3   GCCCCATGCCCCTAGCTCCAGCGGACAAGAACAAGCGG (111bp)
KvLQT1  AACCCTGACTCAGCCACTTGGAAGATCTATGTCCGGAAGCCTGCTCGGAGTCACACGCTTCTGTCCCCCAGCC
minK    GCAACGTGTCGGGCCTGGCTCGTAAGTCTCAGC (106bp)
Kv1.4   AAATTTCGGAGCTCCACTTCTTCTTCCCTGGGGGACAAGTCAGAGTATCTAGAGATGGAAGAAGGGGTCAAGG
Kv1.2   CAGGAGGGAGTTAACAACAGCAATGAGGACTTTAGAGAGG (113bp)

Kv1.5   ATCACCGAGGAGGCGCGCCACACACGAGGATGCGG (181bp)
Kv4.2   CACCCGTTTCCAGACATGGCAAGACACCCTGGAAC (181bp)
KvLQT1  CCAAACCTAAAAAGTCTGTCATGG (170bp)
Kv1.4   AATCATTATGTGGAAAGGAGGAGAAGTGTCAGGG (180bp)
```

Upon sequencing the cloned fragments several nucleotide differences compared with the reference sequences (found in GenBank) were detected. The Kv1.5 fragment had three base changes compared with the published mouse heart Kv1.5 sequence (Attali *et al.*, 1993); C → T (nt. 320), T → G (nt. 361) and T → G (nt. 402). The Kv1.4 fragment had two base changes from the published mouse heart Kv1.4 sequence (Wymore *et al.*, 1994); T → C (nt. 2707) and T → A (nt.2765). The Kv4.2 fragment had numerous differences compared to the rat sequence it was based on (Roberds & Tamkun, 1991). These include; A → G (nt. 259), C → T (nt. 301), C → G (nt. 304), A → T (nt.316), T → G (nt. 319), G → A (nt. 328), A → G (nt. 358), and T → A (nt. 361). The Kv4.3 fragment was also derived from rat-based primers (Dixon *et al.*, 1996) and was found to have two sequence changes G → A (nt. 74) and C → G (nt. 116).

Riboprobe sequences (including transcribed vector) are shown in Figure 3.3. The shaded areas represent the fraction of the probe that will hybridize to the channel mRNA and is, therefore, protected from RNase digestion. The riboprobes were designed such that they could be combined in pairs to probe each tissue sample. The sets of probes were as follows: Kv1.5 and IRK1, Kv4.2 and Kv4.3, $KvLQT_1$ and minK, and Kv1.4 and Kv1.2 (with the first probe of each pair being the largest). Each reaction also contained an internal control riboprobe whose protection product was always the smallest in the assays (sequences not shown).

3.2. Mouse Ventricle RNA Samples

The RNA samples hybridized with the riboprobes in the RNase protection assays were derived from both whole ventricular muscle and isolated cells (myocytes and fibroblasts). Total RNA was prepared from tissues pooled from 4-30 animals depending on age and type of sample. The concentration of the total RNA in each tissue was determined by optical density spectrophotometry. Figure 3.4 consists of a photograph of an agarose gel on which 1 μg of total RNA from a group of representative samples was run. Both the amounts and integrity of RNA were found to be equivalent in all samples.

Figure 3.3: Nucleotide sequence of the antisense RNA fragments made by run-off transcription (MAXIscript™, Ambion). Shaded regions represent the fully protected portion of the RNA and unshaded, leading and trailing, nucleotides correspond to vector (pBluescript® II SK-, Stratagene) sequences. The first nucleotide of the T7 transcribed RNA is numbered 1. Changes in nucleotide length between undigested and protected fragments are given in brackets.

Kv1.5 (258-181)

```
1    gggcgaauug gguaccgggc ccccccucga ggucgacggu aucgauaagc uugauaucga
61   auuccgcgau ccucgugugu ggcgcgccuc cucggugaug uuucuuugga cugauuauug
121  aguccagccg ucggagggca cccacacucu ccccuggggc ucugcacaca gcuugccccu
181  gccucccccuc cuccucugag ggucauggca cugccguucu ccaugggcac cagggagauc
241  uccauggauc cacuaguu
```

IRK_1 (135-106)

```
1    gggcgaauug gguaccuacu cuugccauuc ccaaagccau uggcaacugc cauaguggcc
61   agcuucaugc caucuuccuc cgaagagacg augcuguagc gguugguucu cacacugccc
121  auggauccac uaguu
```

Kv4.2 (258-106)

```
1    gggcgaauug gguaccgggc ccccccucga ggucgacggu aucgauaagc uugauaucga
61   auucguucca gggugucuug ccaugucugg aaacgggugc cacucacguu cagcacaauu
121  agagcguccu gaguccuuuu ucucuccugc cuuggggggag cuggcauagg cccggaggca
181  acaggcaucc acccaauggc ggcugcccug gcaaagggua gccaugcugc aacaccggcu
241  gccauggauc cacuaguu
```

Kv4.3 (140-111)

```
1    gggcgaauug gguaccccgc uuguucuugu cggcuggagc uaggggcaug gggcaguugg
61   ccacuggcau ccacccaaug gccgcagccc gggcaaaagg cagccaggcu gcaacuccug
121  ccgccaugga uccacuaguu
```

$KvLQT_1$ (199-170)

```
1    gggcgaauug gguacccau gacagacuuu uuagguuugg ggcuggggga cagaagcgug
61   ugacuccgag caggcuuccg gacauagauc uuccaagugg cugagucagg guucucagcg
121  gcauagcacc uccaugcagu cuggaugagu gaggcugcag cugggaucug ccgguugaag
181  ugcuucggau ccacuaguu
```

minK (135-106)

```
1    gggcgaauug gguaccgcug agacuuacga gccaggcccg acacguugcc gcccuguuca
61   gcugucuccu gccacagccu ggccagaaag ggcagaacag ucguggaauu gggcaggcuc
121  auggauccac uaguu
```

Kv1.4_3' (218-178)

```
1    gggcgaauug gguacccuga cacuucuccu ccuuuccaca uaaagauucc uugaccccuu
61   cuuccaucuc uagauacucu gacuuguccc ccagggaaga agaaguagag cuccgaaauu
121  ucuugagcaa auuagaaggu agguauggac aacugacugc guuuuguguc agcugggucu
181  guucuucauu uucaggaucc acuaguucua gagcggcc
```

Kv1.2_3' (135-106)

```
1    gggcgaauug gguaccucuc uaaaguccuc auugcuguug uuaacucccu ccuguaucuc
61   cauguaauca gacuuacuua ugguagaggc acuucuacuu uucuuuaggu caggggagga
121  cgggauccac uaguu
```

Figure 3.4: Representative agarose gel electrophoresis of 1μg of mouse ventricular total RNAs. Each sample represents pooled ventricular muscle from 4 to 30 CD-1 mice at different age groups. Total RNA was isolated using TRIzol® Reagent (GibcoBRL). The 28s, 18s and 5s bands represent ribosomal RNA subunits, the 4s band results from tRNA and the backgraound smear is the various sized mRNAs. Samples that appeared brighter were re-analyzed spectrophotometrically to ensure the concentration of the sample was accurate and amounts used were adjusted accordingly.

Mouse Ventricle Total RNA Samples

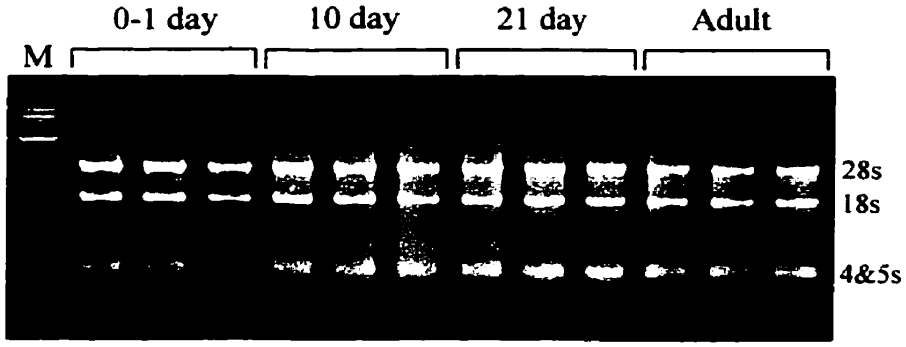

3.3. Internal Controls

Initially, β-actin was used as an internal control for the RPA experiments, however, it was discovered that the level of the β-actin mRNA changes dramatically during development and is also under thyroid hormone control (Figure 3.5A). It was thus of interest to find a protein whose mRNA level did not change significantly under our experimental conditions. GAPDH mRNA levels were found to fluctuate less than β-actin during development (Figure 3.5B), but significant changes were revealed by statistical analysis of the data. As well, GAPDH mRNA expression was found to be significantly greater in hypothyroid diet mouse ventricle (data not shown). Calsequestrin mRNA levels were also examined and found to change significantly during development (Figure 3.5C). A portion of the ribosomal 18s subunit was another candidate internal control, but our experimental conditions were unable to saturate the levels of this message present in the total RNA samples without adding substantial amounts of unlabelled antisense riboprobes, which was not economical. As well, RNase resistant complexes have been reported when 18s is combined with other probes (Ginter *et al.*, 1994)

GAPDH was eventually chosen as the best available internal control. It was used for all of the RPA measurements presented in the following sections. For data analysis purposes, a correction factor was incorporated to adjust the differences in the average GAPDH mRNA expression levels between study groups (see Methods section).

3.4. Ribonuclease Protection Assay: Methodological Findings

Autoradiography was used to visualize radiolabelled bands on the gels for all RPA experiments. Many of the total RNA samples had low quantities of the individual K^+ channel mRNA targets, i.e. only faint bands were detectable (< 10% of GAPDH signal) even when using high specific activity riboprobes. 4 day exposures to MS film with an intensifying screen (Kodak) were therefore required to visualize the protection products. Due to the prolonged exposure times required, background noise increased and faint full-length probe bands were revealed in many of the test lanes.

Figure 3.5: Autoradiograms of RPA gels demonstrating the mRNA expression level of various internal controls examined. A. β-actin mRNA levels in 2.5 μg of 0-1 day, 10 day, 21 day, and hypothyroid diet mouse ventricular total RNA. B. GAPDH mRNA levels in 2.5 μg of 0-1 day, 10 day, 21 day, and adult total RNA. C. Calsequestrin mRNA expression in 2.5 μg of adult (A), 10 day (10d) and 0-1 day (1d) mouse ventricular total RNA. All assays were done using the RPA II™ kit (Ambion). Gels were exposed overnight with an intensifying screen (Transcreen HE) using BioMax MS film (Kodak).

A. β-actin

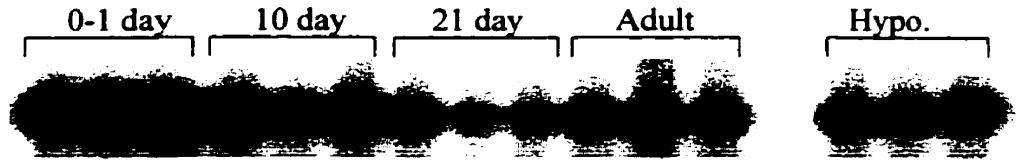

B. GAPDH

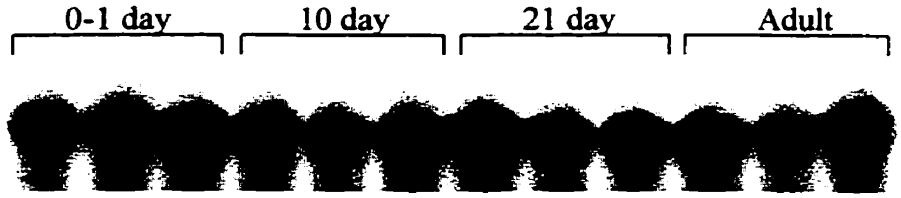

C. Calsequestrin

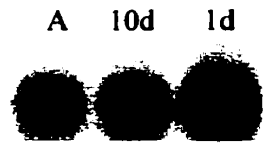

The small amounts of full-length probe may have resulted from adding too much high specific activity riboprobe (>3 fold molar excess is recommended) to the assays or having residual DNA template from the transcription reaction present (incomplete DNasing). These bands were not found to affect the analysis of the protection products.

Two of the K^+ channel probes, IRK1 and $KvLQT_1$, produced unexpected banding patterns (doublets) in the RNase protection assays. A slightly larger less intense band was always present for IRK1; and a slightly smaller less intense band was consistently observed in the $KvLQT_1$ test lanes. The reasons for these "unexpected" bands include: the probe hybridizes to transcripts with differing, but unrelated sequences; the probe detects heterogeneity in initiation, termination, or procession of mRNA transcripts; there are mismatches between probe and mRNA transcript; or there is heterogeneity in riboprobe length (Ambion RPA instruction manual). Through troubleshooting (as suggested by manufacturer), sequence analysis of our clones and GenBank searches for possible complementary transcripts we were unable to determine the exact basis of the double banding (either artifactual or legitimate protection product). The more intense band was used for data analysis purposes in both cases.

Other technical issues were encountered when using the RPA procedure to study K^+ channel mRNA expression in ventricular tissue. For example, double banding of the GAPDH protection product (Figure 3.6A) occurred when using the Hybspeed™ RPA kit (Ambion). The size of the extra band in the test lanes was larger than expected for a fully protected fragment (approximately 69 nucleotides) and smaller than undigested probe (98 nucleotides). This unidentified band was not present when the same sample was processed using either the RPA II™ (see Figure 3.5B) or RPA III™ (Figure 3.6B) kits (Ambion). The smaller or "correct" GAPDH protection product was subsequently used for analysis purposes in RPAs performed using the Hybspeed™ RPA kit since the larger band appeared to be an artifact. It had no effect on the intensity of the lower control band.

Figure 3.6: Autoradiograms of two RPA experiments in which different RPA kits were used. A. Hybspeed™ RPA kit (Ambion). The asterisk (*) indicates the unidentified GAPDH protection product. The size of the GAPDH artifact is between 69 and 98 nucleotides. B. RPA III™ kit (Ambion). No GAPDH artifact is present when the identical experiment was performed with the RPA III™ kit. Note Gel A was exposed for 8 hours and Gel B was exposed for 4 hours with a Transcreen HE intensifying screen (Kodak) using Kodak BioMax MS film.

A. Hybspeed™ RPA

B. RPA III™

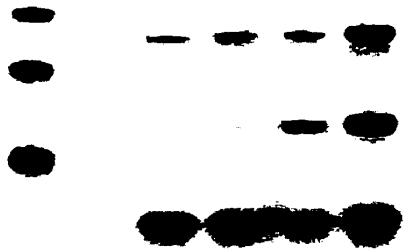

A second technical problem was loss of the RNA pellet during the processing steps of the Hybspeed™ RPA kit protocol. To try and reduce this occurrence seeDNA™ (Amersham Life Sciences), an inert carrier molecule used for quantitative precipitation of nucleic acids, was added to the final precipitation. Figure 3.7 shows an experiment in which seeDNA™ was added to the test samples. A significant amount of radioactive product was retained in the wells when it was added, compared to normal samples. SeeDNA™ was therefore not used in subsequent experiments.

3.5. Mouse Ventricular K^+ Channel mRNA Levels

3.5.1. K^+ channel α-subunit mRNA expression during development

Quantitative comparisons of the K^+ channel α-subunit mRNA expression were made in ventricular muscle from CD-1 mice aged 0-1 days (1d), 10 days (10d), 21 days (21d), and 4-6 weeks (adult). The eight K^+ channel isoforms were all expressed in the mouse ventricle total RNA in at least three of the age groups and all showed statistically significant ($P<0.05$; one-way ANOVA) changes during development (Figures 3.8-3.11). Appendix III (Table A) contains the data used to construct the histograms for the figures in this section. Tukey's post test ($P<0.05$) was used to evaluate inter-age group variation.

Figure 3.8 displays a representative RPA gel (A) and the corresponding histogram (B) showing the mRNA levels of Kv1.5 and IRK1 in mouse ventricle during development. Both transcripts were detected in all of the age groups and were found to increase by approximately 40% during postnatal development. The 1d vs. 21d variation for Kv1.5 and 1d vs. 21d and 1d vs. adult for IRK1 were statistically significant ($P<0.05$).

Kv4.2 and Kv4.3 mRNA levels also increased during development (Figure 3.9). Kv4.2 levels increased between 0-1 days and 10 days (72%), remained constant at 21 days and then peaked in adult mice (27% increase from 10 day). The observed increases between 1d and each age group were significant ($P<0.05$).

Figure 3.7: Autoradiogram of a Hybspeed™ RPA gel. A defined band of radioactivity was retained in the wells of the test samples when seeDNA™ (Amersham Life Sciences) was added in the processing steps of this experiment. Gels were exposed overnight with a Transcreen HE intensifying screen (Kodak) using Kodak BioMax MS film.

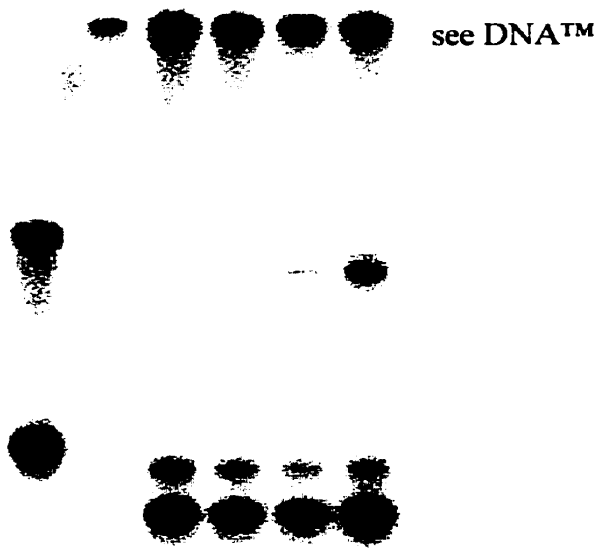
see DNA™

Figure 3.8: Developmental expression of Kv1.5 and IRK1 α-subunits in mouse ventricle. **A.** Autoradiogram of an RPA gel (RPA III™ kit, Ambion). The first lane (P) contains the 258 nt. Kv1.5, 135 nt. IRK1, and 86 nt. GAPDH riboprobes. The second lane (t) is the tRNA control lane. The remaining four test lanes show the 181 nt. Kv1.5, 106 nt. IRK1, and 69 nt. GAPDH protection products present in 2.5μg of total ventricular RNA samples. Each sample contains pooled ventricles (4-20) from adult (A), 21 day, 10 day, or 1 day CD1 mice. **B.** Histogram representing the developmental expression of Kv1.5 and IRK1 α-subunits in mouse ventricle. Molecular Dynamics PhosphorImager™ with ImageQuant® software was used to determine the density of RPA gel bands. Each bar represents the average of three samples of pooled ventricles.

A.

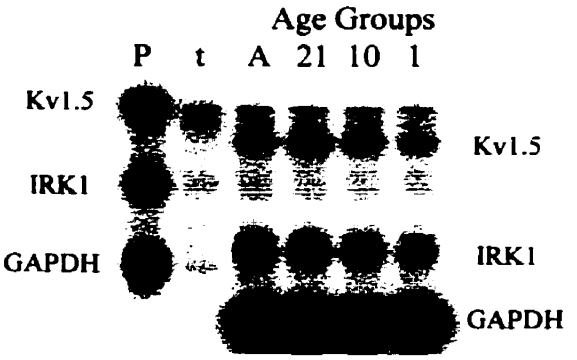
Age Groups
P t A 21 10 1
Kv1.5
IRK1
GAPDH
Kv1.5
IRK1
GAPDH

B.

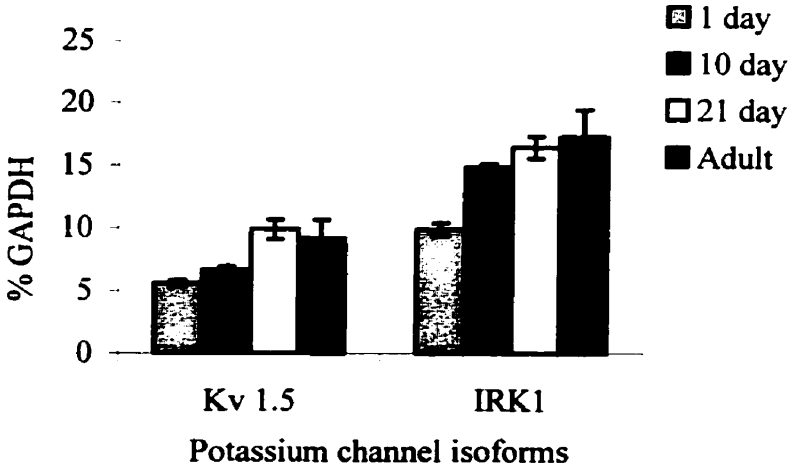
25
20
15
10
5
0
% GAPDH
1 day
10 day
21 day
Adult
Kv 1.5
IRK1
Potassium channel isoforms

Figure 3.9: Developmental expression of Kv4.2 and Kv4.3 α-subunits in mouse ventricle. **A.** Autoradiogram of an RPA gel (RPA III™ kit, Ambion). The first lane (P) contains the 258 nt. Kv4.2, 140 nt. Kv4.3, and 86 nt. GAPDH riboprobes. The second lane (t) is the tRNA control lane. The remaining four test lanes show the 181nt. Kv4.2, 111 nt. Kv4.3, and 69 nt. GAPDH protection products present in 2.5μg of total ventricular RNA samples. Each sample contains pooled ventricles (4-20) from adult (A), 21 day, 10 day, or 1 day CD1 mice. **B.** Histogram representing the developmental expression of Kv4.2 and Kv4.3 α-subunits in mouse ventricle. Molecular Dynamics PhosphorImager™ with ImageQuant® software was used to determine the density of RPA gel bands. Each bar represents the average of three samples of pooled ventricles.

A.

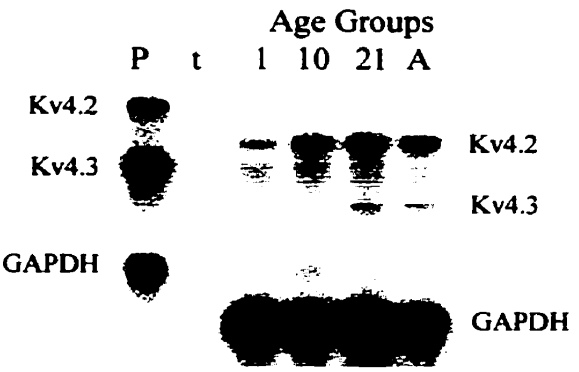
Age Groups
P t 1 10 21 A
Kv4.2
Kv4.3
GAPDH
Kv4.2
Kv4.3
GAPDH

B.

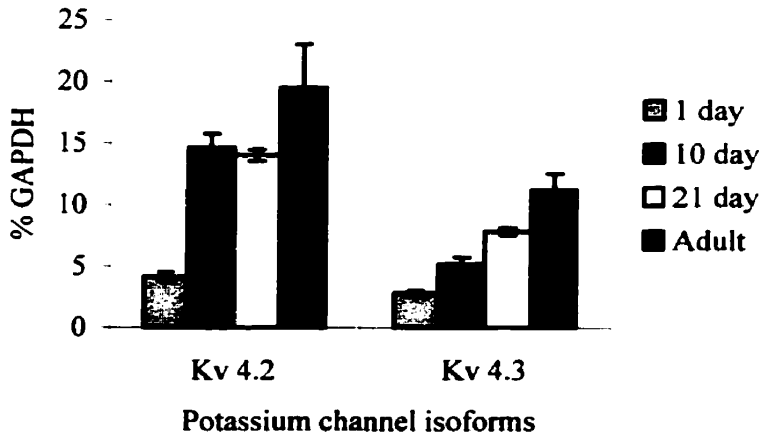
25
20
15
10
5
0
% GAPDH
1 day
10 day
21 day
Adult
Kv 4.2
Kv 4.3
Potassium channel isoforms

Figure 3.10: Developmental expression of $KvLQT_1$ and minK α-subunits in mouse ventricle. **A.** Autoradiogram of an RPA gel (RPA III™ kit, Ambion). The first lane (P) contains the 199 nt. $KvLQT_1$, 135 nt. minK, and 86 nt. GAPDH riboprobes. The second lane (t) is the tRNA control lane. The remaining four test lanes show the 170 nt. $KvLQT_1$, 106 nt. minK, and 69 nt. GAPDH protection products present in 2.5μg of total ventricular RNA samples. Each sample contains pooled ventricles (4-20) from adult (A), 21 day, 10 day, or 1 day CD1 mice. **B.** Histogram representing the developmental expression of $KvLQT_1$ and minK α-subunits in mouse ventricle. Molecular Dynamics PhosphorImager™ with ImageQuant® software was used to determine the density of RPA gel bands. Each bar represents the average of three samples of pooled ventricles.

A.

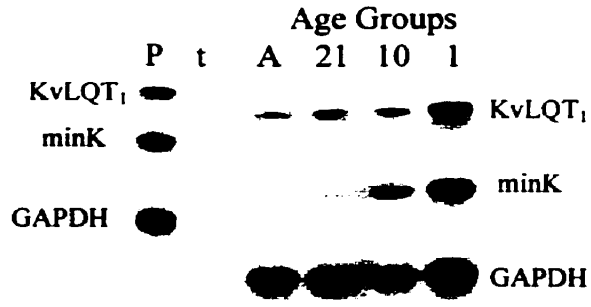
Age Groups
P t A 21 10 1
KvLQT1
minK
GAPDH
KvLQT1
minK
GAPDH

B.

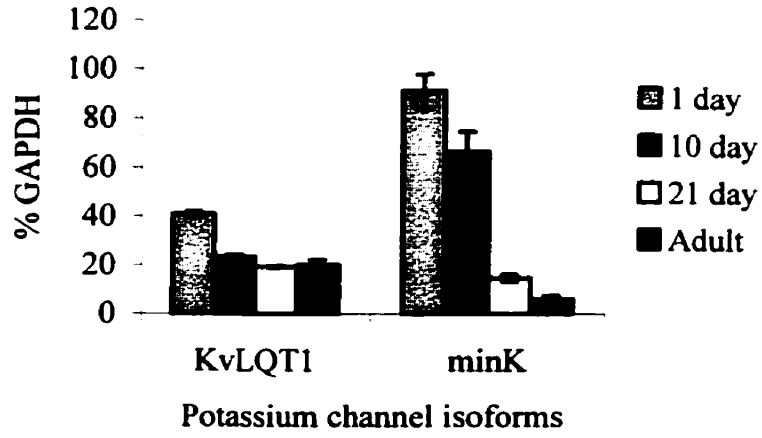
120
100
80
60
40
20
0
% GAPDH
1 day
10 day
21 day
Adult
KvLQT1
minK
Potassium channel isoforms

Figure 3.11: Developmental expression of Kv1.4 and Kv1.2 α-subunits in mouse ventricle. **A.** Autoradiogram of an RPA gel (Hybspeed™ RPA kit, Ambion). The first lane (P) contains the 218 nt. Kv1.4, 135 nt. Kv1.2, and 86 nt. GAPDH riboprobes. The second lane (t) is the tRNA control lane. The remaining four test lanes show the 178 nt. Kv1.4, 106 nt. Kv1.2, and 69 nt. GAPDH protection products present in 2.5μg of total ventricular RNA samples. Each sample contains pooled ventricles (4-20) from adult (A), 21 day, 10 day, or 1 day CD1 mice. **B.** Histogram representing the developmental expression of Kv1.4 and Kv1.2 α-subunits in mouse ventricle. Molecular Dynamics PhosphorImager™ with ImageQuant® software was used to determine the density of RPA gel bands. Each bar represents the average of three samples of pooled ventricles.

A.

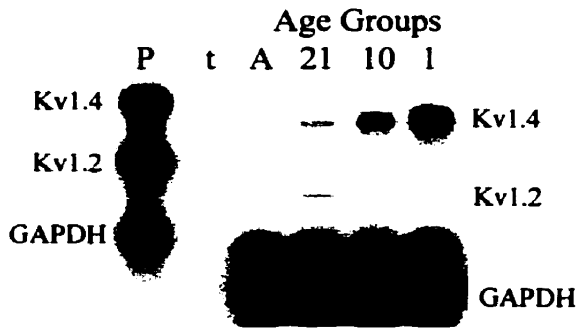
Age Groups
P t A 21 10 1
Kv1.4
Kv1.2
GAPDH
Kv1.4
Kv1.2
GAPDH

B.

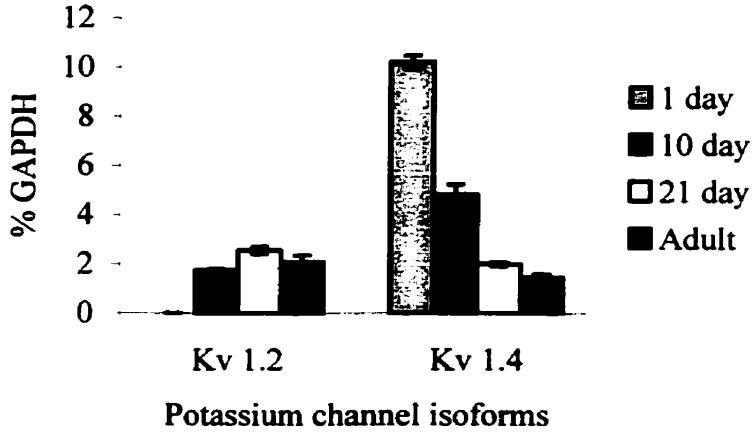
12
10
8
6
4
2
0
% GAPDH
1 day
10 day
21 day
Adult
Kv 1.2
Kv 1.4
Potassium channel isoforms

Kv4.3 mRNA levels rose steadily between age groups by 30 to 46% attaining a total postnatal increase of 75%. The 1d to 10d and 10d to 21d variation was not statistically significant (P>0.05).

$KvLQT_1$ and minK mRNA levels were found to decrease considerably during development (Figure 3.10). $KvLQT_1$ mRNA levels were highest in the postnatal 0-1 day mouse ventricles, and then declined to 57% of their original level by day 10 (10d to 21d, 10d to adult and 21d to adult variation was not significant, P>0.05). MinK mRNA also showed a pronounced decrease during development with levels dropping 94% from 1d to adult with the largest decrease between consecutive groups occurring between postnatal days 10 and 21 (78% decline). Only 21d to adult variation was not significant (P>0.05).

Figure 3.11 shows the developmental changes observed for Kv1.4 and Kv1.2 mRNA expression. Kv1.2 mRNA was undetectable in 1d total RNA, but was present from day 10 though to adult stages at a relatively constant level (no significant difference between the means, 10d vs. adult or 21d vs. adult, P>0.05). Kv1.4 mRNA expression decreased steadily during development with adult levels being only 14% of the 1d maximum. All variation between groups was significant except 21d to adult (P>0.05).

3.5.2. K^+ channel α-subunit mRNA expression in adult hypothyroid diet mice

The level of K^+ channel α-subunit mRNA in untreated (control) and hypothyroid diet C57b6 mouse ventricles was quantified by RPA. All eight K^+ channel isoforms investigated were expressed in both the untreated and hypothyroid mouse ventricular total RNA samples (Figures 3.12-3.15). Appendix III (Table B) contains the numerical data used to construct the histograms for the figures in this section. Unpaired t-tests were used to evaluate the means.

Figure 3.12A illustrates a complete RPA experiment (n=3, for each test group) comparing the levels of Kv1.5 and IRK1 mRNA in control and hypothyroid diet ventricle samples.

Figure 3.12: Kv1.5 and IRK1 α-subunit expression in hypothyroid diet versus control C57b6 mice. **A.** Autoradiogram of an RPA gel (RPA III™ kit, Ambion). The first lane (P) contains the 258 nt. Kv1.5, 135 nt. IRK1, and 86 nt. GAPDH riboprobes. The second lane (t) is the tRNA control lane. The remaining six test lanes show the 181 nt. Kv1.5, 106 nt. IRK1, and 69 nt. GAPDH protection products present in 2.5μg of total ventricular RNA samples. Each sample contains pooled ventricles from four adult hypothyroid diet or control mice. **B.** Histogram representing expression level of Kv1.5 and IRK1 α-subunits in hypothyroid diet and control mouse ventricles. Molecular Dynamics PhosphorImager™ with ImageQuant® software was used to determine the density of RPA gel bands. Each bar represents the average of three samples of pooled ventricles.

A.

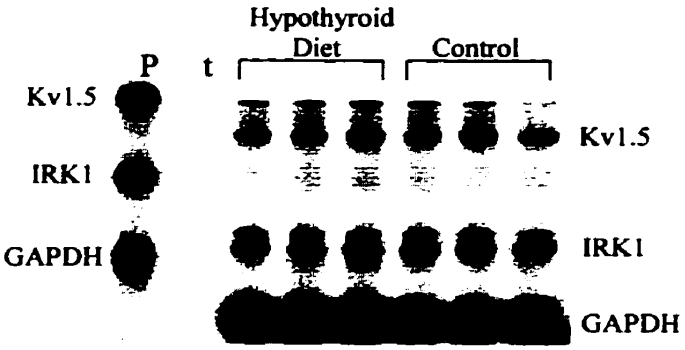
Hypothyroid Diet
Control
P
t
Kv1.5
IRK1
GAPDH
Kv1.5
IRK1
GAPDH

B.

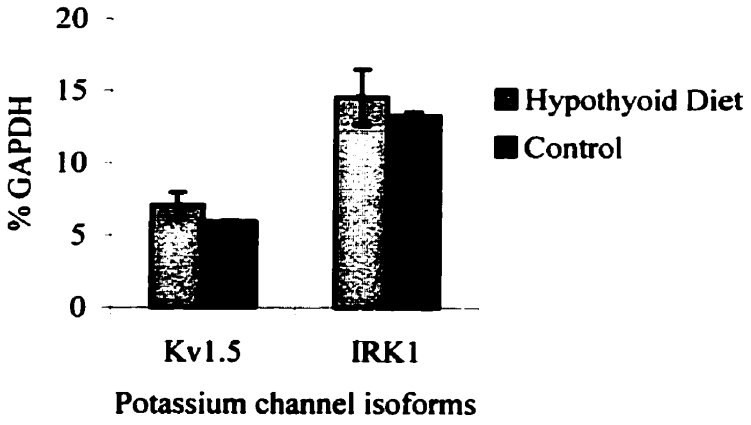
20
15
10
5
0
% GAPDH
Hypothyoid Diet
Control
Kv1.5
IRK1
Potassium channel isoforms

Figure 3.13: Kv4.2 and Kv4.3 α-subunit expression in hypothyroid diet versus control C57b6 mice. **A.** Autoradiogram of an RPA gel (RPA III™ kit, Ambion). The first lane (P) contains the 258 nt. Kv4.2, 140 nt. Kv4.3, and 86 nt. GAPDH riboprobes. The second lane (t) is the tRNA control lane. The remaining six test lanes show the 181nt. Kv4.2, 111 nt. Kv4.3, and 69 nt. GAPDH protection products present in 2.5μg of total ventricular RNA samples. Each sample contains pooled ventricles from four adult hypothyroid diet or control mice. **B.** Histogram representing expression level of Kv4.2 and Kv4.3 α-subunits in hypothyroid diet and control mouse ventricles. Molecular Dynamics PhosphorImager™ with ImageQuant® software was used to determine the density of RPA gel bands. Each bar represents the average of three samples of pooled ventricles.

A.

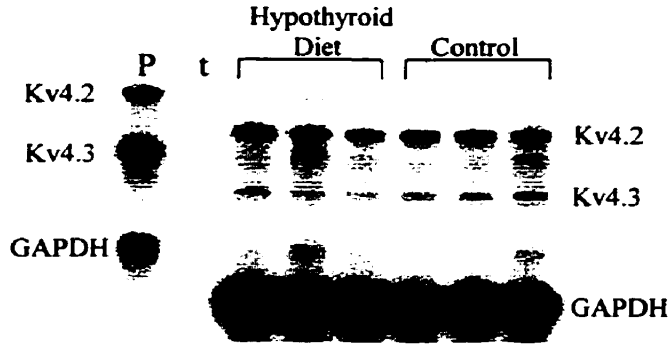
Hypothyroid Diet
Control
P
t
Kv4.2
Kv4.3
GAPDH
Kv4.2
Kv4.3
GAPDH

B.

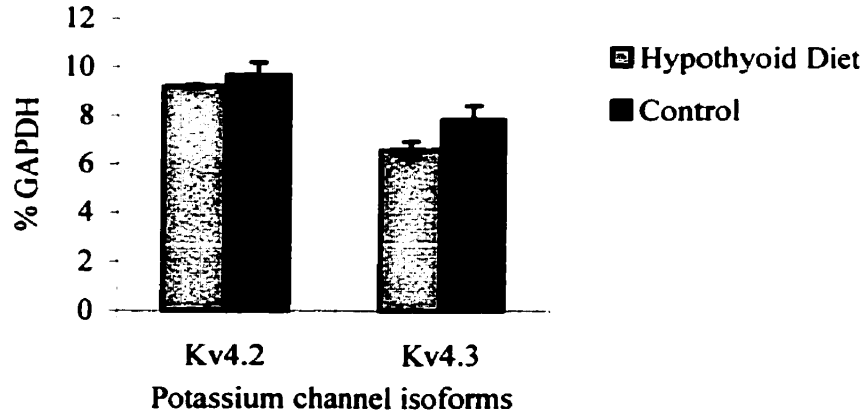
12
10
8
6
4
2
0
% GAPDH
Hypothyoid Diet
Control
Kv4.2
Kv4.3
Potassium channel isoforms

Figure 3.14: $KvLQT_1$ and minK α-subunit expression in hypothyroid diet versus control C57b6 mice. **A.** Autoradiogram of an RPA gel (RPA III™ kit, Ambion). The first lane (P) contains the 199 nt. $KvLQT_1$, 135 nt. minK, and 86 nt. GAPDH riboprobes. The second lane (t) is the tRNA control lane. The remaining six test lanes show the 170 nt. $KvLQT_1$, 106 nt. minK, and 69 nt. GAPDH protection products present in 2.5μg of total ventricular RNA samples. Each sample contains pooled ventricles from four adult hypothyroid diet or control mice. **B.** Histogram representing expression level of $KvLQT_1$ and minK α-subunits in hypothyroid diet and control mouse ventricles. Molecular Dynamics PhosphorImager™ with ImageQuant® software was used to determine the density of RPA gel bands. Each bar represents the average of three samples of pooled ventricles.

A.

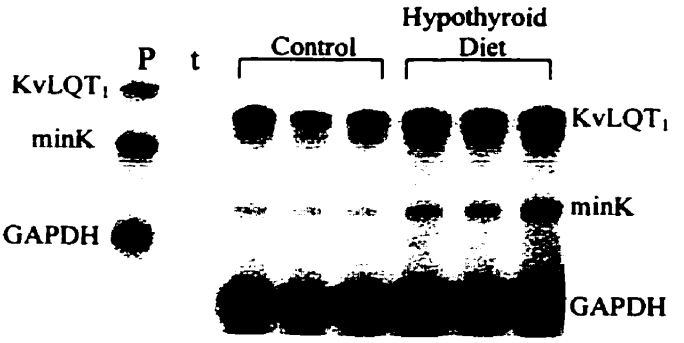
Hypothyroid
Diet
Control
P
t
KvLQT1
minK
GAPDH
KvLQT1
minK
GAPDH

B.

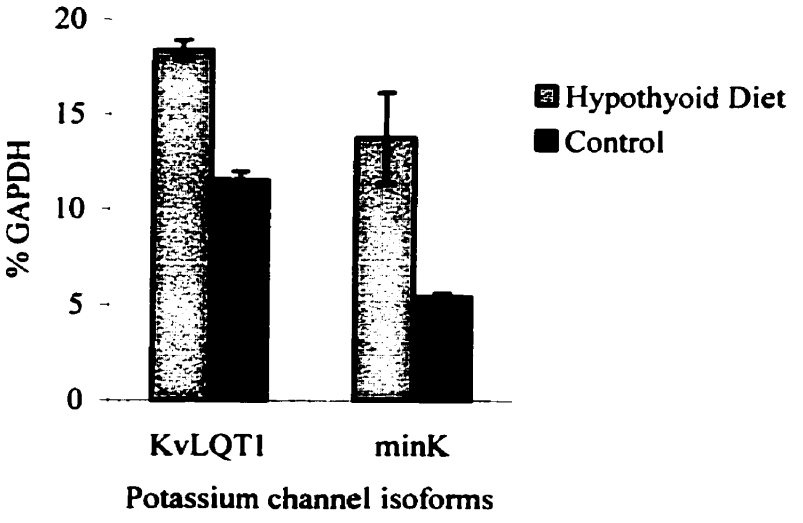
20
15
10
5
0
% GAPDH
Hypothyoid Diet
Control
KvLQT1
minK
Potassium channel isoforms

Figure 3.15: Kv1.4 and Kv1.2 α-subunit expression in hypothyroid diet versus control C57b6 mice. **A.** Autoradiogram of an RPA gel (Hybspeed™ RPA kit, Ambion). The first lane (P) contains the 218 nt. Kv1.4, 135 nt. Kv1.2, and 86 nt. GAPDH riboprobes. The second lane (t) is the tRNA control lane. The remaining six test lanes show the 178 nt. Kv1.4, 106 nt. Kv1.2, and 69 nt. GAPDH protection products present in 2.5μg of total ventricular RNA samples. Each sample contains pooled ventricles from four adult hypothyroid diet or control mice. **B.** Histogram representing expression level of Kv1.4 and Kv1.2 α-subunits in hypothyroid diet and control mouse ventricles. Molecular Dynamics PhosphorImager™ with ImageQuant® software was used to determine the density of RPA gel bands. Data expressed as % GAPDH. Each bar represents the average of three samples of pooled ventricles.

A.

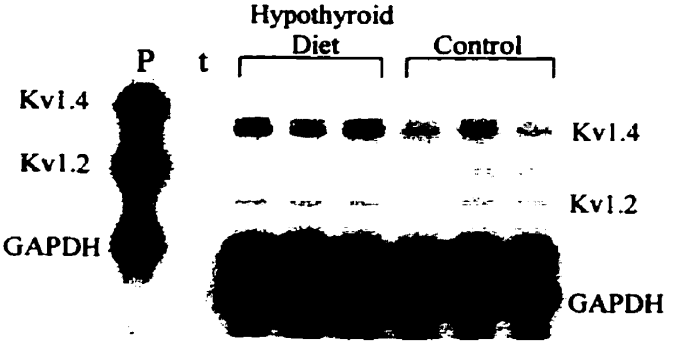
Hypothyroid Diet
Control
P
t
Kv1.4
Kv1.2
GAPDH
Kv1.4
Kv1.2
GAPDH

B.

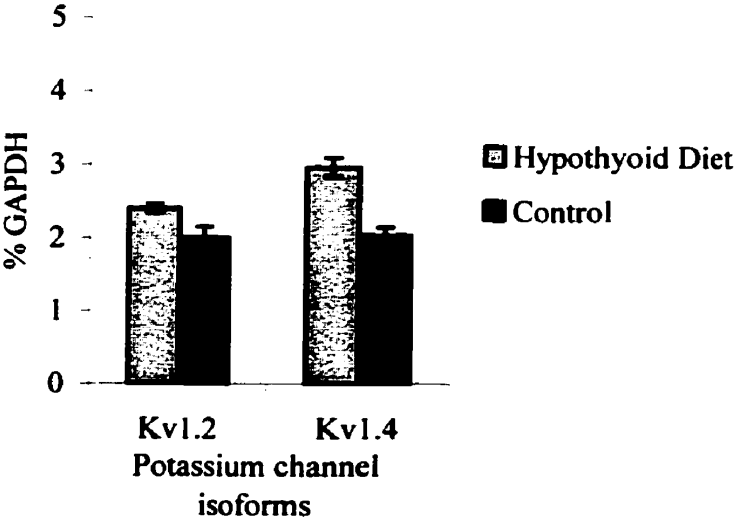
5
4
3
2
1
0
% GAPDH
Hypothyoid Diet
Control
Kv1.2
Kv1.4
Potassium channel isoforms

Neither Kv1.5 nor IRK1 mRNA levels were significantly different ($P>0.05$) between the two groups (Figure 3.12B). Kv4.2 and Kv4.3 message levels were slightly higher in control mice, 5% and 16%, respectively (Figure 3.13), however these differences were also not statistically significant ($P>0.05$).

More pronounced differences between control and hypothyroid diet mice were observed for the $KvLQT_1$, minK, Kv1.2 and Kv1.4 mRNAs (Figure 3.14 and 3.15). All four of the channel transcripts were more abundant in the hypothyroid diet samples at 37%, 61%, 17% and 31% above the control levels, respectively ($P<0.05$).

3.5.3. K^+ channel α-subunit expression in myocytes and fibroblasts

The K^+ channel α-subunit mRNA expression was also examined in isolated ventricular myocytes and fibroblasts from 0-1 day ventricular tissue. The myocytes in this study were cultured in the presence or absence of 100 nM 3,3'5-triiodo-L-thyronine (T_3) for 18-24 hours on 100 mm glass petri dishes prior to total RNA isolation. Comparisons between the isolated cells and whole ventricular samples were made. The data for this section are presented in Figures 3.16-3.19 and in Appendix III (Table C). Unpaired t-tests were used to evaluate the means.

Kv1.5 and IRK1 mRNA expression levels were measured in whole ventricle, control myocyte, T_3-treated myocyte, and fibroblast total RNA samples (Figure 3.16). Kv1.5 was not detectable in myocyte and fibroblast total RNA samples. As expected this transcript was present in 0-1 day whole ventricle. IRK1 mRNA expression was not significantly different between whole ventricle and cultured myocytes, and T_3 treatment had no effect ($P>0.05$). Fibroblasts were found to express IRK1 at 45% of the myocyte level ($P<0.05$).

Figure 3.17 illustrates that Kv4.2 mRNA expression in control myocytes was greater than that seen in whole ventricle, however, this difference was not significant ($P>0.05$). As well, T_3 caused an apparent increase in the amount of Kv4.2 mRNA in myocytes that was

Figure 3.16: Kv1.5 and IRK1 α-subunit mRNA expression in neonatal (0-1 day) whole ventricle tissue (wv), isolated ventricular myocytes [control (mc) and T_3-treated (mt)] and fibroblasts (f). Myocytes and fibroblasts were maintained in serum-free culture for 18-24 hours on 100 mm culture dishes (low-density). **A.** Autoradiogram of an RPA gel (RPA III™ kit, Ambion). The first lane (P) contains the 258 nt. Kv1.5, 135 nt. IRK1, and 86 nt. GAPDH riboprobes. The second lane (t) is the tRNA control lane. The remaining four test lanes show the 181 nt. Kv1.5, 106 nt. IRK1, and 69 nt. GAPDH protection products present in 2.5μg total RNA. The wv sample was prepared from pooled ventricles from 4 adult mice and the mc, mt, and f samples were extracted from isolated cells from 16-26 pups. **B.** Histogram representing average (n=3) mRNA expression level of Kv1.5 and IRK1 α-subunits in test samples. Molecular Dynamics PhosphorImager™ with ImageQuant® software was used to determine the density of RPA gel bands.

A.

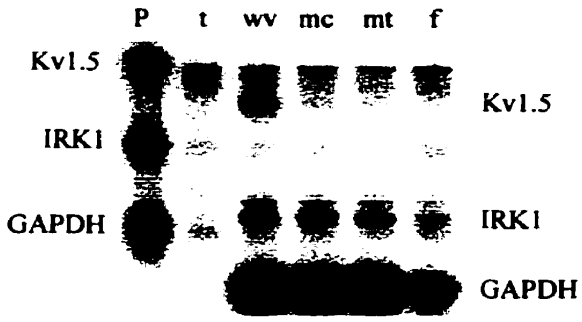
P
t
wv
mc
mt
f
Kv1.5
IRK1
GAPDH
Kv1.5
IRK1
GAPDH

B.

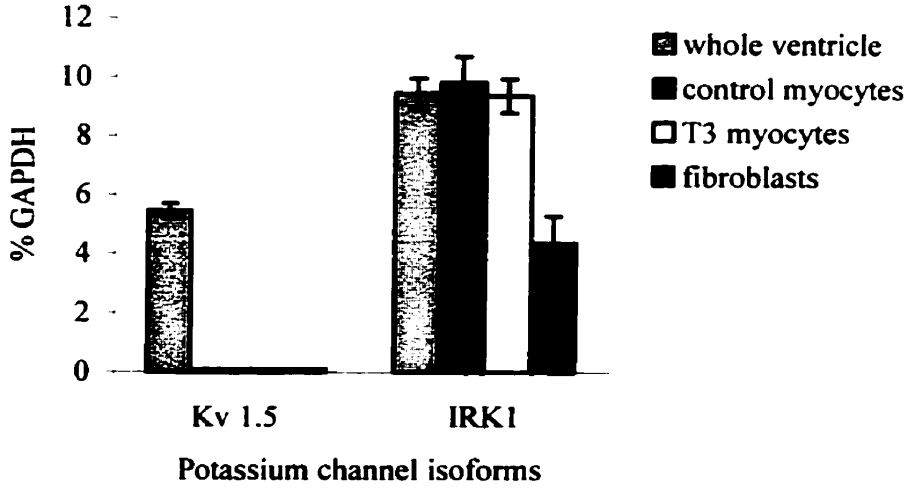
12
10
8
6
4
2
0
% GAPDH
Kv 1.5
IRK1
Potassium channel isoforms
whole ventricle
control myocytes
T3 myocytes
fibroblasts

Figure 3.17: Kv4.2 and Kv4.3 α-subunit mRNA expression in neonatal (0-1 day) whole ventricle tissue (wv), isolated ventricular myocytes [control (mc) and T_3-treated (mt)] and fibroblasts (f). Myocytes and fibroblasts were maintained in serum-free culture for 18-24 hours on 100 mm culture dishes (low-density). **A.** Autoradiogram of an RPA gel (RPA III™ kit, Ambion). The first lane (P) contains the 258 nt. Kv4.2, 140 nt. Kv4.3, and 86 nt. GAPDH riboprobes. The second lane (t) is the tRNA control lane. The remaining four test lanes show the 181nt. Kv4.2, and 69 nt. GAPDH protection products present in 2.5μg total RNA. Note, Kv4.3 expression was not detectable in myocytes or fibroblasts. The wv sample was prepared from pooled ventricles from 4 adult mice and the mc, mt, and f samples were extracted from isolated cells from 16-26 pups. **B.** Histogram representing average (n=3) mRNA expression level of Kv4.2 α-subunits in test samples. Molecular Dynamics PhosphorImager™ with ImageQuant® software was used to determine the density of RPA gel bands

A.

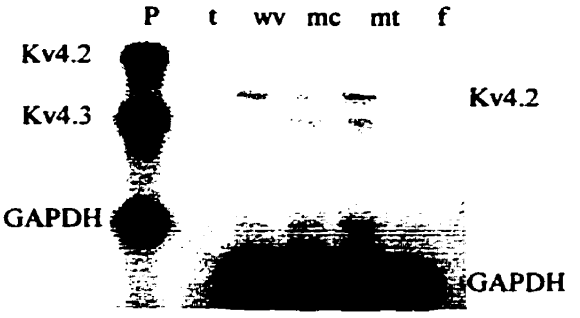
P
t
wv
mc
mt
f
Kv4.2
Kv4.3
GAPDH
Kv4.2
GAPDH

B.

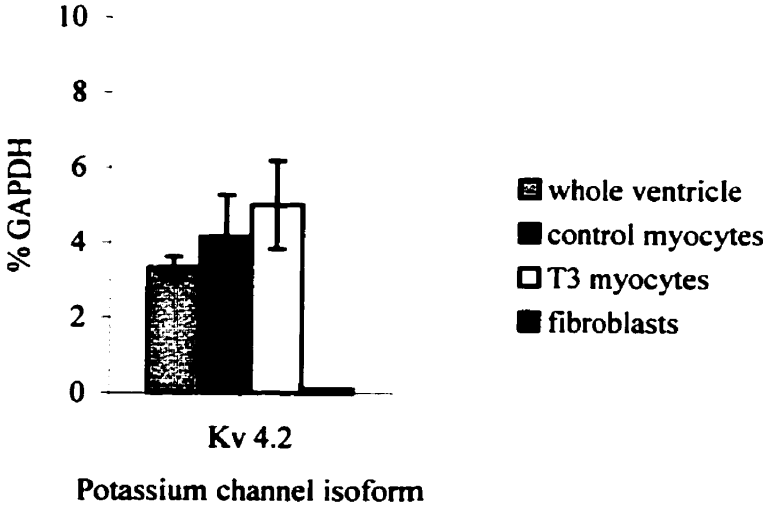
10
8
6
4
2
0
% GAPDH
whole ventricle
control myocytes
T3 myocytes
fibroblasts
Kv 4.2
Potassium channel isoform

Figure 3.18: $KvLQT_1$ and minK α-subunit mRNA expression in neonatal (0-1 day) whole ventricle tissue (wv), isolated ventricular myocytes [control (mc) and T_3-treated (mt)] and fibroblasts (f). Myocytes and fibroblasts were maintained in serum-free culture for 18-24 hours on 100 mm culture dishes (low-density). **A.** Autoradiogram of an RPA gel (RPA III™ kit, Ambion). The first lane (P) contains the 199 nt. $KvLQT_1$, 135 nt. minK, and 86 nt. GAPDH riboprobes. The second lane (t) is the tRNA control lane. The remaining four test lanes show the 170 nt. $KvLQT_1$, 106 nt. minK, and 69 nt. GAPDH protection products present in 2.5μg total RNA. The wv sample was prepared from pooled ventricles from four adult mice and the mc, mt, and f samples were extracted from isolated cells from 16-26 pups. **B.** Histogram representing average (n=3) mRNA expression level of $KvLQT_1$ and minK α-subunits in test samples. Molecular Dynamics PhosphorImager™ with ImageQuant® software was used to determine the density of RPA gel bands.

A.

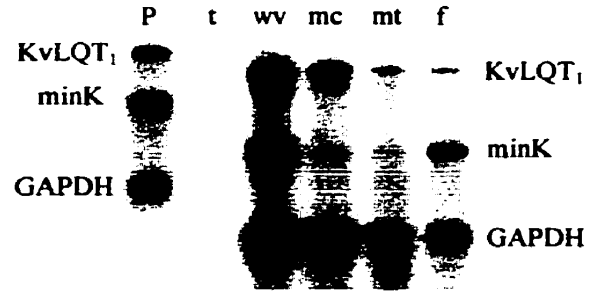
P
t
wv
mc
mt
f
KvLQT1
minK
GAPDH
KvLQT1
minK
GAPDH

B.

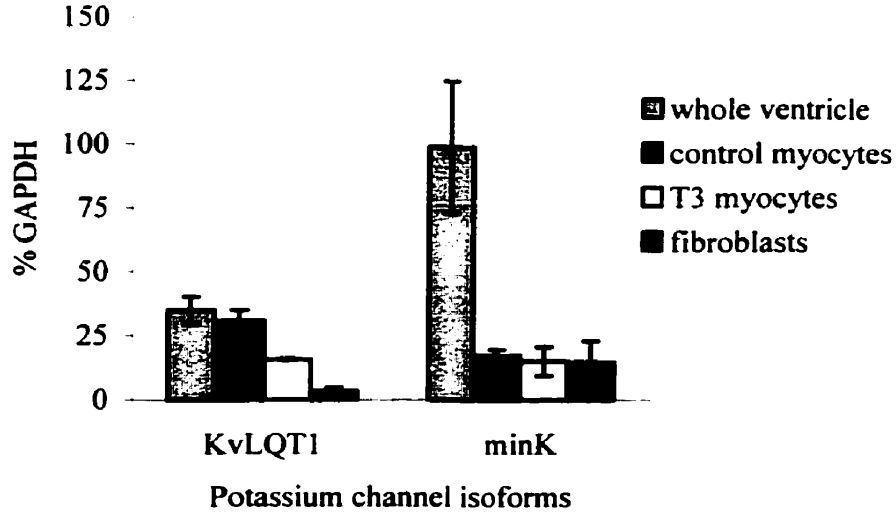
150
125
100
75
50
25
0
% GAPDH
whole ventricle
control myocytes
T3 myocytes
fibroblasts
KvLQT1
minK
Potassium channel isoforms

Figure 3.19: Kv1.4 and Kv1.2 α-subunit mRNA expression in neonatal (0-1 day) whole ventricle tissue (wv), isolated ventricular myocytes [control (mc) and T_3-treated (mt)] and fibroblasts (f). Myocytes and fibroblasts were maintained in serum-free culture for 18-24 hours on 100 mm culture dishes (low-density). **A.** Autoradiogram of an RPA gel (Hybspeed™ RPA kit, Ambion). The first lane (P) contains the 218 nt. Kv1.4, 135 nt. Kv1.2, and 86 nt. GAPDH riboprobes. The second lane (t) is the tRNA control lane. The remaining four test lanes show the 178 nt. Kv1.4, 106 nt. Kv1.2, and 69 nt. GAPDH protection products present in 2.5μg total RNA. Note, Kv1.2 expression was not detectable in myocytes or fibroblasts. The wv sample was prepared from pooled ventricles from four adult mice and the mc, mt, and f samples were extracted from isolated cells from 16-26 pups. **B.** Histogram representing average (n=3) mRNA expression level of Kv1.4 α-subunits in test samples. Molecular Dynamics PhosphorImager™ with ImageQuant® software was used to determine the density of RPA gel bands.

A.

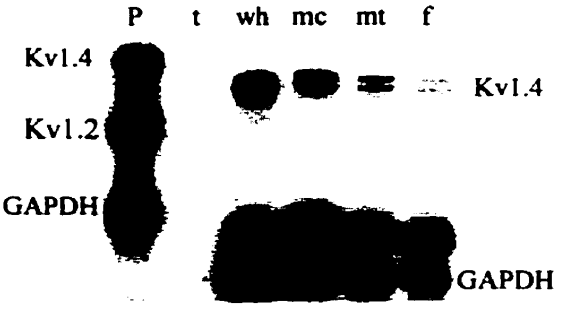
P
t
wh
mc
mt
f
Kv1.4
Kv1.2
GAPDH
Kv1.4
GAPDH

B.

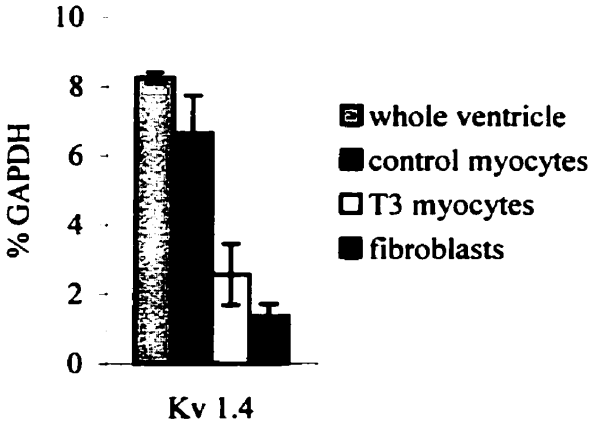
10
8
6
4
2
0
% GAPDH
whole ventricle
control myocytes
T3 myocytes
fibroblasts
Kv 1.4
Potassium channel isoform

not statistically different from control (P>0.05). No detectable level of Kv4.2 mRNA was observed in fibroblasts. Kv4.3 mRNA expression is very low in 0-1 day whole ventricle and was not detectable in myocyte or fibroblast RNA samples (Figure 3.17).

$KvLQT_1$ and minK mRNA was present in all test samples in this section (Figure 3.18). $KvLQT_1$ mRNA levels were not significantly different between whole ventricle and control myocytes (P>0.05). T_3 treatment caused a significant (50%) reduction in the level of $KvLQT_1$ mRNA in myocytes (P<0.05). Low level $KvLQT_1$ expression was detected in fibroblasts. MinK mRNA was significantly lower (P<0.05) in control myocytes compared to whole ventricle, with myocytes only expressing 17% of the whole ventricle level. T_3 had no effect on the amount of minK mRNA and fibroblasts also had low level minK expression that was nearly equivalent to the myocyte expression levels (P>0.05).

Differences in Kv1.4 mRNA expression were also identified between test samples (Figure 3.19). Control myocytes had 20% lower mRNA expression than whole ventricle samples (not statistically significant, P>0.05) and T_3 treatment caused a large 62% decrease in Kv1.4 transcript levels (P<0.05). Fibroblasts were found to have very low Kv1.4 mRNA expression. Kv1.2 mRNA was undetectable in all 0-1 day whole ventricle and isolated cell samples (Figure 3.19).

3.5.4. K^+ channel α-subunit mRNA expression in high-density myocyte cultures

As a result of the findings in section 3.5.3., indicating there were differences in K^+ channel mRNA expression between isolated ventricular myocytes and whole tissue (especially in Kv1.5 mRNA levels), an alternate high-density (pellet) culture methodology was explored (Hershman & Levitan, 1998). All eight K^+ channel riboprobes were tested on total RNA extracted from myocytes maintained in culture in the absence or presence of T_3 for 18-24 hours in 15 ml conical culture tubes (Figures 3.20-3.27; Appendix III, Table D).

Figure 3.20: Kv1.5 and IRK1 α-subunit mRNA expression in neonatal (0-1 day) whole ventricle tissue and isolated ventricular myocytes maintained in high-density serum-free cultures for 18-24 hours in 15 ml conical tubes (myocytes settled under gravity forming a pellet within the first hour). **A.** Autoradiogram of an RPA gel (RPA III^{TM} kit, Ambion). The first (P) lane contains the 258 nt. Kv1.5, 135 nt. IRK1, and 86 nt. GAPDH riboprobes. The second lane (t) is the tRNA control lane. The remaining six test lanes show the 181 nt. Kv1.5, 106 nt. IRK1, and 69 nt. GAPDH protection products present in 2.5μg total RNA. The whole ventricle total RNA samples were prepared from pooled ventricles from four adult mice and the myocyte samples were extracted from isolated cells from 16-26 pups. **B.** Histogram representing average (n=3) mRNA expression level of Kv1.5 and IRK1 α-subunits in test samples. Molecular Dynamics PhosphorImager^{TM} with ImageQuant® software was used to determine the density of RPA gel bands.

A.

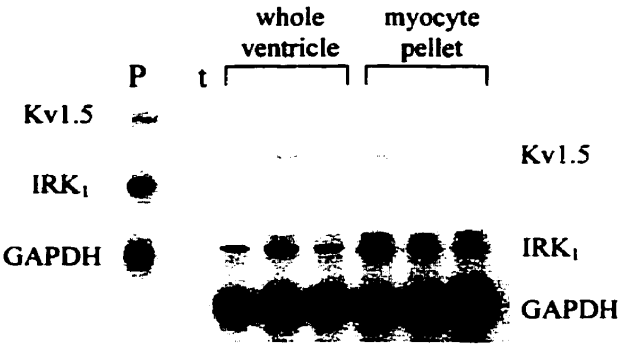
whole ventricle
myocyte pellet
P
t
Kv1.5
IRK1
GAPDH
Kv1.5
IRK1
GAPDH

B.

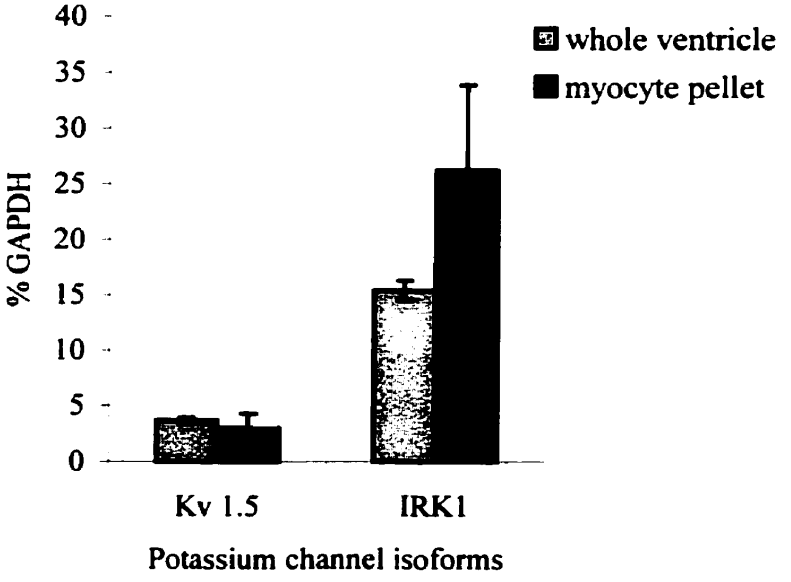
40
35
30
25
20
15
10
5
0
% GAPDH
whole ventricle
myocyte pellet
Kv 1.5
IRK1
Potassium channel isoforms

Figure 3.21: Kv1.5 and IRK1 α-subunit mRNA expression in isolated ventricular myocytes maintained in high-density serum-free cultures in the presence or absence of T_3 (100 nM). Myocytes were cultured in 15 ml conical tubes for 18-24 hours (myocytes settled under gravity forming a pellet within the first hour). **A.** Autoradiogram of an RPA gel (RPA III™ kit, Ambion). The first (P) lane contains the 258 nt. Kv1.5, 135 nt. IRK1, and 86 nt. GAPDH riboprobes. The second lane (t) is the tRNA control lane. The remaining six test lanes show the 181 nt. Kv1.5, 106 nt. IRK1, and 69 nt. GAPDH protection products present in 2.5μg total RNA. The myocyte samples were extracted from isolated cells from 16-26 pups. **B.** Histogram representing average (n=3) mRNA expression level of Kv1.5 and IRK1 α-subunits in test samples. Molecular Dynamics PhosphorImager™ with ImageQuant® software was used to determine the density of RPA gel bands.

A.

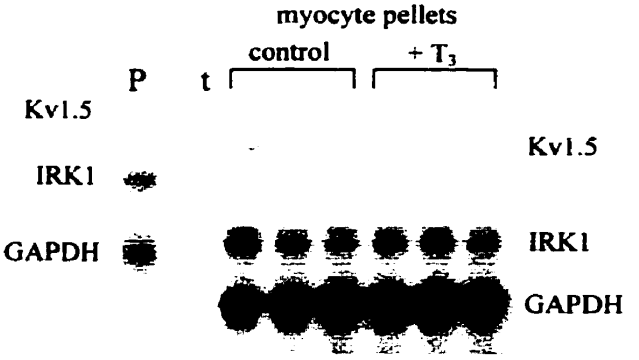
myocyte pellets
control
+ T_3
P
t
Kv1.5
IRK1
GAPDH
Kv1.5
IRK1
GAPDH

B.

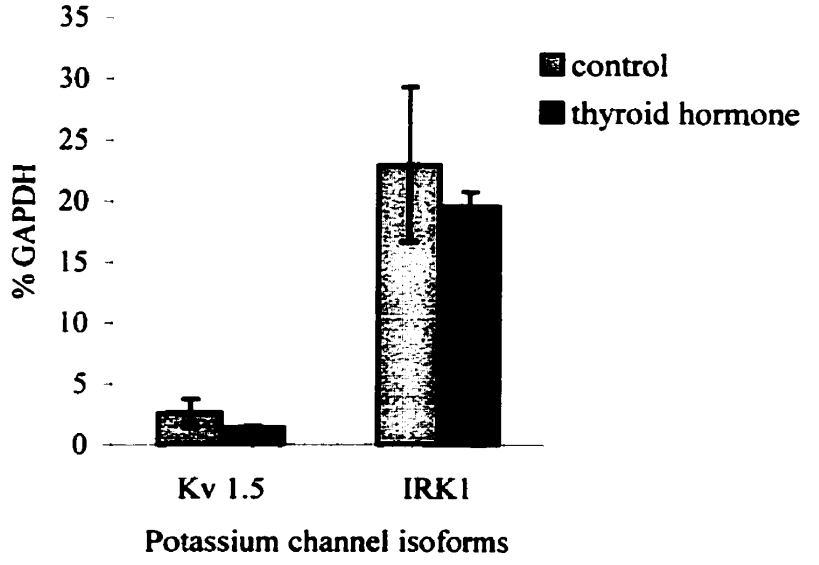
35
30
25
20
15
10
5
0
% GAPDH
control
thyroid hormone
Kv 1.5
IRK1
Potassium channel isoforms

Figure 3.22: Kv4.2 and Kv4.3 α-subunit mRNA expression in neonatal (0-1 day) whole ventricle tissue and isolated ventricular myocytes maintained in high-density serum-free cultures for 18-24 hours in 15 ml conical tubes (myocytes settled under gravity forming a pellet within the first hour). **A.** Autoradiogram of an RPA gel (RPA III™ kit, Ambion). The first lane (P) contains the 258 nt. Kv4.2, 140 nt. Kv4.3, and 86 nt. GAPDH riboprobes. The second lane (t) is the tRNA control lane. The remaining six test lanes show the 181nt. Kv4.2, and 69 nt. GAPDH protection products present in 2.5μg total RNA. Note, Kv4.3 expression was not discernible from background in myocyte samples. The whole ventricle total RNA samples were prepared from pooled ventricles from four adult mice and the myocyte samples were extracted from isolated cells from 16-26 pups. **B.** Histogram representing average (n=3) mRNA expression level of Kv4.2 α-subunits in test samples. Molecular Dynamics PhosphorImager™ with ImageQuant® software was used to determine the density of RPA gel bands.

A.

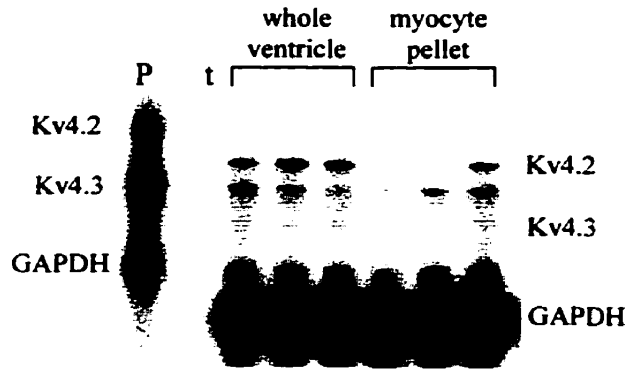
whole ventricle
myocyte pellet
P
t
Kv4.2
Kv4.3
GAPDH
Kv4.2
Kv4.3
GAPDH

B.

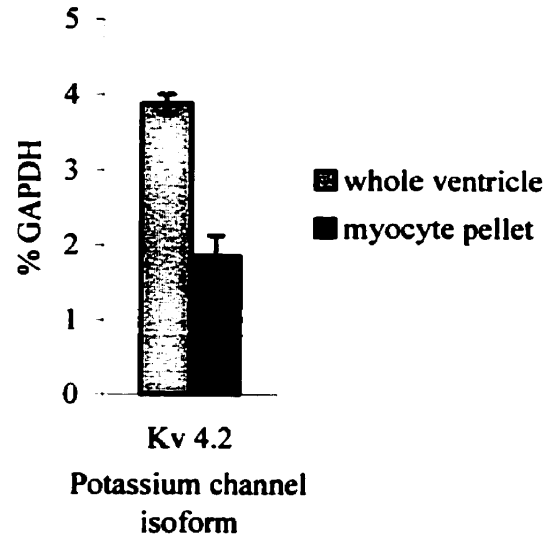
5
4
3
2
1
0
% GAPDH
whole ventricle
myocyte pellet
Kv 4.2
Potassium channel isoform

Figure 3.23: Kv4.2 and Kv4.3 α-subunit mRNA expression in isolated ventricular myocytes maintained in high-density serum-free cultures in the presence or absence of T_3 (100 nM). Myocytes were cultured in 15 ml conical tubes for 18-24 hours (myocytes settled under gravity forming a pellet within the first hour). **A.** Autoradiogram of an RPA gel (RPA III™ kit, Ambion). The first lane (P) contains the 258 nt. Kv4.2, 140 nt. Kv4.3, and 86 nt. GAPDH riboprobes. The second lane (t) is the tRNA control lane. The remaining six test lanes show the 181nt. Kv4.2, and 69 nt. GAPDH protection products present in 2.5μg total RNA. Note, Kv4.3 expression insignificant in myocytes. The myocyte samples were extracted from isolated cells from 16-26 pups. **B.** Histogram representing average (n=3) mRNA expression level of Kv4.2 α-subunits in test samples. Molecular Dynamics PhosphorImager™ with ImageQuant® software was used to determine the density of RPA gel bands.

A.

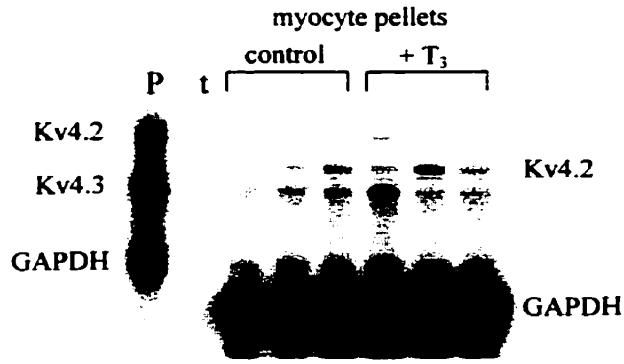
myocyte pellets
control
+ T_3
P
t
Kv4.2
Kv4.3
GAPDH
Kv4.2
GAPDH

B.

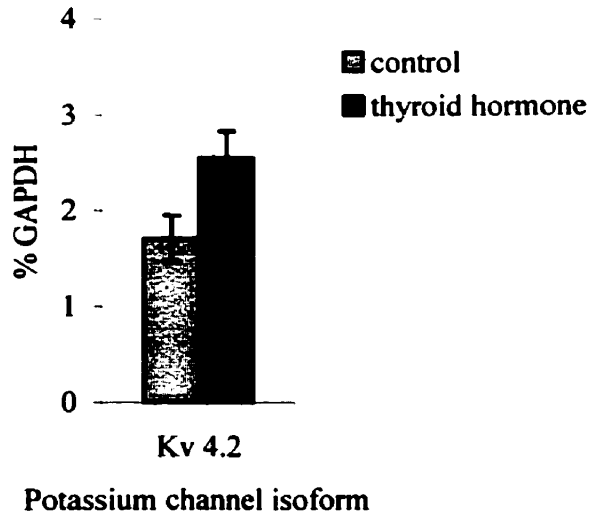
4
3
2
1
0
% GAPDH
control
thyroid hormone
Kv 4.2
Potassium channel isoform

Figure 3.24: $KvLQT_1$ and minK α-subunit mRNA expression in neonatal (0-1 day) whole ventricle tissue and isolated ventricular myocytes maintained in high-density serum-free cultures for 18-24 hours in 15 ml conical tubes (myocytes settled under gravity forming a pellet within the first hour). **A.** Autoradiogram of an RPA gel (RPA III™ kit, Ambion). The first lane (P) contains the 199 nt. $KvLQT_1$, 135 nt. minK, and 86 nt. GAPDH riboprobes. The second lane (t) is the tRNA control lane. The remaining six test lanes show the 170 nt. $KvLQT_1$, 106 nt. minK, and 69 nt. GAPDH protection products present in 2.5μg total RNA. The whole ventricle total RNA samples were prepared from pooled ventricles from four adult mice and the myocyte samples were extracted from isolated cells from 16-26 pups. **B.** Histogram representing average (n=3) mRNA expression level of $KvLQT_1$ and minK α-subunits in test samples. Molecular Dynamics PhosphorImager™ with ImageQuant® software was used to determine the density of RPA gel bands.

A.

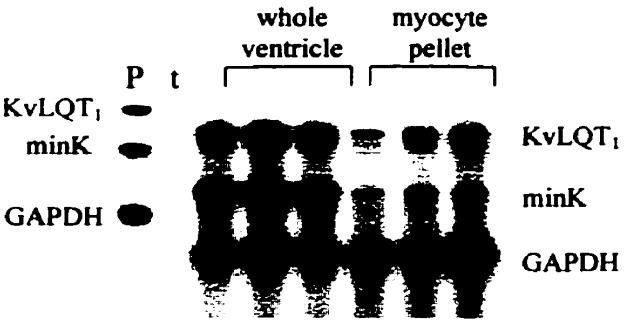
whole ventricle
myocyte pellet
P t
KvLQT1
minK
GAPDH
KvLQT1
minK
GAPDH

B.

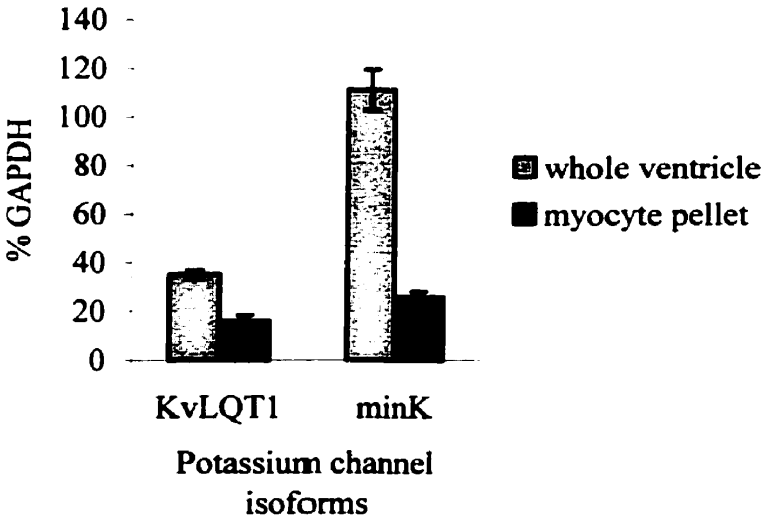
140
120
100
80
60
40
20
0
% GAPDH
KvLQT1
minK
Potassium channel isoforms
whole ventricle
myocyte pellet

Figure 3.25: $KvLQT_1$ and minK α-subunit mRNA expression in isolated ventricular myocytes maintained in high-density serum-free cultures in the presence or absence of T_3 (100 nM) for 18-24 hours in 15 ml conical tubes (myocytes settled under gravity forming a pellet within the first hour). **A.** Autoradiogram of an RPA gel (RPA III™ kit, Ambion). The first lane (P) contains the 199 nt. $KvLQT_1$, 135 nt. minK, and 86 nt. GAPDH riboprobes. The second lane (t) is the tRNA control lane. The remaining six test lanes show the 170 nt. $KvLQT_1$, 106 nt. minK, and 69 nt. GAPDH protection products present in 2.5μg total RNA. The myocyte samples were extracted from isolated cells from 16-26 pups. **B.** Histogram representing average (n=3) mRNA expression level of $KvLQT_1$ and minK α-subunits in test samples. Molecular Dynamics PhosphorImager™ with ImageQuant® software was used to determine the density of RPA gel bands.

A.

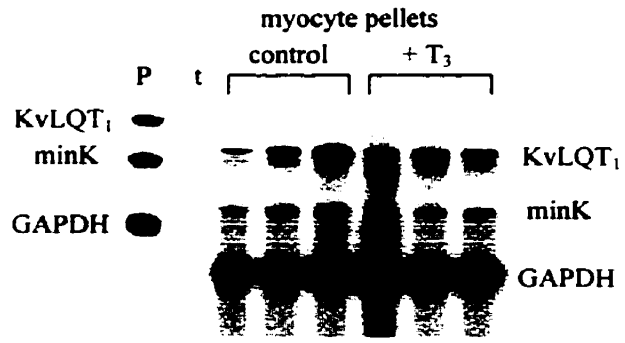
myocyte pellets
control
+ T_3
P
t
$KvLQT_1$
minK
GAPDH
$KvLQT_1$
minK
GAPDH

B.

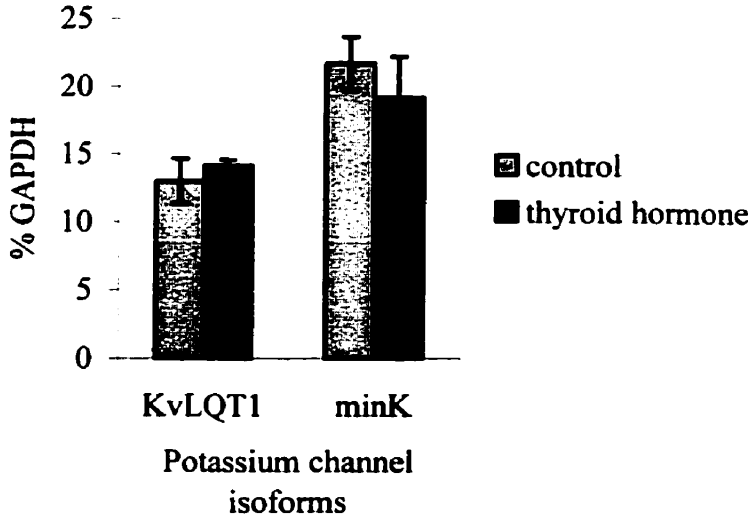
25
20
15
10
5
0
% GAPDH
control
thyroid hormone
KvLQT1
minK
Potassium channel isoforms

Figure 3.26: Kv1.4 and Kv1.2 α-subunit mRNA expression in neonatal (0-1 day) whole ventricle tissue and isolated ventricular myocytes maintained in high-density serum-free culture for 18-24 hours in 15 ml conical tubes (myocytes settled under gravity forming a pellet within the first hour). **A.** Autoradiogram of an RPA gel (RPA III™ kit, Ambion). The first lane (P) contains the 218 nt. Kv1.4, 135 nt. Kv1.2, and 86 nt. GAPDH riboprobes. The second lane (t) is the tRNA control lane. The remaining six test lanes show the 178 nt. Kv1.4 and 69 nt. GAPDH protection products present in 2.5μg total RNA. Note, Kv1.2 expression was not discernible from background in myocyte samples. The whole ventricle total RNA samples were prepared from pooled ventricles from four adult mice and the myocyte samples were extracted from isolated cells from 16-26 pups. **B.** Histogram representing average (n=3) mRNA expression level of Kv1.4 α-subunits in test samples. Molecular Dynamics PhosphorImager™ with ImageQuant® software was used to determine the density of RPA gel bands.

A.

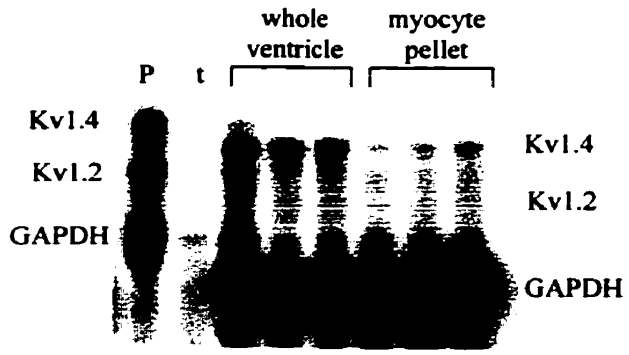
whole ventricle
myocyte pellet
P
t
Kv1.4
Kv1.2
GAPDH
Kv1.4
Kv1.2
GAPDH

B.

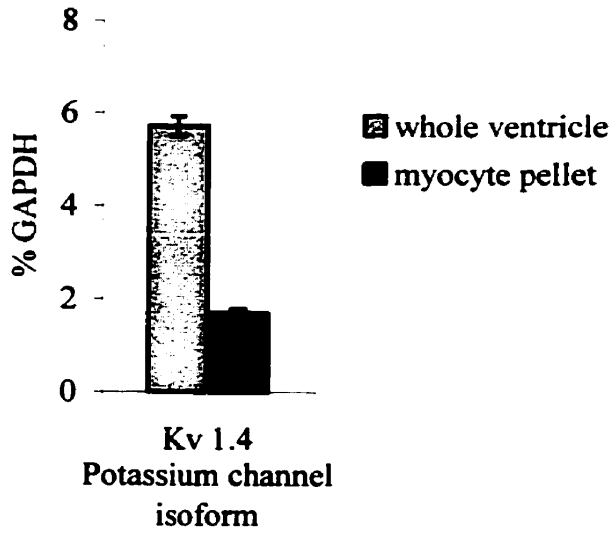
8
6
4
2
0
% GAPDH
whole ventricle
myocyte pellet
Kv 1.4
Potassium channel
isoform

Figure 3.27: Kv1.4 and Kv1.2 α-subunit mRNA expression in isolated ventricular myocytes maintained in high-density serum-free culture in the presence or absence of T_3 (100nM). Myocytes were cultured in 15 ml conical tubes for 18-24 hours (myocytes settled under gravity forming a pellet within the first hour). **A.** Autoradiogram of an RPA gel (RPA III™ kit, Ambion). The first lane (P) contains the 218 nt. Kv1.4, 135 nt. Kv1.2, and 86 nt. GAPDH riboprobes. The second lane (t) is the tRNA control lane. The remaining six test lanes show the 178 nt. Kv1.4 and 69 nt. GAPDH protection products present in 2.5μg total RNA. Note, Kv1.2 protection product not discernible from background in myocyte samples. The myocyte samples were extracted from isolated cells from 16-26 pups. **B.** Histogram representing average (n=3) mRNA expression level of Kv1.4 α-subunits in test samples. Molecular Dynamics PhosphorImager™ with ImageQuant® software was used to determine the density of RPA gel bands.

A.

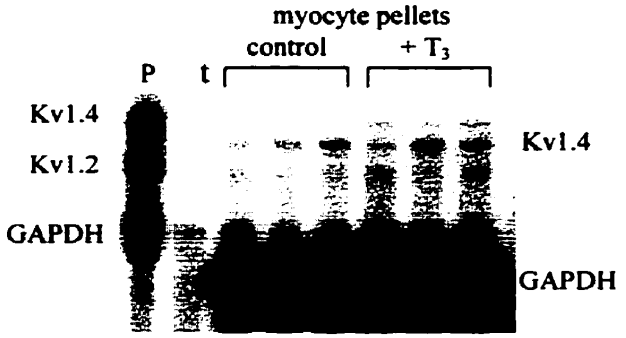
myocyte pellets
control
+ T_3
P
t
Kv1.4
Kv1.2
GAPDH
Kv1.4
GAPDH

B.

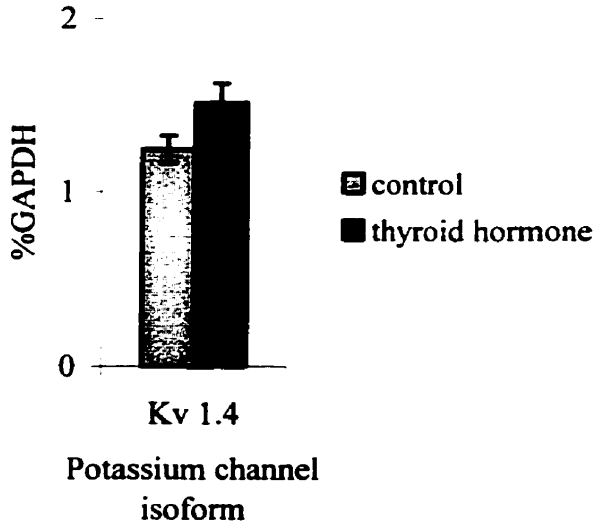
2
1
0
%GAPDH
control
thyroid hormone
Kv 1.4
Potassium channel isoform

Kv1.5 and IRK1 mRNA expression in the high-density cultured myocytes was not significantly different than whole ventricle levels ($P>0.05$; Figure 3.20). Thyroid hormone addition caused Kv1.5 and IRK1 levels to decrease, however, the change was not statistically significant (Figure 3.21, $P>0.05$).

Kv4.2 and Kv4.3 mRNA levels in the high-density myocytes were both significantly lower than whole ventricle ($P<0.05$) with Kv4.2 being 50% less and Kv4.3 being undetectable (Figure 3.22). Culturing in the presence of T_3 caused a significant 33% increase in Kv4.2 message level ($P<0.05$) and no detectable effect on Kv4.3 (Figure 3.23).

Large decreases in $KvLQT_1$ and minK transcripts were observed in the high-density myocyte RNA samples, 55% and 76%, respectively compared to the whole ventricular RNA levels (variation between means highly significant $P<0.001$; Figure 3.24). T_3-treated myocyte $KvLQT_1$ and minK mRNA levels were not significantly different than control ($P>0.05$; Figure 3.25).

Kv1.4 and Kv1.2 mRNA expression levels were also lower in the high-density myocytes compared to whole ventricular levels with Kv1.4 levels decreasing by 70% and Kv1.2 being undetectable in the myocyte samples ($P< 0.05$; Figure 3.26). T_3 treatment caused a small increase in Kv1.4 mRNA expression but it was found to be statistically insignificant ($P>0.05$, Figure 3.27).

The observations summarized above, suggested that a comparison between the two types of myocyte culture, low-density plating and high-density pellet should be made. The results showed that Kv1.5, IRK1, Kv4.2, Kv1.4, $KvLQT_1$, and minK mRNA levels were all dependent on the method of cell culturing used for isolated ventricular myocytes (Kv4.3 and Kv1.2 mRNA bands were not discernible from background in all of the 0-1 day myocyte samples).

Kv1.5, IRK1 and minK levels increased in the high-density myocyte cultures with Kv1.5 and IRK1 attaining the amount measured in whole ventricular samples ($P>0.05$). At low-density Kv4.2, Kv1.4 and $KvLQT_1$ expression was not significantly different than whole ventricle, however, in the high-density pellet culture system all three had significantly lower ($P<0.05$) mRNA levels.

4. DISCUSSION

The primary goal of this project was to identify and quantify specific K^+ channel α-subunit mRNAs present in mouse ventricular tissue by means of the RNase protection assay (RPA). The information obtained complements the detailed electrophysiological work being performed in our lab (and by others) which focuses on establishing the molecular identity, developmental pattern, and hormonal regulation of the K^+ currents in the mouse heart.

The K^+ channels selected for study include: Kv1.5, which is thought to underlie I_{sus} (a rapidly activating, slowly inactivating outward K^+ current); Kv1.2, a second rapidly activating, slowly inactivating K^+ current; Kv1.4, Kv4.2, and Kv4.3, which are candidates for I_{to} (the Ca^{2+}-independent transient outward K^+ current) in mouse heart; $KvLQT_1$ and minK, which are thought to underlie I_{Ks} (the slow component of the cardiac delayed rectifier K^+ current); and IRK1, which generates the inward rectifier K^+ current (I_{K1}).

4.1. Method Evaluation: The RNase Protection Assay

The RPA is a rapid, flexible, highly sensitive method that is commonly used to detect specific hybridization between complimentary RNA transcripts (Kreig & Melton, 1987). This method has been used by others to investigate the K^+ channel mRNA expression in the rat and canine heart (Dixon & McKinnen, 1994; Dixon *et al.*, 1996; Xu *et al.*, 1996; Shimoni *et al.*, 1997; Wickenden *et al.*, 1997; 1999), and was therefore chosen to determine if selected K^+ channel α-subunit mRNAs are expressed in mouse ventricular tissues and cells.

It is difficult to obtain consistent results when using the standard RPA method. A substantial amount of variability was encountered, which was apparently due to error incorporated when working with the small volumes required by the assay (RPA II™, RPA III™ and Hybspeed™ RPA kits, Ambion). Internal controls such as β-actin or

GAPDH are commonly used (and were used in this study) to reduce the variability between sample processing (Dixon & McKinnon, 1994). However, it was discovered that these transcripts are also under developmental control and are regulated by thyroid hormone.

Using more stable housekeeping genes that are not regulated during development or by thyroid hormone or use of an alternate method to help standardize the RPA procedure may have produced less variable results. As well, increasing the number of samples (from n=3) would have reduced the overall error in the assay; thereby enhancing the likelihood of obtaining significant differences between sample groups.

4.2. Neonatal Ventricular Myocyte Cell Culture

In order to study the direct effects of thyroid hormone on K^+ channel α-subunit mRNA expression in the mouse heart we isolated neonatal ventricular myocytes and maintained them in culture for 18 to 24 hours in the absence or presence of 100 nM 3,3'5-triiodo-L-thyronine (T_3). Total RNA samples were subsequently obtained from the cultured cells for RPA analysis. Wickenden *et al.* (1997) utilized a similar approach to study the effect of thyroid hormone on rat ventricular myocyte K^+ channel expression.

Using isolated myocytes avoids the potentially complicating indirect effects associated with thyroid hormone administration *in vivo*, since T_3 can result in increased sympathetic innervation, increased heart rate and cardiac hypertrophy (Dillman 1990; Klein, 1990; Wickenden *et al.*, 1997). However, the enzymatic dispersion and subsequent culture of isolated ventricular myocytes obviously removes the complex myocyte-myocyte and myocyte-fibroblast signaling that occurs in the intact heart (Clark *et al.*, 1998). Therefore it is possible that processes such as transcription or factors that maintain mRNA stability are disrupted when myocytes are isolated and cultured which could lead to inherent changes in K^+ channel mRNA levels. A comparison of the K^+ channel mRNA expression

in isolated myocytes versus whole ventricular samples was therefore undertaken.

The level of K^+ channel mRNA expression in fibroblasts was also determined since $^2/_3$ of the cells that comprise ventricle tissue are non-myocytes, and 90% of these are fibroblasts (Booz & Baker, 1995). The majority of the RPA measurements in my study, and RPA and Northern Blot experiments reported by others (Roberds & Tamkun, 1991; Dixon & McKinnen, 1994; Dixon *et al.*, 1996; Xu *et al.*, 1996; Nishiyama *et al.*, 1997; Shimoni *et al.*, 1997; Nishiyama *et al.*, 1998; Wickenden *et al.*, 1999), utilize total RNA isolated from whole ventricular or atrial samples. Thus, it was of interest to ensure that the mRNA signals obtained from whole tissue are a result of K^+ channel mRNA expression in myocytes and not fibroblasts. This is important since the electrophysiological recordings of the K^+ currents in the heart are routinely performed in freshly isolated myocytes. If the K^+ channel mRNA level in fibroblasts is significant it may contribute to discrepancies observed when making comparisons between whole ventricle mRNA message levels and the observed currents in myocytes measured by patch clamp recordings.

4.2.1. K^+ channel α-subunit mRNA levels in ventricular myocytes and fibroblasts

In the present study we observed that when 0-1 day ventricular myocytes were cultured at low density on 100 mm glass plates for 18 to 24 hours (see Figures 3.16-3.19) the mRNA levels for Kv4.2, IRK1, $KvLQT_1$, and Kv1.4 were approximately equal to those detected in whole ventricular tissue. However, Kv1.5 and minK mRNA levels in ventricular myocyte total RNA were significantly lower than what was detected in whole heart. Neither Kv4.3 nor Kv 1.2 mRNA transcripts could be separated from background in isolated myocyte total RNA, however, Kv4.3 mRNA expression was very low and Kv1.2 mRNA expression was undetectable in 0-1 day whole ventricle samples.

Fibroblasts were found to have no significant Kv1.5, Kv4.2, Kv4.3, Kv1.4 or Kv1.2 mRNA expression, however, low-level expression of IRK1 and $KvLQT_1$ mRNA and a

significant amount of minK mRNA was detected. Both $KvLQT_1$ and IRK1 mRNAs are abundant in myocytes thus the low-level expression in the fibroblast samples may have resulted from contamination of the fibroblast samples with a small population of myocytes.

The finding that Kv1.5 was not present in fibroblasts eliminates the possibility that the discrepancy between whole heart and myocytes Kv1.5 mRNA levels resulted from a high level of non-myocyte Kv1.5 expression. An alternate explanation for the significant difference in Kv1.5 mRNA expression is that the processes of isolating and/or culturing the myocytes affected the Kv1.5 transcript. Rapid downregulation of Kv1.5 mRNA expression has been described when adult rat ventricular myocytes are cultured over a 3 hour period on 100 mm dishes at low density (Hershman & Levitan, 1998). It was therefore postulated that the large decrease in Kv1.5 mRNA levels observed in the present study might result from culturing the neonatal mouse myocytes at low density.

Increasing cell-cell contact by culturing the myocytes on smaller plates (60 mm) or in 15 ml conical tubes was found to maintain the Kv1.5 mRNA levels in isolated rat ventricular myocytes (Hershman & Levitan, 1998). Thus to determine if the low Kv1.5 mRNA expression in mouse ventricular myocytes was due to maintaining the cells at low-density, we cultured the neonatal mouse myocytes in 15 ml conical tubes (one of the high-density culture systems used by Hershman & Levitan; see Figures 3.20 to 3.27). Kv1.5 mRNA expression was significantly greater in total RNA isolated from myocytes cultured at high-density compared to low-density culture, with the level of Kv1.5 mRNA in high-density myocyte samples being equivalent to the expected whole ventricle expression level (Figure 3.20). This suggests that the apparent discrepancy observed between myocyte and whole ventricle mRNA levels for Kv1.5 was a direct result of the culture conditions used, and that slight modifications to the culture system can have a dramatic impact on the results obtained.

The level of minK mRNA expression was also increased in high-density myocyte cultures, however, the minK levels were not restored to the whole ventricle levels (Figure 3.24). It can therefore be postulated that the large minK mRNA levels detected in whole heart samples may not be due to minK mRNA expression in myocytes alone. Fibroblasts were found to have a significant amount of minK mRNA expression, which may account for some of the disagreement between whole ventricular and myocyte expression levels. Alternately, high levels of minK expression have been localized to cells of the conduction system of the mouse heart (Kupershmidt *et al.*, 1999) which may not be adequately represented in the isolated ventricular myocyte population studied.

It is important to note that the mRNA expression levels for Kv4.2, $KvLQT_1$, and Kv1.4 were significantly lower in the high-density culture system. The reason for this is unknown, however, there is a possibility that there was inadequate oxygen available to the myocyte pellet that formed by gravity at the bottom of the 15 ml tube. Hypoxia has been reported to inhibit gene expression of voltage-gated K^+ channel α-subunits in pulmonary artery smooth muscle cells (Wang *et al.*, 1997). Furthermore, anoxia has been reported to decrease the transient K^+ outward current in isolated ventricular heart cells of the mouse (Thierfelder *et al.*, 1994), which could potentially result from downregulation of K^+ channel α-subunit gene transcription.

Hershman & Levitan (1997) found no change in $KvLQT_1$ mRNA expression between high and low-density systems; however, their incubation time was short (1-3 hours) compared to the 18-24 hour incubation times used in our study. Furthermore, Hershman & Levitan (1998) reported that Kv4.2 mRNA expression was inversely affected by cell-cell contact with high-density culture causing a decrease in Kv4.2 expression compared to low-density culture. Thus, the decreased Kv4.2, $KvLQT_1$ and Kv1.4 mRNA expression in the present study may also be a direct result of cell density. To determine whether the K^+

channel mRNAs were downregulated as a result of insufficient gas exchange as opposed to increased cell-cell contact; a study could be done where the myocytes are plated at high density (on 60 mm plates) instead of culturing them in the 15 ml conical tubes.

Overall the mRNA expression levels of the majority of K^+ channel α-subunits (excluding minK) were comparable in isolated neonatal myocytes and neonatal whole ventricular samples. However, K^+ channel mRNA expression was highly dependent on culture conditions, specifically the density of the cells. Thus, caution must be used when interpreting the data obtained from both *in vivo* and *in vitro* studies of mRNA expression.

4.3. K^+ Channels in the Developing Mouse Heart

It has been demonstrated that distinct changes in the action potential waveform and in excitation-contraction coupling occur in the mammalian myocardium during development (Wetzel & Klitzner, 1996; Nerbonne, 1998). The molecular mechanisms underlying these changes are not fully understood and may involve transcriptional, translational, and/or post-translational modifications of a number of ion channels or antiporters, as well as progressive changes in cellular microanatomy (Wetzel & Klitzner, 1996). The action potentials recorded from neonatal myocytes have a prolonged repolarization phase in most species. The mature, much more rapid repolarization phenotype, does not appear until a few weeks after birth (Adolph, 1966; Wang *et al.*, 1996; Wetzel & Klitzner, 1996; Wang & Duff, 1997). It has been postulated that an increase in the density of the repolarizing K^+ currents is responsible for this phenomena (Nerbonne, 1998).

4.3.1. K^+ channel α-subunit mRNA expression during development

In this study, significant developmental changes in K^+ channel α-subunit mRNA expression were identified in mouse ventricular total RNA (Figures 3.8-3.11). Kv1.5, IRK1, Kv4.2, Kv4.3, and Kv1.2 mRNA levels increased postnatally, in contrast, $KvLQT_1$, minK and Kv1.4 mRNA levels decreased. Developmental expression patterns

of some K^+ channel α-subunits have also been studied in rat ventricle. As in mouse, Kv1.5, Kv4.2 and Kv1.2 were found to increase significantly, and Kv1.4 was found to decrease significantly (Xu *et al.* 1996; Nakamura & Iijima, 1994; Matsubara *et al.*, 1991; 1993).

The temporal pattern of the developmental increases and decreases of some of the K^+ channel mRNA appears to be somewhat different in mouse and rat. The largest mRNA level increases in the developing mouse ventricle occurred between postnatal days 10 and 21 for Kv1.5 and between postnatal days 0-1 and 10 for Kv1.2. Mouse ventricular Kv4.2 mRNA levels showed large increases between both 0-1 and 10 day, and 21 day and adult, while Kv4.3 mRNA levels increased steadily during development. In rat, the timing of the increases for Kv1.2 and Kv1.5 mRNA expression were largest between day 5 and 16 and for Kv4.2 mRNA expression between postnatal day 20 and adult (age groups in study 0, 5, 10, 16, 24, and 30 days; Xu *et al.*, 1996). Xu *et al* (1996) also reported that Kv1.4 mRNA peaked between day 5 and 10 and then steadily decreased during development. In contrast, peak Kv1.4 mRNA levels in mouse ventricles occurred at day 0-1.

4.3.2. Relationship between mRNA levels and electrophysiological findings

4.3.2.1. Kv4.2, Kv4.3 and Kv1.4: I_{to}

Research in several species has shown that the density of the Ca^{2+}-independent transient outward current, I_{to}, increases during postnatal development (Kilborn & Fedida, 1990; Jeck & Boyden, 1992; Nuss & Marban, 1994; Wahler *et al.*, 1994; Sanchez-Chapula, 1994; Guo *et al.*, 1996; Xu *et al.*, 1996; Guo *et al.*, 1997b; Shimoni *et al.*, 1997, Wang & Duff, 1997; Wickenden *et al.*, 1997). As well, it has been reported that postnatal cardiac development involves an increase in the rate of recovery from inactivation of I_{to}, since neonatal I_{to} exhibits a slowly recovering component while the recovery from inactivation of adult I_{to} is rapid with a single fast time constant (Sanchez-Chapula, 1994; Wickenden *et al.*, 1997). It is not known if these changes reflect developmental switches in Kv α and

β-subunits contributing to ventricular I_{to} or age dependent changes in post translational processing of the Kv subunits (Nerbonne, 1998).

Benndorf & Nilius (1988) reported that I_{to} is the dominant repolarizing K^+ current in adult mouse ventricular myocytes. Recently, a detailed analysis of the depolarization-activated K^+ currents in adult mouse ventricular myocytes has been interpreted in terms of there being two distinct I_{to} currents, $I_{to,fast}$ ($I_{to,f}$) and $I_{to,slow}$ ($I_{to,s}$) (Xu *et al.*, 1999). $I_{to,f}$ and $I_{to,s}$ appear to be differently distributed in the adult mouse ventricle with some cells having both I_{to} currents (80% of septum myocytes express $I_{to,f}$ and $I_{to,s}$) while other cells have just one or the other (the apex only has $I_{to,f}$ and 20% of septum cells only have $I_{to,s}$). $I_{to,f}$ was identified as the relatively large I_{to} current that exhibits rapid activation and inactivation and resembles the I_{to} currents reported by others in mouse (Benndorf *et al.*, 1987; Benndorf & Nilius, 1988; Wang & Duff, 1997; Fiset *et al.*, 1997a) and in other species (Campbell *et al.*, 1995; Barry & Nerbonne, 1996; Giles *et al.*, 1996), while $I_{to,s}$ was deemed a novel current which has only been identified in adult mouse ventricle (Barry *et al.*, 1998; Xu *et al.*, 1999).

In newborn mouse ventricular myocytes, $I_{to,f}$ density was found to be low (Nuss & Marban, 1994) and to increase more than fivefold between birth and postnatal day 14. A further small increase is also seen between postnatal day 14 and adult (Wang & Duff, 1997). The postnatal development of $I_{to,s}$ has not been reported to date.

The candidate K^+ channel α-subunits underlying Ca^{2+}-independent transient I_{to} currents in mouse ventricle include Kv4.2, Kv4.3 and Kv1.4. Considerable evidence suggests that Kv4 α-subunits underlie $I_{to,f}$ in mouse and other species (Dixon & McKinnon, 1994; Dixon *et al.*, 1996; Fiset *et al.*, 1997; Johns *et al.*, 1997; Barry *et al.*, 1998). The postnatal increases in both Kv4.2 and Kv4.3 α-subunit mRNA in mouse correlate quite closely with the developmental increase of $I_{to,f}$ described by Wang & Duff (1997). The slowly

inactivating transient outward current $I_{to,s}$ found in adult ventricular myocytes (Xu *et al.*, 1999), however, does not appear to result from Kv4 α-subunit expression since $I_{to,s}$ was recorded in all of the myocytes from transgenic animals expressing the dominant negative construct, Kv4.2W362F (which lack Kv4 α-subunits; Barry *et al.*, 1998).

Kv1.4 α-subunits generate transient K^+ currents that display very slow recovery from inactivation compared to Kv4 subfamily α-subunits (Tseng-Crank *et al.*, 1990, Po *et al.*, 1992). Kv1.4 has been suggested to underlie the endocardium, slow I_{to} in ferret left ventricle (Brahmajothi *et al.*, 1999) and the small, slowly recovering component of I_{to} detected in rat ventricular tissues (septum and right free wall; Wickenden *et al.*, 1999). It could therefore be postulated that Kv1.4 α-subunits generate $I_{to,s}$ in the mouse ventricle (Xu *et al.*, 1999). There is evidence from knock-out mice, homozygous for a truncated Kv1.4 gene that the Kv1.4 gene does not affect the normal cardiac action potential or I_{to} (London *et al.* 1998a). However, this study focused on the fast $I_{to,f}$ current, as opposed to the novel $I_{to,s}$.

In the present study Kv1.4 α-subunit mRNA was found to decrease significantly during development with relatively low levels being present in adult mouse ventricle compared to Kv4.2 and Kv4.3 mRNAs. Presently there is no data available on the postnatal development of the $I_{to,s}$ current in mouse, however, if this current was found to decrease in density during development the possible role of Kv1.4 in underlying mouse ventricular $I_{to,s}$ may be substantiated.

4.3.2.2. Kv1.5 and Kv1.2: I_{sus}

Developmental changes have been reported in a K^+ current described as the ultrarapid component of the delayed rectifier, or more specifically, the rapidly activating, slowly inactivating outward K^+ current, I_{sus} (also called $I_{K,slow}$). In rat, Guo *et al.* (1997a) detected I_{sus} in neonatal rat ventricular myocytes but found it to decrease to nearly undetectable

levels in the adult, while Shimoni *et al.* (1997) reported that I_{sus} remained unchanged during development. In contrast, the I_{sus} current density has been found to increase postnatally in mouse ventricle: neonatal mice have no detectable I_{sus} (C. Fiset and R. Clark, unpublished observations) and adult mice have a prominent slowly inactivating I_{sus}-type current (Xu *et al.*, 1999).

The K^+ channel isoforms which are potential candidates for I_{sus} include Kv1.2 and Kv1.5 (Paulmichl *et al.*, 1991; Roberds & Tamkun, 1991; Fiset *et al.*, 1997b). The kinetics of these two channels are nearly indistinguishable, however, there are major pharmacological differences between Kv1.2 and Kv1.5 in their sensitivity to α-dendrotoxin (α-DTX) and 4-aminopyridine (4-AP). Kv1.5 is relatively insensitive to α-DTX and highly sensitive to 4-AP, while Kv1.2 is highly sensitive to α-DTX and less sensitive to 4-AP (Snyders *et al.*, 1993; Wang *et al.*, 1993; Grissmer *et al.*, 1994). Xu *et al.* (1999) reported that none of the outward K^+ currents in adult mouse ventricles were sensitive to α-DTX. This suggests that Kv1.5 channels, not Kv1.2, underlie I_{sus} in adult mouse ventricle. Furthermore, London *et al.* (1998b) recently characterized transgenic mice expressing a truncated Kv1.1 α-subunit that co-assembles with Kv1.5 α-subunits, such that no Kv1.5 channel proteins are expressed at the cell surface. The functional consequence of blocked Kv1.5 channel expression was inhibition of an I_{sus}-type current ($I_{K,slow}$) in the mouse ventricular myocytes (London *et al.*, 1998b; Zhou *et al.*, 1998).

In the present study, Kv1.5 and Kv1.2 α-subunit mRNAs were both detected in adult mouse ventricle and were found to increase significantly during postnatal development (no Kv1.2 mRNA was detectable in 0-1 day samples). This increase in Kv1.5 mRNA expression correlates closely with the developmental increase in I_{sus} current density. The presence of Kv1.2 mRNA in the mouse ventricle is unexpected since there appears to be no functional Kv1.2 channels, as judged by the absence of α-DTX sensitive currents. The presence of Kv α-subunit mRNA, however, does not necessarily mean that functional Kv

channel proteins are expressed at the cell membrane. Kv channel protein expression and mRNA expression patterns in the rat have been found to be divergent for some channels (e.g. Kv1.5 and Kv 2.1). However, in rat heart the Kv1.2 protein and message levels were found to vary in parallel (Xu *et al.*, 1996; Barry *et al.*, 1995; Guo *et al.*, 1997a).

An alternate explanation for the presence of Kv1.2 α-subunit mRNAs is that functional Kv1.2 α-subunits are present but form heteromultimeric K^+ channels with other Shaker Kv α-subunits (like Kv1.5). The formation of heteromultimeric K^+ channels consisting of α-subunits from different K^+ channel clones has been described (Roberds *et al.*, 1993; Po *et al.*, 1993). These α-DTX insensitive heteromultimers could underlie a component of the rapidly activated slowly inactivating K^+ currents observed. Xu *et al.* (1999) reported that the steady state inactivation for $I_{K,slow}$ has two components which may reflect the fact that there are two molecularly distinct populations of $I_{K,slow}$. It could therefore be postulated that there are distinct populations of Kv1.5 homomultimers and Kv1.5 and Kv1.2 heteromultimers with slightly different kinetics in the mouse.

4.3.2.3. $KvLQT_1$ and minK: I_{Ks}

The slow component of the cardiac delayed rectifier K^+ current, I_{Ks}, changes significantly during development in mouse ventricle (Nuss & Marban, 1994; Wang *et al.*, 1996). I_{Ks} density increases in the late embryonic heart, becoming consistently detectable just before birth (Davies *et al.*, 1996). It then subsequently decreases during postnatal development (Nuss & Marban, 1994; Davies *et al.*, 1996; Wang *et al.*, 1996). I_{Ks} is not a prominent repolarizing current in the adult mouse ventricle (Nerbonne, 1998). In contrast, I_{Ks} plays a major role in action potential repolarization in adult myocytes from other species such as canine, guinea pig, and human (Tseng & Hoffman, 1989; Sanguinetti & Jurkiewicz, 1991; Wang *et al.*, 1994).

From studies in heterologous expression systems, it is evident that $KvLQT_1$ and minK

(Isk) proteins combine to form a slowly activating K^+ current very similar to I_{Ks} (Barhanin *et al.*, 1996; Sanguinetti *et al.*, 1996). Direct biochemical evidence for coassembly of $KvLQT_1$ and minK in the mammalian heart has not been provided to date (Nerbonne, 1998), however, in the inner ear it has been shown that the cytoplasmic C-terminal end of minK interacts directly with the pore region of $KvLQT_1$ creating a very slowly activating K^+ current (Romey *et al.*, 1997). As well, minK-deficient mice have been generated (by homologous recombination of the minK gene with lacZ). The heart cells isolated from these animals were found to have no I_{Ks}, which supports the role for minK in modulating this current (Kupershmidt *et al.*, 1999).

The mRNA levels of both $KvLQT_1$ and minK were found to decrease during postnatal development, with peak levels being detected in 0-1-day-old mouse ventricular tissue. This finding correlates with the functional expression of I_{Ks} being predominantly in neonatal mouse ventricular myocytes, and supports the hypothesis that $KvLQT_1$ and minK underlie I_{Ks} in mouse. Felipe *et al.* (1994) also reported that minK mRNA decreases dramatically during development in the mouse heart. Recently, minK expression has been localized to the conduction system in mouse heart (sinus node region, caudal atrial septum, and proximal conducting system) and its transient expression has been implicated as a key event in conduction system development (Kupershmidt *et al.*, 1999). In contrast, *in situ* hybridization has demonstrated $KvLQT_1$ mRNA in left ventricular cells from all regions of the ferret heart (Brahmajothi *et al.*, 1996; 1997).

4.3.2.4. IRK1(Kir2.1): I_{K1}

The inward rectifier, I_{K1}, is prominent in adult mouse ventricular myocytes and has been reported to change during development in mouse ventricle (Nakamura *et al.*, 1999). Similar increases in the inwardly rectifying K^+ currents of rat and rabbit ventricular myocytes during postnatal development have also been reported (Wahler, 1992; Masuda

& Sperelakis, 1993; Sanchez-Chapula *et al.*, 1994) with this increase in rat ventricle occurring almost entirely between days 3 and 9 to 13 (Wahler, 1992).

IRK1 (or Kir 2.1) is thought to underlie I_{K1} in adult mouse ventricular myocytes (Nakamura *et al.*, 1999). In the present study, IRK1 mRNA was identified at all developmental stages. It increased significantly during development, with the largest increase being detected between 0-1 and 10 day samples. Low IRK1 mRNA expression in fetal mouse ventricular myocytes has been reported (Nakamura *et al.*, 1999) which agrees with the lower neonatal levels identified in my experiments.

4.4. Thyroid Hormone and Postnatal Development of the Mouse Heart

A large increase in the serum levels of thyroid hormone(s) (3,3'5-triiodo-L-thyronine, T_3 and thyroxine, T_4) takes place in mammals shortly after birth. Early neonates are strongly hypothyroid due to a poorly developed hypothalamic pituitary-thyroid axis (Vigouroux, 1976; Dubois & Dussault, 1977). In mice the variation in thyroid hormone levels is complex (D'Albis *et al.*, 1987; Calikoglu *et al.*, 1996), however, the general trend is an increase in T_3 and T_4 levels after birth until day 6 to day 10, followed by a decrease, then a secondary increase reaching a maximum between day 16 and day 20. T_3 and T_4 levels then decrease progressively within the first month of life to the adult values (that are still significantly higher than those of young mice; D'Albis *et al.*, 1987).

Thyroid hormone levels are known to have an effect on cardiac output including specific influences on the electrical activity of the heart (Morkin *et al.*, 1983). For example, in rat and rabbit ventricle, action potential duration is prolonged in hypothyroid animals and is shortened in hyperthyroid animals (Sharp *et al.*, 1985; Di Meo *et al.*, 1991; Shimoni *et al.*, 1997; Wickenden *et al.*, 1997). Several depolarization activated K^+ currents play key roles in determining the amplitude and duration of the cardiac action potential (Campbell *et al.*, 1995; Giles *et al.*, 1996). Thus, changes in action potential duration resulting from

altered thyroid hormone levels may be explained by altered expression of various K^+ currents.

The thyroid hormone surge has been related to a number of physiological and structural changes occurring in various tissues during the postnatal period (Greenberg *et al.*, 1974; Schwartz & Oppenheimer, 1978). Thus, the developmental changes in K^+ currents and expression of K^+ channel α-subunit mRNA and subsequent shortening of the action potential duration may be due to the developmental increase in thyroid hormone. If there is a relationship between thyroid status and postnatal K^+ channel mRNA expression it could be postulated that hypothyroid animals express a neonatal cardiac phenotype, while neonatal myocytes treated with T_3 would express a more "adult-like" phenotype.

4.4.1. Effect of thyroid hormones on K^+ currents

K^+ currents are known to be regulated by hormones and neuropeptides such as glucocorticoids, thyrotrophin releasing hormone, and thyroid hormone (Nerbonne, 1998). Shimoni *et al.* (1992; 1995; 1997) reported that elevations in plasma thyroid hormone levels increased the density of I_{to} in rabbit and rat heart, while hypothyroid conditions decreased I_{to} current amplitude. In contrast, the background inward rectifier current, I_{K1}, and I_{sus} (a rapidly activating slowly inactivating K^+ current) are not changed when thyroid hormone levels are altered in the rat (Shimoni *et al.*, 1997). However, Wickenden *et al.* (1997) have reported that treatment of neonatal rat myocytes in culture with T_3 increased the current density of I_{sus} and accelerated the recovery kinetics of I_{to} but had no effect on the amplitude of I_{to}. Since I_{to} can increase with time in culture, the effects of T_3 on I_{to} may have been obscured (Wickenden *et al.*, 1997). A study of the current-voltage relations in hypothyroid mice (R. Clark, unpublished results) showed that the peak outward K^+ currents were 50% smaller in hypothyroid ventricular myocytes than in controls. More detailed analysis revealed that the magnitudes of I_{sus} and I_{to}, two of the major components

of the total outward K^+ current in mouse ventricle, were both depressed significantly (30% and 50% of the control value, respectively). The current density of I_{K1} was not found to be significantly different between hypothyroid and control ventricular myocytes (R. Clark, unpublished results).

Overall, the effect of thyroid hormone on I_{to} appears to coincide with the developmental changes in these currents discussed previously (Kilborn & Fedida, 1990; Wang *et al.*, 1997; Shimoni *et al.*, 1997; Wickenden *et al.*, 1997). The developmental increase in I_{K1} (Nakamura *et al.*, 1999) does not appear to be related to the T_3 surge since thyroid hormone levels do not modulate this current. Furthermore, the decreased expression of I_{sus} in hypothyroid mice correlates with the low levels of this current in neonatal mouse ventricles (R. Clark, unpublished results). The data available on the regulation of I_{sus} in the rat is conflicting. Developmental decreases (Guo *et al.*, 1997a) as well as no developmental changes (Shimoni *et al.*, 1997) have been reported, and positive thyroid hormone regulation and no effect of thyroid hormone have been observed (Wickenden *et al.*, 1997 and Shimoni *et al*, 1997, respectively).

4.4.2. Effect of thyroid hormones on K^+ channel α-subunit mRNA expression

Thyroid hormone-induced changes in the formation of specific proteins appear to be controlled primarily at the steps regulating the transcription of specific genes and by the influences on the stability of the mRNA in the cytoplasm (Dillmann, 1990). Thyroid hormone-induced effects on K^+ currents would therefore be expected to result from changes in the mRNA levels of the K^+ channel α-subunits that underlie the modulated currents.

Two methodologies were used to evaluate the effects of thyroid hormone on K^+ channel α-subunit mRNA expression in the mouse ventricle. The first approach compared the K^+ channel mRNA expression in normal adult mice versus hypothyroid mice (mice were

made hypothyroid by feeding them a low iodine diet supplemented with the thyroid hormone synthesis inhibitor propylthrouracil, PTU). The second approach studied the effect of directly adding 100 nM T_3 to isolated neonatal mouse myocardial cells maintained in serum-free medium.

4.4.2.1. K^+ channel α-subunit mRNA expression in hypothyroid ventricles

The mRNA expression levels of $KvLQT_1$, minK, Kv1.2 and Kv1.4 were all found to be significantly greater (37%, 61%, 17%, and 31% increased, respectively, see Figures 3.1.4 and 3.15) in mice on a hypothyroid diet than in age-matched control animals. However, Kv1.5, Kv4.2, Kv4.3 and IRK1 mRNA levels were not significantly different in the treated and control mice (see Figures 3.12 and 3.13).

Similar studies have been completed in rats made hypothyroid by treatment with either PTU or methimazole (MMI, another thyroid hormone synthesis inhibitor). Abe *et al.* (1998) reported large increases in Kv1.2 and Kv1.4 (51% and 86%, respectively) and a large decrease in Kv1.5 (80%) mRNA levels with no change in Kv4.2 in adult rats treated with PTU compared to controls. Nishiyama *et al.* (1997; 1998) observed similar changes in Kv1.2, Kv1.4 and Kv1.5 mRNA expression levels with no significant effect on Kv4.3 levels in MMI-treated adult rats, but in contrast found decreased Kv4.2 (61% of the control value) mRNA levels. Recently, Ojamaa *et al.* (1999) reported a 70% decrease in Kv1.5 mRNA in ventricles of PTU-treated rats.

The findings summarized above suggest that Kv1.4 and Kv1.2 are regulated similarly by thyroid hormone in the mouse and rat ventricle. However, there are some apparent discrepancies in the effect of hypothyroidism on the Kv4 and Kv1.5 α-subunit mRNA expression levels between species, and also between studies of the same species. For example, Kv1.5 mRNA expression appears to be highly regulated by thyroid hormone in rat ventricle but no apparent effect was detected in mouse ventricle. This may suggest that

there are thyroid hormone response elements on rat ventricular Kv1.5 gene and not on the mouse ventricular gene. Alternately, T_3 may be required to stabilize Kv1.5 mRNA transcripts in the rat and under hypothyroid conditions Kv1.5 mRNA levels decline due to increased degradation. Recently, Ojamaa *et al.* (1999) reported that atrial Kv1.5 mRNA content in rat showed no dependence on thyroid status while the ventricle Kv1.5 mRNA was regulated. Different effects of thyroid status on a single transcript are thus plausible, this may explain the lack of effect on mouse Kv1.5 ventricular mRNA.

Electrophysiological recordings from isolated ventricular myocytes from hypothyroid mice revealed that the peak current density of I_{sus} and I_{to} were decreased compared to controls (R. Clark, unpublished results). The finding that hypothyroidism did not effect the levels of Kv1.5 or Kv4 α-subunit mRNA (the K^+ channel α-subunits proposed to underlie I_{sus} and I_{to}, respectively in mouse ventricle, see above discussion) suggests thyroid hormone may regulate these K^+ currents directly at the protein level rather than at the level of gene transcription.

4.4.2.2. Effect of T_3 on myocyte K^+ channel α-subunit mRNA expression

Short-term culture (18-24 hours) of 0-1 day mouse ventricular myocytes in the presence of 100 nM T_3 significantly altered the mRNA expression levels of three of the eight K^+ channel isoforms. Specifically, T_3 addition caused a 33% increase in Kv4.2 mRNA levels (observed in the high-density culture system) compared to control myocytes (see Figure 3.23); while Kv1.4 and $KvLQT_1$ mRNA levels were significantly decreased (50% and 62%, respectively) compared to control (the low-density culture method was employed, see Figures 3.19 and 3.18).

In a comparable study using neonatal rat ventricular myocytes, Wickenden *et al.* (1997) reported that the addition of 100 nM T_3 significantly decreased expression of Kv1.4 mRNA (86%). In contrast, increased expression of Kv4.3 (106%) mRNA was observed

while no change in Kv4.2 mRNA levels were identified in the T_3-treated cells compared to control (Wickenden *et al.*, 1997). This suggests that the Kv1.4 channel may be similarly regulated while the Kv4 channel mRNAs are differently regulated by T_3 in mouse and rats.

Other studies have been completed that investigate the effect of hyperthyroid conditions on rat ventricle K^+ channel mRNA expression *in vivo*. Subcutaneous injection of T_3 was found to significantly increase Kv4.2 and Kv4.3 and decrease Kv1.4 mRNA levels in neonatal (8-day-old) rat pups (Shimoni *et al.*, 1997). However, Abe *et al.* (1998) found that T_3-treatment (by gastric tube) did not increase Kv1.5 or Kv4.2 mRNA or decrease Kv1.4 mRNA expression in adult rats. Similarly, Ojamaa *et al* (1999) reported that T_4 injection did not increase Kv1.5 mRNA expression in adult rats. In a separate study, Nishiyama *et al.* (1998) reported that hyperthyroid conditions caused Kv1.2 and Kv1.4 mRNA levels to significantly decrease and Kv4.2 and Kv1.5 levels to significantly increase over control levels in rats. Note that in the latter study MMI-treated rats were injected with T_4 to induce hyperthyroidism. It has been reported that the expression of T_3-receptors in the hypothyroid myocardium differs from that in the euthyroid (normal) heart (Balkman *et al.*, 1992). The hypothyroid heart is said to have increased sensitivity to thyroid hormones resulting in T_3-induced gene expression that is higher than that observed in the euthyroid heart (Balkman *et al.*, 1992; Ojamaa *et al.*, 1999). This may explain some of the apparent discrepancies in mRNA levels observed between the study by Nishiyama's group (1998) and the studies by Abe *et al* (1998) and Ojamaa *et al* (1999) in rat ventricle.

The age of the rats used may also contribute to the variability between studies since endogenous thyroid hormone levels increase postnatally in the rat (Vigouroux, 1976). Thus, K^+ channel gene expression may be maximally stimulated in adult animals, and no apparent effect of exogenous addition of thyroid hormones would therefore be expected.

4.5. Correlation of mRNA Levels: Development and Thyroid Hormone

In the mouse ventricle, Kv1.5, Kv4.2, Kv4.3, Kv1.2, and IRK1 mRNA levels increased during postnatal development while Kv1.4, $KvLQT_1$, and minK mRNA levels decreased. It was proposed that adult hypothyroid mice would have K^+ channel α-subunit expression patterns similar to those in neonatal mice if the thyroid hormone surge contributed to the developmental changes in K^+ channel α-subunit expression. The results revealed that Kv1.4, $KvLQT_1$ and minK mRNA levels were in fact higher in hypothyroid diet mice, which correlates well with the higher levels observed in neonatal ventricular tissue compared to adult.

The level of Kv1.2 α-subunit mRNA was also increased in hypothyroid animals; however, this change does not correlate well with the developmental regulation of this transcript which increases postnatally from near zero levels at birth. The other K^+ channel α-subunit mRNA levels, however, were not significantly lower in the hypothyroid animals compared to control as was expected. This suggests that the developmental increase of these K^+ channel α-subunits is not dependent on thyroid hormone, since normal adult mRNA levels were attained in absence of T_3 throughout postnatal development.

The second method used to determine if thyroid hormone may be responsible for the developmental changes in K^+ channel mRNA expression was addition of T_3 to neonatal myocytes. If thyroid hormone is responsible for the developmental changes in K^+ channel mRNA expression, addition of T_3 to neonatal mouse ventricular myocytes would be expected to produce more adult-like mRNA levels in the neonatal cells.

The levels of Kv1.4 and $KvLQT_1$ mRNA were again found to modulated by thyroid hormone status. Both transcripts decreased upon T_3 addition, which correlates well with

the developmental decreases observed. T_3 treatment also caused a significant increase in Kv4.2 mRNA expression, which corresponds with the developmental increase of this transcript reported in whole mouse ventricle. However, this finding conflicts with the data obtained from the hypothyroid mice that suggested Kv4.2 mRNA is not regulated by thyroid hormone. A possible explanation for this finding is that in the absence of thyroid hormones other factors regulate the postnatal increase in Kv4.2 α-subunit expression thereby compensating for the lack of thyroid hormones.

Kv1.5, Kv4.3, Kv1.2, IRK1 and minK mRNA expression levels in neonatal ventricular myocytes were not influenced by addition of T_3 suggesting that they are not modulated by thyroid hormone. The lack of effect of T_3 on minK mRNA levels did not correlate well with the large increase observed in hypothyroid ventricles. This discrepancy may result from the fact that minK expression is localized to cells of the conduction system of the mouse heart (Kupershmidt *et al.*, 1999) which may not be adequately represented in the isolated ventricular myocytes studied. Note that minK mRNA expression levels were greatly reduced in isolated myocytes compared to whole ventricle in both culture systems.

In summary, thyroid hormone treatment resulted in changes in mRNA levels for the Kv4.2, Kv1.4, $KvLQT_1$, and minK transcripts somewhat similar to those seen during development. However, our data suggests that thyroid hormone is not the only factor controlling K^+ channel mRNA expression levels during development in the mouse heart.

4.6. Limitations of Study and Future Directions

Overall RPA is a powerful technique for the identification of rare messages such as those for ion channels (Dixon & McKinnon, 1994; Wickenden *et al.*, 1999). Using RPA, we were able to evaluate the mRNA expression level of eight K^+ channel α-subunits in a variety of ventricular muscle samples and in isolated ventricular cells. The ultimate goal of the present study was to correlate the molecular information obtained at the mRNA

level with functional studies of the K^+ currents. It must therefore be remembered that the presence of mRNA does not guarantee the presence of the encoded protein. mRNA mapping only provides information on the cell specificity of K^+ channel gene expression (Deal *et al.*, 1996). Further work at the protein level is required to provide more concrete evidence to correlate specific currents with identified K^+ channel isoforms.

In the future, localizing K^+ channel mRNA and protein expression to specific areas of the heart will be increasingly important since a significant amount of regional variability in K^+ currents has been described (Wickenden *et al.*, 1999; Xu *et al.*, 1999). Immunohistochemistry techniques (using specific K^+ channel antibodies) combined with *in situ* hybridization studies (using specific K^+ channel probes) will be useful tools to permit localization of selected K^+ channels in specific cells/tissues of the heart. As well, methodologies, such as quantitative competitive-PCR and laser-assisted cell picking, will enable absolute quantitation of mRNA species to be made in a single cell type (Fink *et al.*, 1998). This type of technology has the potential to yield much more accurate information (moles of mRNA per specific cell type) compared to the currently used RPA studies that reflect average expression of mRNA in a whole tissue (containing heterogeneous cell types) relative to a housekeeping gene (Fink *et al.*, 1998).

The use of transgenic mice and dominant negative strategies have recently become very powerful tools for the dissection of the role of individual K^+ channel genes in cardiac electrophysiology (Barry *et al.*, 1998; Kupershmidt *et al.*, 1998; London *et al.*, 1998a; 1998b). Accordingly, further gene knockout studies, including every identified K^+ channel α- and β-subunits in cardiac tissue, could be employed to gain more insight into the specific function and importance of each isoform. Ultimately, the information obtained from these types of specific gene-targeting studies, in combination with detailed molecular and functional analyses, should eventually lead to the elucidation of the exact molecular basis of the K^+ currents in the mouse heart.

4.7. Overall Relevance

Changes in the properties and densities of voltage-gated K^+ currents have been identified in a variety of cardiovascular disorders including myocardial infarction and cardiac arrhythmias (Gidh-Jain *et al.*, 1994; Van Waghoner *et al.*, 1997). It is therefore of interest to determine the molecular correlates underlying the voltage-gated K^+ currents in the heart. Advances in molecular, cellular and genetically based technologies have created the possibility of generating genetically engineered mice having physiological phenotypes with direct relevance to human pathological states (Chien, 1995). For example, cardiovascular abnormalities including hypertension, hypertrophy, and some cardiomyopathies (Boyden & Jeck, 1995; Kubalak *et al.*, 1996; Ackerman & Clapham, 1997) have begun to be evaluated using transgenic mouse models. Thus, determining the molecular basis of the cardiac action potential in mice and humans is important to help determine if complex cardiac disease phenotypes can result from direct mutations or altered regulation of individual ion channel genes. As well, knowledge of the molecular basis of the cardiac action potential in health and disease, and the potential to develop models of the disease in the mouse, are useful apparatuses for testing gene-targeted drug therapies.

Understanding the electrophysiological properties of neonatal myocytes and the factors that can regulate postnatal cardiac development (such as thyroid hormone) are also of interest since re-expression of a neonatal genetic program is a common feature of cardiac hypertrophy and failure (Lompre *et al.*, 1979; Schwartz *et al.*, 1986).

Overall, the continued evaluation of the voltage-gated K^+ channels responsible for repolarization of the cardiac action potential and maintaining the resting membrane potential is warranted. The continued use of multidisciplinary approaches make it likely that the details of the mouse cardiac action potential will be resolved in the near future.

5. REFERENCES

ABE, A., YAMAMOTO, T., ISOME, M., MA, M., YAOITA, E., KAWASAKI, K., KIHARA, I. & AIZAWA, Y. (1998). Thyroid hormone regulates expression of shaker-related potassium channel mRNA in rat heart. *Biochem. Biophys. Res. Commun.* **245**, 226-230.

ACKERMAN, M.J. & CLAPHAM, D.E. (1997). Ion channels - Basic science and clinical disease. *New Engl. J. Med.* **336**, 1575-1586.

ADOLPH, E.F. (1966). Ranges of heart rates and their regulations at various ages (rat). *Am. J. Physiol.* **212**, 595-602.

ALTSCHUL, S.F., GISH, W., MILLER, W., MYERS, E.W. & LIPMAN, D.J. (1990). Basic local alignment search tool. *J. Mol. Bio.* **215**, 403-410.

APKON, M. & NERBONNE, J.M. (1991). Characterization of two distinct depolarization-activated K^+ currents in isolated adult rat ventricular myocytes. *J. Gen. Physiol.* **97**, 973-1101.

ATTALI, B., LESAGE, F., ZILIANI, P., GUILLEMARE, E., HONORE, E., WALDMANN, R., HUGNOT, J.P., MATTEI, M.G., LAZDUNSKI, M. & BARHANIN, J. (1993). Multiple mRNA isoforms encoding the mouse cardiac Kv1.5 delayed rectifier K^+ channel. *J. Biol. Chem.* **268**, 24283-24289.

ATTALI, B., GUILLEMARE, E., LESAGE, F., HONORE, E., ROMEY, G., LAZDUNSKI, M. & BARHANIN, J. (1993). The protein IsK is a dual activator of K^+ and Cl^- channels. *Nature* **365**, 850-852.

ATTALI, B. (1996). Ion channels. A new wave for heart rhythms. *Nature* **384**, 24-25.

BALKMAN, C., OJAMAA, K. & KLEIN, I. (1992). Time course of the *in vivo* effects of thyroid hormone on cardiac gene expression. *Endocrinol.* **130**, 2001-2006.

BARHANIN, J., LESAGE, F., GUILLEMARE, E., FINK, M., LAZDUNSKI, M. & ROMEY, G. (1996). K(V)LQT1 and lsK (minK) proteins associate to form the I(Ks) cardiac potassium current. *Nature* **384**, 78-80.

BARRY, D.M., TRIMMER, J.S., MERLIE, J.P. & NERBONNE, J.M. (1995). Differential expression of voltage-gated K^+ channel subunits in adult rat heart. Relation to functional K^+ channels? *Circ. Res.* **77**, 361-369.

BARRY, D.M. & NERBONNE, J.M. (1996). Myocardial potassium channels: electrophysiological and molecular diversity. *Ann. Rev. Physiol.* **58**, 363-394.

BARRY, D.M., XU, R.B., SCHUESSLER, R.B. & NERBONNE, J.M. (1998). Functional knockout of the cardiac transient outward current, long QT syndrome and cardiac remodeling in mice expressing a dominant negative Kv4 α subunit. *Circ. Res.* **83**, 560-567.

BECKER, K.D., GOTTSHALL, K.R. & CHIEN, K.R. (1996). Strategies for studying cardiovascular phenotypes in genetically manipulated mice. *Hypertension* **27**, 495-501.

BEN-YEHUDA, O. & ROCKMAN, H.A. (1996). Regulation of myocardial contractility: Insights from transgenic mice. *Trends Cardiovasc. Med.* **6**, 95-99.

BENNDORF, K., MARKWARDT, F. & NILUS, B. (1987). Two types of transient outward currents in cardiac ventricular cells of mice. *Pflugers Archiv.* **409**, 641-643.

BENNDORF, K. & NILUS, B. (1988). Properties of an early outward current in single cells of the mouse ventricle. *Gen. J. Physiol. Biophys.* 7, 449-466.

BLAIR, T.A., ROBERDS, S.L., TAMKUN, M.M. & HARTSHORNE, R.P. (1991). Functional characterization of RK5, a voltage-gated K^+ channel cloned from the rat cardiovascular system. *FEBS Letters.* **295**, 211-213.

BOOZ, G.W. & BAKER, K. (1995). Molecular signalling mechanisms controlling growth and function of cardiac fibroblasts. *Cardiovasc. Res.* **30**, 537-543.

BOYDEN, P.A. & JECK, C.D. (1995). Ion channel function in disease. *Cardiovasc. Res.* **29**, 312-318.

BRAHMAJOTHI, M.V., MORALES, M.J., RASMUSSON, R.L., CAMPBELL, D.L. & STRAUSS, H.C. (1997). Heterogeneity in K^+ channel transcript expression detected in isolated ferret cardiac myocytes. *Pacing Clin. Electrophysiol.* **20**, 388-396.

BRAHMAJOTHI, M.V., CAMPBELL, D.L., RASMUSSON, R.L., MORALES, M.J., TRIMMER, J.S., NERBONNE, J.M. & STRAUSS, H.C. (1999). Distinct transient outward potassium current (Ito) phenotypes and distribution of fast-inactivating potassium channel alpha subunits in ferret left ventricular myocytes. *J. Gen. Physiol.* **113**, 581-600.

BREITWIESER, G.E. (1996). Mechanism of K^+ channel regulation. *J. Membr. Biol.* **152**, 1-11.

CALIKOGLU, A.S., GUTIERREZ-OSPINA, G. & D'ERCOLE, A.J. (1996). Congenital hypothyroidism delays the formation and retards the growth of the mouse primary somatic sensory cortex (S1). *Neurosci. Lett.* **213**, 132-136.

CAMPBELL, D.L., RASMUSSON, R.L., COMER, M.B. & STRAUSS, H.C. (1995). The cardiac calcium-independent transient outward potassium current: kinetics, molecular properties, and role in ventricular repolarization. In *Cardiac Electrophysiology: From Cell to Bedside*, eds. ZIPES, D. & JALIFE, J., pp. 83-96. Philadelphia: W.B. Saunders Co.

CARMELIET, E. (1993). Mechanisms and control of repolarization. *Euro. Heart J.* **14**, Suppl-13

CHANDY, K.G., GHANSHANI, S., TEMPEL, B.L. & GUTMAN, G.A. (1990). A family of three mouse potassium channel genes with intronless coding regions. *Science* **247**, 943-975.

CHANDY, K.G. (1991). Simplified gene nomenclature. *Nature* **352**, 26

CHANDY, K.G. & GUTMAN, G.A. (1993). Nomenclature for mammalian potassium channel genes. *TIPS.* **14**, 434

CHIEN, K.R. (1995). Cardiac muscle diseases in genetically engineered mice: evolution of molecular physiology. *Am. J. Physiol.* **269**, H755-H766

CHRISTENSEN, G., WANG, Y. & CHIEN, K.R. (1997). Physiological assessment of complex cardiac phenotypes in genetically engineered mice. *Am. J. Physiol.* **272**, H2513-H2524

CHRISTIE, M.J., NORTH, R.A., OSBORN, P.B., DOUGLASS, J. & ADELMAN, J.P. (1990). Heteropolymeric potassium channels expressed in Xenopus oocytes from cloned subunits. *Neuron* **2**, 405-411.

CLARK, R.B., BOUCHARD, R.A., SALINAS-STEFANON, E., SANCHEZ-CHAPULA, J. & GILES, W.R. (1993). Heterogeneity of action potential waveforms and potassium currents in rat ventricle. *Cardiovasc. Res.* **27**, 1795-1799.

CLARK, W.A., DECKER, M.L., BEHNKE-BARCLAY, M., JANES, D.M. & DECKER, R.S. (1998). Cell contact as an independent factor modulating cardiac myocyte hypertrophy and survival in long-term primary culture. *J. Mol. Cell Cardiol.* **30**, 139-155.

COVARRUBIAS, M., WEI, A. & SALKOFF, L. (1991). Shaker, Shal, Shab, and Shaw express independent K^+ current systems. *Neuron* **7**, 763-773.

D'ALBIS, A., LENFANT-GUYOT, M., JANMOT, C., CHANOINE, C., WEINMAN, J. & GALLIEN, C.L. (1987). Regulation by thyroid hormones of terminal differentiation in the skeletal dorsal muscle. *Developmental Bio.* **123**, 25-32.

DAVIES, M.P., AN, R.H., DOEVENDANS, P.A., KUBALAK, S.W. & CHIEN, K.R. (1996). Developmental changes in ionic channel activity in the embryonic murine heart. *Circ. Res.* **78**, 15-25.

DEAL, K.K., ENGLAND, S.K. & TAMKUN, M.M. (1996). Molecular physiology of cardiac potassium channels. *Physiol. Rev.* **76**, 49-67.

DI MEO, S., DE MARINO ROSAROLL, P. & DE LEO, T. (1991). Thyroid state and electrical properties of rat papillary muscle fibers. *Arch. Int. Physiol. Biochim. Biophys.* **99**, 377-383.

DILLMANN, W. (1990). Biochemical basis of thyroid hormone action in the heart. *Am. J. Med.* **88**, 626-630.

DIXON, J.E. & MCKINNON, D. (1994). Quantitative analysis of potassium channel mRNA expression in atrial and ventricular muscle of rats. *Circ. Res.* **75**, 252-260.

DIXON, J.E., SHI, W., WANG, H.S., MCDONALD, C., YU, H., WYMORE, R.S., COHEN, I.S. & MCKINNON, D. (1996). Role of the Kv4.3 K^+ channel in ventricular muscle. A molecular correlate for the transient outward current [published erratum appears in Circ Res 1997 Jan;80(1):147]. *Circ. Res.* **79**, 659-668.

DOUPNIK, C.A., DAVIDSON, N. & LESTER, H.A. (1995). The inward rectifier potassium channel family. *Current Opin. Neurobiol.* **5**, 268-277.

DRICI, M., ARRIGHI, I., CHOUABE, C., MANN, J.R., LAZDUNSKI, M., ROMEY, G. & BARHANIN, J. (1998). Involvement of IsK-associated K^+ channel in heart rate control of repolarization in a murine engineered model of Jervell and Lange-Nielsen Syndrome. *Circ. Res.* **83**, 95-102.

DUBOIS, J.D. & DUSSAULT, J.H. (1977). Ontogenesis of thyroid function in the neonatal rat. Thyroxine (T4) and triiodothyronine (T3) production rates. *Endocrinol.* **101**, 435-440.

ESCANDE, D., COULOMBE, A., FAIVRE, J.F., DEROUBAIX, E. & CORABOEUF, E. (1985). Two types of transient outward currents in adult human atrial cells. *Am.J.Physiol.* **252**, H142-H148

FEDIDA, D. & GILES, W.R. (1991). Regional variations in action potentials and transient outward current in myocytes isolated from rabbit left ventricle. *J. Physiol.* **442**, 191-201.

FELIPE, A., KNITTLE, T.J., DOYLE, K.L., SNYDERS, D.J. & TAMKUN, M.M. (1994). Differential expression of Isk mRNAs in mouse tissue during development and pregnancy. *Am. J. Physiol.* **267**, C700-C705

FENG, J., WIBLE, B., LI, G.R., WANG, Z. & NATTEL, S. (1997). Antisense oligonucleotides directed against Kv1.5 mRNA specifically inhibit ultrarapid delayed rectifier K^+ current in cultured adult human atrial myocytes. *Circ. Res.* **80**, 572-579.

FINK, L., SEEGER, W., ERMERT, L., HANZE, J., STAHL, U., GRIMMINGER, F., KUMMER, W. & BOHLE, R.M. (1998). Real-time quantitative RT-PCR after laser-assisted cell picking. *Nature Med.* **4**, 1329-1333.

FISET, C., CLARK, R.B., SHIMONI, Y. & GILES, W.R. (1997a). Shal-type channels contribute to the Ca^{2+}-independent transient outward K^+ current in rat ventricle. *J. Physiol.* **500**, 51-64.

FISET, C., CLARK, R.B., LARSEN, T.S. & GILES, W.R. (1997b). A rapidly activating sustained K^+ current modulates repolarization and excitation-contraction coupling in adult mouse ventricle. *J. Physiol.* **504**, 557-563.

FOLANDER, K., SMITH, J.M., ANTANAVAGE, J., BENNETT, C., STEIN, R.B. & SWANSON, R. (1990). Cloning and expression of the delayed rectifier IsK channel from neonatal rat heart and diethylstilbestrol-primed rat uterus. *Proc. Natl. Acad. Sci.* **87**, 2975-2979.

FOZZARD, H.A. (1994). Cardiac electrogenesis and the sodium channel. In *Cardiovascular system: Function and dysfunction*, eds. SPOONER, P.M. & BROWN, A.M., pp. S1-99. Mount Krisco, New York: Futura.

FREEMAN, L.C. & KASS, R.S. (1993). Expression of a minimal K^+ channel protein in mammalian cells and immunolocalization in Guinea Pig heart. *Circ. Res.* **73**, 968-973.

GIDH-JAIN, M., HUANG, B., JAIN, P. & EL-SHERIF, N. (1996). Differential expression of voltage-gated K^+ channel genes in left ventricular remodeled myocardium after experimental myocardial infarction. *Circ. Res.* **79**, 669-675.

GILES, W.R. & IMAIZUMI, Y. (1988). Comparison of potassium currents in rabbit atrial and ventricular cells. *J. Physiol.* **405**, 123-145.

GILES, W.R. (1989). Intracellular electrical activity in the heart. In *Textbook of Physiology*, eds. PATTON, H.D., FUCHS, A.F., HILLE, B., SCHER, A.M. & STEINER, R., pp. 782-795. Philidelphia: W.B. Saunders.

GILES, W.R., CLARK, R.B. & BRAUN, A.P. (1996). Ca^{2+}-independent transient outward current in mammalian heart. In *Molecular Physiology and Pharmacology of Cardiac Ion Channels and Transporters*, eds. MORAD, M., KURACHI, Y., NOMA, A. & HOSADA, M., pp. 141-168. Amsterdam: Kluwer Press.

GINTANT, G.A., COHEN, I.S., DATYNER, N.B. & KLINE, R.P. (1992). Time-dependent outward currents in the heart. In *The heart and cardiovascular system*, eds. FOZZARD, H.A., JENNINGS, R.B., HABER, E., KATZ, A.M. & MORGAN, H.E., pp. 1121-1169. New York: Raven Press.

GINTER, H.B., BAILEY, K. & ROHAN, R.M. (1994). Overlapping protection assay due to complementary vector sequences. *Biotech.* **16**, 584-585.

GREENBERG, A.H., NAJJAR, S. & BLIZZARD, R.M. (1974). Effects of thyroid hormone on growth, differentiation and development. In *Handbook of Physiology*, eds. GREER, M.A. & SOLOMON, D.H., pp. 377-389. Washington: Amer. Physiol. Soc.

GRISSMER, S., NGUYEN, A.N., AIYAR, J., HANSON, D.C., MATHER, R.J., GUTMAN, G.A., KARMILOWICZ, M.J., AUPERIN, D.D. & CHANDY, K.G. (1994). Pharmacological characterization of five cloned voltage-gated K^+ channels, types Kv1.1, 1.2, 1.3, 1.5, and 3.1, stably expressed in mammalian cell lines. *Mol. Pharmacol.* **45**, 1227-1234.

GUO, W., KAMIYA, K. & TOYAMA, J. (1996). Modulated expression of transient outward current in cultured neonatal rat ventricular myocytes: comparison with development in situ. *Card. Res.* **32**, 524-533.

GUO, W., KAMIYA, K. & TOYAMA, J. (1997). Roles of the voltage-gated K^+ channel subunits, Kv 1.5 and Kv 1.4, in the developmental changes of K^+ currents in cultured neonatal rat ventricular cells. *Pflugers Archiv.* **434**, 206-208.

GUO, W., KAMIYA, K., LIU, S. & TOYAMA, J. (1997). Developmental changes of the ultrarapid delayed rectifier K^+ current in rat ventricular myocytes. *Pflugers Archiv.* **434**, 206-208.

GUSTAFSON, T.A., MARKHAM, B.E., BAHL, J.J. & MORKIN, E. (1987). Thyroid hormone regulates expression of a transfected α-myosin heavy chain fusion gene in fetal heart cells. *Nat. Acad. Sci. U.S.A.* **84**, 3122-3126.

HEIDBUCHEL, H., VEREECKE, J. & CARMELIET, E. (1990). Three different potassium channels in human atrium. Contribution to the basal potassium conductance. *Circ. Res.* **66**, 1277-1286.

HERSHMAN, K.M. & LEVITAN, E.S. (1998). Cell-cell contact between adult rat cardiac myocytes regulates Kv1.5 and Kv4.2 K^+ channel mRNA expression. *Am. J. Physiol.* **275**, C1473-C1480

HO, K., NICHOLS, C.G., LEDERER, W.J., LYTTON, J. & VASSELEV, P.M. (1993). Cloning and expression of an inwardly rectifying ATP-regulated potassium channel. *Nature* **362**, 31-38.

HOFFMAN, B.F. & CRANEFIELD, P.F. (1960). *Electrophysiology of the heart.* New York: McGraw-Hill Book Co.

HONORE, E., ATTALI, B., ROMEY, G., HEURTEAUX, C., RICARD, P., LESAGE, F., LAZDUNSKI, M. & BARHANIN, J. (1991). Cloning, expression, pharmacology and regulation of a delayed rectifier K^+ channel in mouse heart. *EMBO J.* **10**, 2805-2811.

HYDE, A., BLONDEL, B., MATTER, A. & CHENEVAL, J.P. (1969). Homo- and heterocellular junctions in cell cultures: An electrophysiological and morphological study. *Prog. Brain. Res.* **31**, 283-311.

IIZUKA, M., KUBO, Y., TSUNENARI, I., PAN, C.X., AKIBA, I. & KONO, T. (1995). Functional characterization and localization of a cardiac-type inwardly rectifying K^+ channel. *Receptors & Channels* **3**, 299-315.

ISACOFF, E.Y., JAN, Y.N. & JAN, L.Y. (1990). Evidence for the formation of heteromultimeric potassium channels in Xenopus oocytes. *Nature* **345**, 530-534.

ISHII, K., YAMAGISHI, T. & TAIRA, N. (1994). Cloning and functional expression of a cardiac inward rectifier K^+ channel. *FEBS Letters.* **338**, 107-111.

ISOM, L.L., DEJOGH, K.S. & CATTERALL, W.A. (1994). Auxiliary subunits of voltage-gated ion channels. *Neuron* **12**, 1183-1194.

JAN, L.Y. & JAN, Y.N. (1992). Structural elements involved in specific K^+ channel functions. *Ann. Rev. Physiol.* **54**, 537-555.

JANVIER, N.C. & BOYETT, M.R. (1996). The role of Na-Ca exchange current in the cardiac action potential. *Cardiovasc. Res.* **32**, 69-84.

JECK, C.D. & BOYDEN, P.A. (1992). Age-related appearance of outward currents may contribute to developmental differences in ventricular repolarization. *Circ. Res.* **71**, 1390-1403.

JOHNS, D.C., NUSS, H.B. & MARBAN, E. (1997). Suppression of neuronal and cardiac transient outward currents by viral gene transfer of dominant-negative Kv4.2 constructs. *J. Biol. Chem.* **272**, 31598-31603.

KAAB, S., DIXON, J.E., DUC, J., ASHEN, D., NABAUER, M., BEUCKELMANN, D.J., STEINBECK, G., MCKINNON, D. & TOMASELLI, G.F. (1998). Molecular basis of transient outward potassium current downregulation in human heart failure: a decrease in Kv4.3 mRNA correlates with a reduction in current density. *Circulation* **98**, 1383-1393.

KAMITANI, T., IKEDA, U., MUTO, S., KAWAKAMI, K., NAGANO, K., TSURUYA, Y., OGUCHI, A., YAMAMOTO, K., HARA, Y., KOJIMA, T., MEDFORD, R.M. & SHIMADA, K. (1992). Regulation of Na/K-ATPase gene expression by thyroid hormone in rat cardiomyocytes. *Circ. Res.* **71**, 1757-1764.

KATZ, A.M. (1993). Cardiac ion channels. *New Engl. J. Med.* **328** , 1244-1251.

KILBORN, M.J. & FEDIDA, D. (1990). A study of the developmental changes in rat ventricular myocytes. *J. Physiol.* **430**, 37-60.

KLEIN, I. (1990). Thyroid hormone and the cardiovascular system. *Am. J. Med.* **88**, 631-637.

KLEMPERER, J.D., KLEIN, I. & OJAMAA, K. (1996). Thyroid hormone therapy in cardiovascular disease. *Prog. Cardiovasc. Dis.* **38**, 329-336.

KRIEG, P.A. & MELTON, D.A. (1987). In vitro RNA synthesis with SP6 RNA polymerases. *Meth. Enzymol.* **55**, 397-415.

KUBALAK, S.W., DOEVENDANS, P.A., ROCKMAN, H.A., HUNTER, J.J., TANAKA, N., ROSS, J.Jr. & CHIEN, K.R. (1996). Molecular analysis of cardiac muscle diseases via mouse genetics. In *Methods in Molecular Genetics*, ed. ADOLPH, K.W., pp. 470-487. San Diego: Academic Press.

KUBO, Y., BALDWIN, T.J., JAN, Y.N. & JAN, L.Y. (1993). Primary structure and functional expression of mouse inward rectifier potassium channel. *Nature* **362**, 127-133.

KUPERSHMIDT, S., YANG, T., ANDERSON, M.E., WESSELS, A., NISWENDER, K.D., MAGNUSON, MA & RODEN, D.M. (1999). Replacement by homologous recombination of the minK gene with lacZ reveals restriction of minK expression to the mouse cardiac conduction system. *Circ. Res.* **84**, 146-152.

LESAGE, F., ATTALI, B., LAZDUNSKI, M. & BARHANIN, J. (1992). IsK, a slowly activation voltage-sensitive K^+ channel. Characterization of multiple cDNA and gene organization in the mouse. *FEBS Letters* **301**, 168-172.

LEVITAN, E.S., HERSHMAN, K.M., SHERMAN, T.G. & TAKIMOTO, K. (1996). Dexamethasone and stress upregulated Kv1.5 K^+ channel expression in rat ventricular myocytes. *Neuropharmacol.* **35**, 1001-1006.

LEVITAN, E.S. & TAKIMOTO, K. (1998). Dynamic regulation of K^+ channel gene expression in differentiated cells. *J. Neurobiol.* **37**, 60-68.

LINDBLAD, D.S., MURPHEY, C.R., CLARK, J.W. & GILES, W.R. (1996). A model of the action potential and underlying membrane currents in a rabbit atrial cell. *Am. J. Physiol* **271**, H1666-H1696

LOMPRE, A.M., SCHWARTZ, K., SWYNGHEDAUW, A., LACOMBE, G., VAN THEIM, N. & SWYNGHEDAUW, B. (1979). Myosin iso-enzyme distribution in chronic heart overload. *Nature* **282**, 105-107.

LONDON, B., WANG, D.W., HILL, J.A. & BENNETT, P.B. (1998a). The transient outward current in mice lacking the potassium channel gene Kv1.4. *J. Physiol.* **509**, 171-182.

LONDON, B., JERON, A., ZHOU, J., BUCKETT, P., HAN, X., MITCHELL, G.F. & KOREN, G. (1998b). Long QT and ventricular arrhythmias in transgenic mice expressing the N terminus and first transmembrane segment of a voltage-gated potassium channel. *Proc. Natl. Acad. Sci.* **95**, 2926-2931.

MACKINNON, R. (1991). Determination of the subunit stoichiometry of a voltage-activated potassium channel. *Nature* **350**, 232-235.

MANIATIS, T., FRITSCH, E.F. & SAMBROOK, J. (1982). *Molecular Cloning: A laboratory manual*. Cold Spring Harbor: Cold Spring Harbor Laboratory Press.

MASUDA, H. & SPERELAKIS, N. (1993). Inwardly rectifying potassium currents in rat fetal and neonatal ventricular cardiomyocytes. *Am. J. Physiol* **265**, H1107-H1111

MATHUR, R., ZHENG, J., YAN, Y. & SIGWORTH, F.J. (1997). Role of the S3-S4 linker in Shaker potassium channel activation. *J. Gen. Physiol.* **109**, 191-199.

MATSUBARA, H., LIMAN, E.R., HESS, P. & KOREN, G. (1991). Pretranslational mechanisms determine the type of potassium channel expressed in the rat skeletal and cardiac muscles. *J. Biol. Chem.* **266**, 13324-13328.

MATSUBARA, H., SUZUKI, J. & INADA, M. (1993). Shaker-related potassium channel, Kv1.4, mRNA regulation in cultured rat heart myocytes and differential expression of Kv1.4 and Kv1.5 genes in myocardial development and hypertrophy. *J. Clin. Invest.* **92**, 1659-1666.

MILANO, C.A., ALLAN, L.F., ROCKMAN, H.A., DOLBER, P.C., MCMINN, T.R., CHIEN, K.R., JOHNSON, T.D., BOND, R.A. & LEFKOWITZ, R.J. (1994). Enhanced myocardial function in transgenic mice over expressing the b_2-adrenergic receptor. *Science* **264**, 582-586.

MORKIN, E., FLINK, I.L. & GOLDMAN, S. (1983). Biochemical and physiological effects of thyroid hormone on cardiac performance. *Prog. Cardiovasc .Dis.* **25**, 435-464.

NAKAMURA, T.Y. & IIJMA, T. (1985). Postnatal changes in mRNA expression in the K^+ channel in rat cardiac ventricles. *Jpn. J. Pharmacol.* **66**, 489-492.

NAKAMURA, T.Y., LEE, K.S., ARTMAN, M., RUDY, B. & COETZEE, W.A. (1999). The role of Kir2.1 in the genesis of native cardiac inward-rectifier K^+ currents during pre- and postnatal development. *Ann. NY Acad. Sci.* **868**, 434-437.

NERBONNE, J.M. (1998). Regulation of voltage-gated K^+ channel expression in the developing mammalian myocardium. *J. Neurobiol.* **37**, 37-59.

NICHOLS, C.G., MAKHINA, E.N., PEARSON, W.L., SHA, Q. & LOPATIN, A.N. (1996). Inward rectification and implications for cardiac excitability. *Circ. IRes.* **78**, 1-7.

NISHIYAMA, A., KAMBE, F., KAMIYA, K., YAMAGUCHI, S., MURATA, Y., SEO, H. & TOYAMA, J. (1997). Effects of thyroid and glucocorticoid hormones on Kv1.5 potassium channel gene expression in the rat left ventricle. *Biochem. Biophysic. Res. Commun.* **237**, 521-526.

NISHIYAMA, A., KAMBE, F., KAMIYA, K., SEO, H. & TOYAMA, J. (1998). Effect of thyroid status on expression of voltage-gated potassium channels in rat left ventricle. *Cardiovasc. Res.* **40**, 343-351.

NOBLE, D. (1984). The surprizing heart: A review of recent progress in cardiac electrophysiology. *J. Physiol.* **353**, 1-50.

NUSS, H.B. & MARBAN, E. (1994). Electrophysiological properties of neonatal mouse cardiac myocytes in primary culture. *J. Physiol.* **479**, 265-279.

OJAMAA, K., SABET, A., KENESSEY, A., SHENOY, R. & KLEIN, I. (1999). Regulation of rat cardiac Kv1.5 gene expression by thyroid hormone is rapid and chamber specific. *Endocrinol.* **140**, 3170-3176.

PAK, M.D., BAKER, K., COVARRUBIAS, M., BUTLER, A. & RATCLIFFE, A. (1991). mShal, a subfamily of A-type K^+ channel cloned from mammalian brain. *Proc. Natl. Acad. Sci.* **88**, 4386-4390.

PAPAZIAN, D.M., SCHWARTZ, T.L., TEMPEL, B.L., JAN, Y.N. & JAN, L.Y. (1987). Cloning of genomic and complementary DNA from *Shaker*, a putative potassium channels gene from *Drosophila*. *Science* **237**, 749-753.

PAPAZIAN, D.M. (1999). Potassium channels: some assembly required. *Neuron* **25**, 7-10.

PAULMICHL, M., NASMITH, P., HELLMISS, R., REED, K., BOYLE, W., NERBONNE, J.M., PERALTA, E. & CLAPHAM, D.E. (1991). Cloning and

expression of a rat delayed rectifier potassium channel. *Proc. Natl. Acad. Sci.* **88**, 7892-7895.

PETERSON, K.R. & NERBONNE, J.M. (1999). Expression environment determines K^+ current properties: Kv1 and Kv4 α-subunit-induced K^+ currents in mammalian cell lines and cardiac myocytes. *Pflugers Archiv.* **437**, 381-392.

PO, S., SNYDERS, D.J., BAKER, R., TAMKUN, M.M. & BENNETT, P.B. (1992). Functional expression of an inactivating potassium channel cloned from human heart. *Circ. Res.* **71**, 732-736.

PO, S., ROBERDS, S.L., SNYDERS, D.J., TAMKUN, M.M. & BENNETT, P.B. (1993). Heteromultimeric assembly of human potassium channels: molecular basis of a transient outward current? *Circ.Res.* **72**, 1326-1336.

PONGS, O., KECSKEMTHY, N., MULLER, R., KRAHJENTGENS, I., BAUMANN, A., KILTZ, H.H., CANAL, I., LLAMAZARES, S. & FERRUS, A. (1988). *Shaker* encodes a family of putative potassium channel proteins in the nervous system of *Drosophila*. *EMBO J.* **7**, 1087-1096.

PONGS, O. (1993). Structure-function studies on the pore of potassium channels. *J. Mem. Biol.* **136**, 1-8.

RAYNAL, F., MICHOT, B. & BACHELLERIE, J.P. (1984). Complete nucleotide sequence of mouse 18S rRNA gene: comparison with other available homologs. *FEBS Letters* **167**, 263-268.

RETTIG, J., HEINEMANN, S.H., WUNDER, F., LORRA, C., PARCEJ, D.N., DOLLY, J.O. & PONGS, O. (1994). Inactivation properties of voltage-gated K^+ channels altered by presence of β-subunit. *Nature* **369**, 289-294.

ROBERDS, S.L. & TAMKUN, M.M. (1991). Cloning and tissue-specific expression of five voltage-gated potassium channel cDNAs expressed in rat heart. *Proc. Natl. Acad. Sci.* **88**, 1798-1802.

ROBERDS, S.L., KNOTH, K.M., PO, S., BLAIR, T.A., BENNETT, P.B., HARTSHORNE, R.P., SNYDERS, D.J. & TAMKUN, M.M. (1993). Molecular biology of the voltage-gated potassium channels of the cardiovascular system. *J. Cardiovasc. Electrophysiol.* **4**, 68-80.

ROMEY, G., ATTALI, B., CHOUABE, C., ABITBOL, I., GUILLEMARE, E., BARHANIN, J. & LAZDUNSKI, M. (1997). Molecular mechanism and functional significance of the MinK control of the KvLQT1 channel activity. *J. Biol. Chem.* **272**, 16713-16716.

RUDY, B., KENTROS, C. & VEGA-SAENZ DE MIERA, E. (1991). Families of K channel genes in mammals: toward an understanding of the molecular basis of K channel diversity. *Mol. Cell. Neurosci.* **2**, 89-102.

RUPPERSBERG, J.P., SCHROTER, K.H., SAKMANN, B., STOCKER, M., SEWING, S. & PONGS, O. (1990). Heteromultimeric channels formed by rat brain potassium-channel proteins. *Nature* **345**, 535-537.

RYBIN, V. & STEINBERG, S.F. (1996). Thyroid hormone represses protein kinase C isoform expression and activity in rat cardiac myocytes. *Circ. Res.* **79**, 388-398.

SABATH, D.E., BROOME, H.E. & PRYSTOWSKY, M.B. (1990). Glyceraldehyde-3-phosphate dehydrogenase mRNA is a major interleukin 2-induced transcript in a cloned T-helper lymphocyte. *Gene* **91**, 185-191.

SALINAS, M., DUPRAT, F., HEURTEAUX, C., HUGNOT, J.P. & LAZDUNSKI, M. (1997). New modulatory alpha subunits for mammalian Shab K^+ channels. *J. Biol. Chem.* **272**, 24371-24379.

SANCHEZ-CHAPULA, J., ELIZALDE, A., NAVARRO-POLANCO, R. & BARAJAS, H. (1994). Differences in outward currents between neonatal and adult rabbit ventricular cells. *Am. J. Physiol* **266**, H1184-H1194

SANGUINETTI, M.C. & JURKIEWICZ, N.K. (1991). Delayed rectifier outward potassium current is composed of two currents in guinea pig atrial cells. *Am. J. Physiol.* **260**, H393-H399

SANGUINETTI, M.C., CURRAN, M.E., ZOU, A., SHEN, J., SPECTOR, P.S., ATKINSON, D.L. & KEATING, M.T. (1996). Coassembly of K(V)LQT1 and minK (IsK) proteins to form cardiac I(Ks) potassium channel. *Nature* **384**, 80-83.

SATO, Y., FERGUSON, D.G., SAKO, H., DORN, G.W., KADAMBI, V.J., YATANI, A., HOIT, B.D., WALSH, R.A. & KRANIAS, E.G. (1998). Cardiac-specific overexpression of mouse cardiac calsequestrin is associated with depressed cardiovascular function and hypertrophy in transgenic mice. *J. Biol. Chem.* **273**, 28470-28477.

SCHOUTEN, V.J.A. & TER KEURS, H.E.D.J. (1985). The slow repolarization phase of the action potential in rat heart. *J. Physiol.* **360**, 13-25.

SCHWARTZ, H.L. & OPPENHEIMER, J.H. (1978). Physiologic and biochemical actions of thyroid hormone. *Pharmacol. Ther.* **3**, 349-376.

SHARP, N.A., NEEL, D.S. & PARSONS, R.L. (1985). Influence of thyroid hormone levels on the electrical and mechanical properties of rabbit papillary muscle. *J. Mol. Cell Cardiol.* **17**, 119-132.

SHI, G., NAKAHIRA, K., AMMOND, S., HODES, K.J., CHECHTER, L.E. & RIMMER, J.S. (1996). Beta subunits promote K^+ channel surface expression through effects early in biosynthesis. *Neuron* **16**, 843-852.

SHIBATA, E.F., DRURY, T., REFSUM, H., ALDRETE, V. & GILES, W.R. (1989). Contribution of transient outward currents to repolarization in human atrium. *Am. J. Physiol.* **257**, H1773-H1781

SHIMONI, Y., BANNO, H. & CLARK, R.B. (1992). Hyperthyrodism selectively modifies a transient outward potassium current in rabbit ventricular and atrial myocytes. *J. Physiol.* **457**, 369-389.

SHIMONI, Y., SEVERSON, D. & GILES, W.R. (1995). Thyroid status and diabetes modulate regional differences in potassium currents in rat ventricle. *J. Physiol.* **488**, 673-688.

SHIMONI, Y., FISET, C., CLARK, R.B., DIXON, J.E., MCKINNON, D. & GILES, W.R. (1997). Thyroid hormone regulates postnatal expression of transient K^+ channel isoforms in rat ventricle. *J. Physiol.* **500**, 65-73.

SNYDERS, D.J., TAMKUN, M.M. & BENNETT, P.B. (1993). A rapidly activating and slowly inactivating potassium channel cloned from human heart. Functional analysis after stable mammalian cell culture expression. *J. Gen. Physiol.* **101**, 513-543.

SPLAWSKI, I., TRISTANI-FIROUZI, M., LEHMANN, M.H., SANGUINETTI, M.C. & KEATING, M.T. (1997). Mutations in hminK gene cause long-QT syndrome and suppress IKs function. *Nat. Genet.* **17**, 338-340.

SUAWICS, B. (1992). Role of potassium channels in cycle length dependent regulation of action potential duration in mammalian cardiac Purkinje and ventricular muscle fibres. *Cardiovasc. Res.* **26**, 1021-1029.

TAKIMOTO, K., LI, D., HERSHMAN, K.M., LI, P., JACKSON, E.K. & LEVITAN, E.S. (1997). Decreased expression of Kv4.2 and novel Kv4.3 K^+ channel subunit mRNAs in Ventricles of renovascular hypertensive rats. *Circ. Res.* **81**, 533-539.

TAMKUN, M.M., KNOTH, K.M., WALBRIDGE, J.A., KROEMER, H., RODEN, D.M. & GLOVER, D.M. (1991). Molecular cloning and characterization of two voltage-gated K^+ channel cDNAs from human ventricle. *FASEB Journal.* **5**, 331-337.

TEMPEL, B.L., PAPAZIAN, D.M., SCHWARTZ, T.L., JAN, Y.N. & JAN, L.Y. (1987). Sequence of a probable potassium channel component encoded at *Shaker* locus of *Drosophila*. *Science* **237**, 770-775.

TEMPEL, B.L., JAN, Y.N. & JAN, L.Y. (1988). Cloning of a probable potassium channel gene from mouse brain. *Nature* **332**, 837-839.

THIERFELDER, S., HIRCHE, H. & BENNDORF, K. (1994). Anoxia decreases the transient K^+ outward current in isolated ventricular heart cells of the mouse. *Pflugers Archiv.* **427**, 547-549.

THOMPSON, J.D., HIGGINS, D.G. & GIBSON, T.J. (1994). CLUSTAL W: improving the sensitivity of progressive multiple sequence alignment through sequence weighting, position-specific gap penalties and weight matrix choice. *Nuc. Acids Res.* **22**, 4673-4680.

TIMPE, L.C., SCHWARTZ, T.L., TEMPEL, B.L., PAPAZIAN, D.M., JAN, Y.N. & JAN, L.Y. (1988). Expression of functional potassium channels from Shaker cDNA in Xenopus oocytes. *Nature* **331**, 143-145.

TOKUNAGA, K., TANIGUCHI, H., YODA, K., SHIMIZU, M. & SAKIYAMA, S. (1986). Nucleotide sequence of a full-length cDNA for mouse cytoskeletal beta-actin mRNA. *Nuc. Acids Res.* **14**, 2829

TSENG-CRANK, J.C., TSENG, G.N., SCHWARTZ, A. & TANOUYE, M.A. (1990). Molecular cloning and functional expression of a potassium channel cDNA isolated from a rat cardiac library. *FEBS Letters* **268**, 63-68.

TSENG, G.N. & HOFFMAN, B.F. (1989). Two components of transient outward current in canine ventricular myocytes. *Circ. Res.* **64**, 633-647.

VAN WAGONER, D.R., POND, A.L., MCCARTHY, P.M., TRIMMER, J.S. & NERBONNE, J.M. (1997). Outward K^+ current densities and Kv 1.5 expression are reduced in chronic human atrial fibrillation. *Circ. Res.* **80**, 772-781.

VANDENBERG, C.A. (1995). Cardiac inward rectifier potassium channel. In *Ion channels in the cardiovascular system*, eds. SPOONER, P.M. & BROWN, A.M., New York: Futura Publishing Co.

VIGOUROUX, E. (1976). Dynamic study of postnatal thyroid function in the rat. *Acta Endocrinol.* **83** , 752-758.

WAHLER, G.M. (1992). Developmental increases in the inwardly rectifying potassium current in rat ventricular myocytes. *Am. J. Physiol* **262**, C1266-C1272

WAHLER, G.M., DOLLINGER, S.J., SMITH, J.M. & FLEMAL, K.L. (1994). Time course of postnatal changes in rat heart action potential and in transient outward current is different. *Am. J. Physiol* **267**, H1157-H1166

WANG, J., JUHASZOVA, M., RUBIN, L.J. & YUAN, X.J. (1997). Hypoxia inhibits gene expression of voltage-gated K^+ channel alpha subunits in pulmonary artery smooth muscle cells. *J. Clin. Invest.* **100**, 2347-2353.

WANG, L., FENG, Z.P., KONDO, C.S., SHELDON, R.S. & DUFF, H.J. (1996). Developmental changes in the delayed rectifier K^+ channels in mouse heart. *Circ. Res.* **79**, 79-85.

WANG, L. & DUFF, H.J. (1996). Identification and characterization of delayed rectifier K^+ currents in fetal mouse ventricular myocytes. *Am. J. Physiol.* **270**, H2088-H2093

WANG, L. & DUFF, H.J. (1997). Developmental changes in transient outward current in mouse ventricle. *Circ. Res.* **81**, 120-127.

WANG, Q., CHEN, Q. & TOWBIN, J.A. (1998). Genetics, molecular mechanisms and management of long QT syndrome. *Ann. Med.* **30**, 58-65.

WANG, Z., FERMINI, B. & NATTEL, S. (1993). Sustained depolarization induced outward current in human atrial myocytes: evidence for a novel delayed rectifier potassium current similar to Kv1.5 cloned channel currents. *Circ. Res.* **73**, 1061-1076.

WANG, Z., FERMINI, B. & NATTEL, S. (1994). Rapid and slow components of delayed rectifier current in human atrial myocytes. *Cardiovasc. Res.* **28**, 1540-1546.

WEI, A., COVARRUBIAS, M., BUTLER, A., BAKER, K., PAK, M.D. & SALKOFF, L. (1990). K^+ current diversity is produced by an extended gene family conserved in Drosophila and mouse. *Science* **248**, 599-603.

WEIDMANN, S. (1956). Resting and action potentials of cardiac muscle. *Ann. NY Acad. Sci.* **65**, 663-678.

WETZEL, G.T. & KLITZNER, T.S. (1996). Developmental cardiac electrophysiology: recent advances in cellular physiology. *Cardiovasc. Res.* **31**, E52-E60

WIBLE, B.A., DE BIASI, M., MAJUMDER, K., TAGLIALATELA, M. & BROWN, A.M. (1995). Cloning and functional expression of an inwardly rectifying K^+ channel from human atrium. *Circ. Res.* **76**, 343-350.

WICKENDEN, A.D., KAPRIELIAN, R., PARKER, T.G., JONES, O.T. & BACKX, P.H. (1997). Effects of development and thyroid hormone on K^+ currents and K^+ channel gene expression in rat ventricle. *J. Physiol.* **504**, 271-286.

WICKENDEN, A.D., JEGLA, T.J., KAPRIELIAN, R. & BACKX, P.H. (1999). Regional contributions of Kv1.4, Kv4.2, and Kv4.3 to transient outward K^+ current in rat ventricle. *Am. J. Physiol.* **276**, H1599-H1607

WOOD, L.S., TSAI, T.D., LEE, K.S. & VOGELI, G. (1995). Cloning and functional expression of a human gene, hIRK1, encoding the heart inward rectifier K^+-channel. *Gene* **163**, 313-317.

WYMORE, R.S., KORENBERG, J.R., KINOSHITA, K.D., AIYAR, J., COYNE, C., CHEN, X.N., HUSTAD, C.M., COPELAND, N.G., GUTMAN, G.A., JENKINS, N.A. & CHANDY, K.G. (1994). Genomic organization, nucleotide sequence, biophysical properties, and localization of the voltage-gated K^+ channel gene KCNA4/Kv1.4 to mouse chromosome2/human 11p14 and mapping of KCNC1/Kv3.1 to mouse 7/Human 11p14.3-p15.2 and KCNA1/Kv1.1 to human 12p13. *Genomics* **20**, 191-202.

XU, H., DIXON, J.E., BARRY, D.M., TRIMMER, J.S., MERLIE, J.P., MCKINNON, D. & NERBONNE, J.M. (1996). Developmental analysis reveals mismatches in the expression of K^+ channel α subunits and voltage gated K^+ channel currents in rat ventricular myocytes. *J. Gen. Physiol.* **108**, 405-419.

XU, H., GUO, W. & NERBONNE, J.M. (1999). Four kinetically distinct depolarization-activated K^+ currents in adult mouse ventricular myocytes. *J. Gen. Physiol.* **113**, 661-677.

YEOLA, S.W. & SNYDERS, D.J. (1997). Electrophysiological and pharmacological correspondence between Kv4.2 current and rat cardiac transient outward current. *Cardiovasc. Res.* **33**, 540-547.

YUE, L., FENG, J., LI, G.R. & NATTEL, S. (1996). Transient outward and delayed rectifier currents in canine atrium. *Am. J. Physiol* **270**, H2157-H2168

ZHOU, J., JERON, A., LONDON, B., HAN, X. & KOREN, G. (1998). Characterization of a slowly inactivating outward current in adult mouse ventricular myocytes. *Circ. Res.* **83**, 806-814.

APPENDIX I: pBluescript® II SK (+/-) phagemid (Stratagene)

The pBluescript® II SK (+/-) phagemid is derived from pUC19. The SK designation indicates the polylinker in oriented such that *lacZ* transcription proceeds from Sac I to Kpn I. Genbank Accession # X52328, SK+ and X52330, SK-. Vector map and polylinker

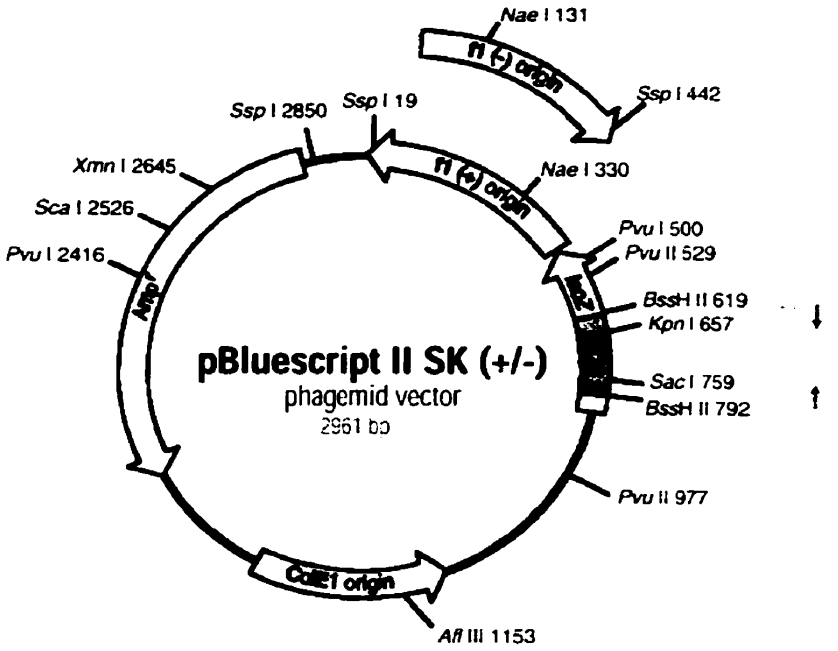

Polylinker sequence

BssH II T3 promoter +1→

5' GGAAACAGCT**ATG**ACCATGATTACGCCAAGCGCGC**AATTAACCCTCACTAAAGGG**AACAAAAGCTG
3' CCTTTGTCGA**TAC**TGGTACTAATGCGGTTCGCGCG**TTAATTGGGAGTGATTTCCC**TTGTTTTCGACCTC

816 792

Sac II Eag I Spe I Sma I
Sac I BstX I Not I Xba I BamH I Pst I EcoR I EcoR V
GAGCTCCACCGCGGTGGCGGCCGCTCTAGAACTAGTGGATCCCCCGGGCTGCAGGAATTCGATATC
GAGGTGGCGCCACCGCCGGCGAGATCTTGATCACCTAGGGGGCCCGACGTCCTTAAGCTATAGTTC

Bsp106 I Hinc III Eco0109 I
Cla I Acc I Dra II
Hind III Sal I Xho I Apa I Kpn I
AAGCTTATCGATACCGTCGACCTCGAGGGGGGGCCCGGTACCCAATTCG**CCCTATAGTGAGTCGTATTA**
GAATAGCTATGGCAGCTGGAGCTCCCCCCCGGGCCATGGGTTAAGC**GGGATATGACTCAGCATAAT**GCG

657 ←+1 T7 promoter

BssH II
CGCGCGCTCACTGGCCGTCGTTTTACAA 3' (+)
CGCGAGTGACCGGCAGCAAAATGTT 5' (-)

619

sequence obtained from http:www.stratagene.com/vectors/selection/plasmid1.htm.

DNA Ladder

The 1kb DNA Ladder (GibcoBRL, U.S. Patent No. 4,403,036) is used to size linear double- stranded DNA fragments from approximately 200bp to 12kb. The ladder shown results from running loading 0.5μg on a 0.9% agarose gel.
(http://www2.lifetech.com:80/images/1kb.gif)

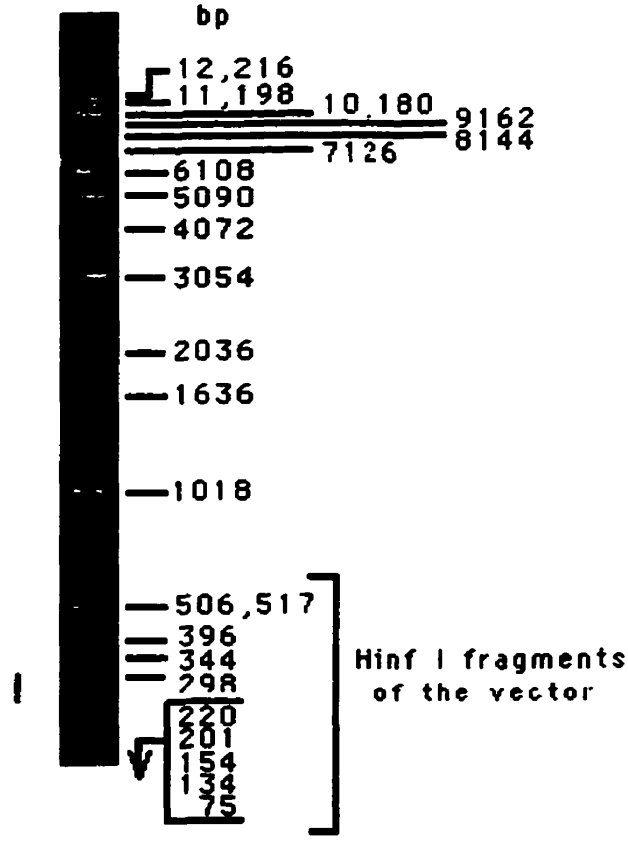

APPENDIX II: Detailed RPA Protocols

RPA Kits - Hybspeed™ RPA Kit, RPA II™ Kit and RPA III™ Kit (Ambion)

1. Hybridization and RNase Digestion:

Combine: 2.5 µg total RNA, 60,000 counts·min^{-1}labelled riboprobe (>3 fold molar excess over message), 100 µl Precipitation mix [10µl (5 µg/µl) yeast RNA, 12 µl (5M) NH_4OAc, 73 µl H_2O], and. 2.5X 100% EtOH (300 µl). Two tubes should be prepared without RNA to act as controls. Precipitate the mixture for at least 15 minutes at -20°C. Pellet the RNA by centrifugation (15minutes at 10,000 x *g*) and discard supernatant. Dissolve the RNA pellet in hybridization solution provided with kit and incubate the samples as per manufacturers' protocol.

Hybspeed™	**RPA II™**	**RPA III™**
- 10 µl Hybspeed Buffer (pre-heated to 90°C) - incubate 90°C, 2-3 minutes with frequent vortexing - incubate 68°C, 10 minutes	- 20 µl Soln.A - vortex briefly - heat 90°C, 3-4 minutes - incubate 42-45°C overnight	- 10 µl RPA III Hybridization Buffer - vortex briefly - heat 90°C, 3-4 minutes - incubate 42-45°C overnight

During the hybridization incubation it is necessary to prepare the RNase digestion mix. RNase digestion Buffer (see below for amount) is combined with RNase A/RNase T1 Mix (250 units/ml RNase A and 10,000 units/ml RNase T1) at room temperature with a 1:100 dilution for all protocols. Do not add enzyme to one of the control tubes. Vortex the samples and place at 37°C for 30 minutes. Vortex after 15 minutes of incubation.

Hybspeed™	**RPA II™**	**RPA III™**
- 100 µl Hybspeed RNase Digestion Buffer x number of assay tubes.	- 200 µl Soln.Bx x number of assay tubes	- 150 µl RNase Digestion III Buffer x number of assay tubes

2. Precipitation and Electrophoresis:

Add 150 µl Hybspeed Inactivation/Precipitation mix, 300 µl Soln. Dx, or 225 µl of RNase Inactivation/Precipitation III Solution depending on the RPA kit. Add 100 µl EtOH, and precipitate for at least 15 minutes at -20°C. Note 1µl of SeeDNA™ (Amersham Life Sciences) was added to some of the Hybspeed™ experiments at this precipitation step to aid in visualization of the RNA pellet. Pellet the RNA for 15 minutes at 10,000 x *g*. Re-suspend in 8 µl Gel Loading Buffer II for denaturing gels 95% formamide, 0.025% xylene cyanol, 0.025% bromophenol blue, 18 mM EDTA, 0.2% SDS). Pre-warm the samples for 3-4 minutes at 95°C before loading 4 µl on an 8% urea denaturing polyacrylamide mini gel.

Run samples at 200 volts in Mini Protean II Electrophoresis Cells (Bio-Rad) until the xylene cyanol band is near the bottom of the gel, since the smallest protection product (internal controls) runs with this band. Fix the gel with 20% methanol, 5% acetic acid and place gel on a piece of Whatman 3MM chromatography paper. Vacuum dry with heating for 1-2 hours.

APPENDIX III : RPA Gel Phosphorimaging Data

Table A: Developmental changes in K^+ channel α-subunit mRNA expression in CD-1 mouse ventricular muscle.

	mRNA expression level			
Channel	0-1 day	10 day	21 day	Adult
Kv 1.5	5.60±0.23	6.65±0.27	9.87±0.78	9.16±1.50
IRK_1	9.87±0.48	14.82±0.24	16.42±0.88	17.27±2.14
Kv 4.2	4.14±0.37	14.65±1.14	14.03±0.46	19.48±3.54
Kv 4.3	2.82±0.21	5.22±0.51	7.84±0.27	11.24±1.31
$KvLQT_1$	40.77±0.95	23.39±0.65	19.32±0.28	19.97±2.18
minK	91.01±6.90	66.47±8.02	14.69±1.45	5.87±1.45
Kv 1.4	10.20±0.26	4.82±0.41	2.00±0.07	1.46±0.13
Kv 1.2	---	1.74±0.05	2.56±0.14	2.08±0.27

The mRNA expression levels are given as % GAPDH. Average GAPDH mRNA levels varied with age, thus all groups corrected to 0-1 day levels (See Methods). Values expressed as mean ± standard error of the mean, n=3. One-way ANOVA for each channel showed statistically significant changes during development ($P<0.05$).

Table B: Effect of hypothyroid diet on K^+ channel α-subunit mRNA expression in C57b6 mouse ventricular muscle.

	mRNA expression level	
Channel	Hypothyroid Diet	Adult Control
Kv 1.5	7.06±0.90	5.95±0.04
IRK_1	14.53±1.93	13.24±0.27
Kv 4.2	9.20±0.06	9.65±0.52
Kv 4.3	6.59±0.34	7.83±0.57
$KvLQT_1$	18.36±0.51*	11.52±0.44
MinK	13.73±2.40*	5.42±0.17
Kv 1.4	2.96±0.13*	2.03±0.11
Kv 1.2	2.40±0.06*	2.00±0.15

The mRNA expression levels are given as % GAPDH. Average GAPDH mRNA levels varied between groups, thus correction factor used (see Methods). Values expressed as mean ± standard error of the mean, n=3. * Statistically significant differences between hypothyroid diet and control C57b6 ventricular samples (Unpaired t-test; $P<0.05$).

Table C: K^+ channel α-subunit mRNA expression in 0-1 day CD-1 mouse ventricular muscle, isolated myocytes (control and T_3-treated) and fibroblasts.

	mRNA expression level			
Channel	0-1 day w.v.	control myocytes	T_3-myocytes	Fibroblasts
Kv 1.5	5.46±0.24*	---	---	---
IRK_1	9.45±0.50	9.81±0.88^S	9.35±0.57	4.34±0.94
Kv 4.2	3.32±0.28	4.14±1.11^S	5.00±1.18	---
$KvLQT_1$	34.94±5.25	30.69±4.12$^{\#S}$	15.62±0.21	3.39±1.28
minK	98.73±25.75*	17.25±2.29	15.02±5.60	14.67±8.13
Kv 1.4	8.25±0.15	6.65±1.09$^{\#S}$	2.56±0.89	1.35±0.37

The mRNA expression levels are given as % GAPDH. Average GAPDH mRNA levels varied, thus all groups corrected to 0-1 day w.v. levels (see Methods). Values expressed as mean ± standard error of the mean, n=3. Myocytes were cultured for 18-24 hours on 100 mm glass petri dishes (low-density culture). Kv4.3 and Kv1.2 protection products were not discernible from background in myocyte and fibroblast samples. * Statistically significant difference between 0-1 day whole ventricle (w.v.) and isolated myocytes (Unpaired t-test; $P<0.05$). # Statistically significant difference between control myocytes and T_3-treated myocytes (Unpaired t-test; $P<0.05$). S Statistically significant difference between control myocytes and fibroblasts (Unpaired t-test; $P<0.01$).

Table D: K^+ channel α-subunit mRNA expression in 0-1 day CD-1 mouse ventricular muscle and isolated myocytes (control and T_3-treated).

	MRNA expression level			
Channel	0-1 day w.v.	0-1 day myocytes	Control myocytes	T_3-myocytes
Kv 1.5	3.69±0.24	2.97±1.31$^{\varnothing}$	2.58±1.13	1.38±0.12
IRK_1	15.40±0.87	26.25±7.59$^{\varnothing}$	22.94±6.32	19.53±1.22
Kv 4.2	3.88±0.13*	1.85±0.27$^{\varnothing}$	1.70±0.24$^{\#}$	2.55±0.28
$KvLQT_1$	35.17±1.61*	16.13±2.15$^{\varnothing}$	12.97±1.67	14.12±0.42
minK	110.96±8.28*	25.82±2.14$^{\varnothing}$	21.67±1.95	19.12±3.04
Kv 1.4	5.72±0.21*	1.70±0.08$^{\varnothing}$	1.24±0.08	1.51±0.11

The mRNA expression levels are given as % GAPDH. Average GAPDH mRNA levels varied between groups, thus correction factor used (see Methods). Values expressed as mean ± standard error of the mean, n=3. Myocytes were cultured for 18-24 hours in 15 ml snap-cap tubes (high-density culture). Kv 4.3 and Kv 1.2 protection products were not discernible from background in myocyte samples. 0-1 day myocytes and control myocytes are the same RPA samples run on different gels. * Statistically significant difference between 0-1 day whole ventricle (w.v.) and isolated myocytes (Unpaired t-test; $P<0.05$). # Statistically significant difference between control myocytes and T_3-treated myocytes (Unpaired t-test; $P<0.05$). ∅ Statistically significant difference between control (high-density) and control (low-density, Table C) myocytes (Unpaired t-test; $P<0.05$).